

# **Experimental and theoretical study of S(IV)/S(VI) ratio in rain and cloud events**

Von der Fakultät für Umweltwissenschaften und Verfahrenstechnik der  
Brandenburgischen Technischen Universität Cottbus zur Erlangung des akademischen  
Grades eines

Doktor der Naturwissenschaften  
(Dr. rer. nat.)

genehmigte Dissertation

vorgelegt von

Master of Science  
(Universität Peking)

Xiangshan Tian-Kunze, geb. Tian

aus Yanji, Jilin Provinz, Volksrepublik China

Gutachter: Prof. Dr. D. Möller  
Gutachter: Prof. Dr. W. Jaeschke  
Tag der mündlichen Prüfung: 26. April 2001

---



**Für meine lieben Eltern.**



## Zusammenfassung

Die Bildung von Sulfat aus emittiertem  $\text{SO}_2$  in der Troposphäre ist eine Schlüsselfrage zur Einschätzung wichtiger Umweltfragen wie saurer Regen, Waldsterben und negativer Klimaantrieb, von dem in der Forschung angenommen wird, daß er den Treibhauseffekt abmildern kann. Seit ungefähr einem Jahrzehnt sind viele Wissenschaftler einig darüber, daß Sulfatbildung hauptsächlich in der atmosphärischen Flüssigphase abläuft (80-90 %), wobei die Dissoziation von  $\text{SO}_2$  der erste Reaktionsschritt ist. Aber es herrscht noch sehr große Unsicherheit über das quantitative Verhältnis von oxidiertem zu flüssig deponiertem Sulfit. Ziel dieser Arbeit ist es, diese wichtige Frage zu beantworten und damit die Konversionsrate von Sulfit zu Sulfat als wichtige Eingangsdaten für Klimamodelle bereitstellen zu können.

Diese Arbeit präsentiert experimentelle und theoretische Ergebnisse unserer Untersuchungen des Verhältnisses von Sulfit zu Sulfat im Regen- und Wolkenwasser zur Abschätzung des S(IV)-Beitrages zur gesamten Schwefelmenge in der Flüssigphase.

Die nasse Deposition von S(IV) im Regenwasser ist im Rahmen einer Meßkampagne in Berlin-Frohnau untersucht worden. Niederschlagswasser ist gleichzeitig in 324 m Höhe und am Boden gesammelt und auf S(IV) neben vielen anderen Komponenten analysiert worden. Die Zunahme des Flusses von naß deponiertem S(IV) durch „sub-cloud scavenging“ (Auswaschprozeß unterhalb der Wolkenbasis) ist signifikant. 13-51 % (36 % als Mittelwert) des Schwefels im Regenwasser am Boden werden als S(IV) gefunden. Dieses experimentelle Ergebnis, daß S(IV) somit eine wichtige Form des Schwefels im Regenwasser ist, wird durch unsere theoretischen Untersuchungen mit einem ein-dimensionalen zeit-abhängigen physikochemischen Wolkenmodell bestätigt. Modellrechnungen zeigen, daß der überwiegende Teil des durch „sub-cloud scavenging“ abgelagerten  $\text{SO}_2$  als freies S(IV) im Regenwasser gefunden wird. In stark verschmutzten Gebieten kann dieses Verhältnis bis zu 90 % erreichen.

Unsere Meßkampagne der Station auf dem Brocken (Harz) zeigt, daß dieses Verhältnis im Wolkenwasser viel kleiner ist als im Regenwasser. Trotzdem kann es

unter bestimmten Bedingungen Werte bis 0.2 erreichen. Das bedeutet, daß S(IV) auch im Wolkenwasser eine nicht zu vernachlässigende Rolle spielt. Unsere Resultate unterstützen die wenige veröffentlichte Meßdaten von S(IV) in der Literatur, die die Wichtigkeit der nassen Deposition von Sulfit nahelegen.

Unsere Ergebnisse zeigen, daß ein erheblicher Teil von emittiertem SO<sub>2</sub> nicht zu Sulfat umgewandelt wird, insbesondere in der Schicht unterhalb der Wolkenbasis. Damit ist die Bildung von klimaeffektiven Sulfataerosolen aus gelöstem SO<sub>2</sub> in der Flüssigphase stärker limitiert als bislang von Klimamodelliern postuliert wird.

## Abstract

Production of atmospheric sulfate from  $\text{SO}_2$  emitted into the troposphere is the key question we have to answer for assessing main problems like acid rain, forest decline and negative climate forcing which is believed to counteract the green house effect. About one decade ago many researchers agreed that sulfate formation occurs dominantly (80-90 %) via the aqueous phase chemical transformation, where the  $\text{SO}_2$  dissociation is the first step. However, there is still a high uncertainty on the amount of sulfite (dissolved  $\text{SO}_2$ ) being oxidized and on that removed by wet deposition in the reduced form S(IV) (sulfite). This important question, whose answer gives climate modellers an essential input on the percentage of emitted  $\text{SO}_2$  converted into sulfate, was the aim of this work.

This work presents experimental and theoretical results from studies of the ratio sulfite/sulfate in rainwater and cloudwater to assess the contribution of S(IV) to the total sulfur amount in the aqueous phase.

The wet deposition of S(IV) in rainwater was studied by collecting rainwater samples from two different levels using a 324 m high tower. The increase of S(IV) wet deposition flux from the 324 m level to the ground level via sub-cloud scavenging of  $\text{SO}_2$  is significant. 13-51 % (36 % in average) of sulfur in rainwater on the ground level was found to be in the form of S(IV). The result that S(IV) is an important form of sulfur in rainwater was further confirmed by our theoretical study using a one-dimensional time-dependant physical-chemical cloud model. Model calculations show that most of sub-cloud scavenged  $\text{SO}_2$  will remain as free S(IV) in rainwater. In highly polluted areas the ratio can be as high as 0.9.

This ratio in cloudwater is much less than that in rainwater according to our field experiment carried out at Mt. Brocken. Nevertheless, under some special conditions, this ratio can be as high as 0.2, which means that the role of S(IV) in cloudwater is not ignorable. Thus, this study has confirmed the very few S(IV) measurements found in literature, suggesting the importance of S(IV) wet deposition.

Our findings suggest that considerable part of emitted  $\text{SO}_2$  will not be transformed to sulfate especially in the sub-cloud layer. Therefore, the production of climate affecting sulfate aerosol via aqueous phase transformation of dissolved  $\text{SO}_2$  is more limited than believed by climate modellers.



# Danksagung

Viele Menschen haben mich bei der Erstellung dieser Arbeit auf verschiedene Weise unterstützt, ohne deren Mithilfe diese Dissertation nicht hätte entstehen können. Dafür möchte ich mich hier herzlich bedanken.

Mein Dank gilt zuerst Herren Prof. Dr. D. Möller für die Betreuung meiner Arbeit und die Gelegenheit in Deutschland zu promovieren.

Ganz besonderer Dank gilt Dr. Acker und Dr. Wieprecht, die durch ihre Kollegialität und Diskussionsbereitschaft wesentlich zum Erfolg dieser Arbeit beigetragen haben.

Veit Schmidt, Dr. Auel, Dieter Kalas und Jürgen Hofmeister danke ich für die Unterstützung bei Experimenten und Meßkampagnen.

Mein herzlicher Dank gilt Dr. Mauersberger für die Mithilfe bei Modellierungen. Birgit Drabow, Ralf Fabian danke ich für die schöne Zeit in Cottbus.

Vielen Dank an Dr. Biermann und Dr. Acker für das Korrekturlesen des Manuskriptes.

Ich danke Dr. Andreas Becker für das Korrekturlesen der meteorologischen Analyse und Herrn Schmidt für die Analyse der Wetterlage.

Ich danke der Deutschen Forschungsgemeinschaft für die finanzielle Unterstützung dieser Promotionsarbeit, der Institut für Meteorologie an der Freien Universität für die Berechnung der Trajektorien, der Senatsverwaltung für Stadtentwicklung, Umweltschutz und Technologie und dem Bundesumweltamt für die Übermittlung von Meßdaten und der Deutschen Telekom für die Nutzung des Berlin-Frohnau Turmes.

Mein besonderer Dank gilt meinen Eltern und Marco für die ganze Liebe und Unterstützung während meiner Arbeit in Deutschland.



# Contents

<b>Zusammenfassung</b> .....	I
<b>Abstract</b> .....	III
<b>Danksagung</b> .....	V
<b>Introduction</b> .....	1
<b>Chapter 1 SO<sub>2</sub>-Sulfate aerosol-Cloud-Climate</b> .....	5
1.1 Atmospheric precursors of sulfate aerosols.....	5
1.2 Transformation of SO <sub>2</sub> to sulfate in the troposphere.....	9
1.2.1 Gas phase oxidation of SO <sub>2</sub> .....	9
1.2.2 Mass transfer of SO <sub>2</sub> into liquid phase.....	9
1.2.3 Formation of hydroxymethanosulfonate (HMS).....	10
1.2.4 Aqueous phase oxidation of SO <sub>2</sub> .....	11
1.2.4.1 Oxidation with H <sub>2</sub> O <sub>2</sub> .....	12
1.2.4.2 Oxidation with ozone.....	12
1.2.4.3 Oxidation with O <sub>2</sub> catalyzed by trace metals.....	13
1.3 Sulfate aerosols and climate forcing.....	14
<b>Chapter 2 Experimental observations of atmospheric S(IV)/S(VI) ratio in rainwater</b> .....	17
2.1 Introduction.....	17
2.2 Measurement site.....	18
2.3 Experimental.....	18
2.4 Result and discussions.....	20
2.5 Conclusion.....	35

<b>Chapter 3 Case studies of S(IV)/S(VI) ratio in cloud events from Brocken experiment</b>	37
3.1 Introduction	37
3.2 Measurement site	38
3.3 Experimental	41
3.4 Results and discussions	43
Event #1	44
Event #2	55
Event #3	63
Event #4	70
3.5 Summaries and Conclusions	78
<b>Chapter 4 One-dimensional physical-chemical stratiform cloud model</b>	81
4.1 Introduction	81
4.2 Cloud physics	83
4.3 Scavenging of aerosols and dissolution of gases into the liquid phase	87
4.4 RADM2 gas phase chemical reaction system	88
4.5 Aqueous phase chemical reaction system	89
4.6 Numerical solvers	90
4.7 Initial and boundary conditions	90
4.8 Results and discussions	91
4.8.1 Physical model results	91
4.8.2 Chemical model results	94
4.9 Summaries and Conclusions	103
<b>Chapter 5 Summary and outlook</b>	105
<b>References</b>	109
<b>Appendix—Measurement methods and Instruments</b>	121

## Introduction

Sulfur in the oxidation state IV (S(IV)) are atmospherically abundant in different compounds and phases: sulfur dioxide  $\text{SO}_2$ , sulfite  $\text{SO}_3^{2-}$ , bisulfite  $\text{HSO}_3^-$ , hydroxymethanesulfonate HMS. In the following we refer to the sum of the three compounds ( $\text{SO}_2$ ,  $\text{SO}_3^{2-}$  and  $\text{HSO}_3^-$ ) as free S(IV). Sulfur in oxidation state VI (S(VI)) is present as sulfate ions. The ratio between S(IV) and S(VI) in rain and cloudwater is regarded as a key factor with respect to the problems like acid rain (Galloway et al., 1982; Cowling, 1982; Andreae et al., 1990; Huang et al, 1993) and forest decline (Pahl and Winkler, 1995; Gravenhorst et al., 2000) as well as the formation of sulfate aerosols acting as cloud condensation nuclei (CCN) (Möller, 1995a; Laj et al., 1997; Eisele, 1997). Gaseous man-made and natural sulfur emissions remain as a key question because of their possible contribution to build particulate sulfates which affect negative climate forcing directly by scattering solar radiation and indirectly via their influence on the cloud albedo (Charlson et al., 1994; Möller, 1995a; Lelieveld et al., 1999).

Remark that not the entire amount of  $\text{SO}_2$  can be transformed to climate affecting sulfate aerosols in the troposphere.

In non-precipitating clouds dissolved  $\text{SO}_2$  is found to be in the form of free S(IV) and HMS, which is an adduct of sulfite ion with formaldehyde or oxidized into sulfate. Many groups have observed the S(IV) concentrations in cloudwater, which were much higher than the concentrations expected from measured  $\text{SO}_2$  concentrations basing on Henry equilibrium (Table 1). The excess S(IV) was found to be HMS (Munger et al., 1984). The concentrations of free S(IV) and HMS in cloudwater vary strongly with time and place. However, it can be seen from the measurements that especially HMS can significantly contribute to the total sulfur in cloudwater. In non-precipitating clouds, HMS and free S(IV) should be considered separately. This is necessary because in a dissipating cloud free S(IV) may turn back to  $\text{SO}_2$  during the evaporation of the cloud droplets, while HMS mainly remains in the aerosol particles and is slowly oxidized into sulfate (Warneck, 1989). Therefore, HMS in non-precipitating clouds may contribute to

the formation of sulfate aerosols, while free S(IV) in these clouds is not climate affecting.

In precipitating clouds, most of the S(IV) and sulfate ions is removed by rainwater to the ground and consequently does not contribute to direct climate forcing. The remaining part of S(IV) and sulfate in the cloud layer has the same effect as in the non-precipitating clouds. The wet removal of S(IV) and sulfate includes in-cloud and sub-cloud processes. The contribution of sub-cloud scavenging of S(IV) to the total amount of sulfur in rainwater on the ground was systematically observed for the first time by Davies (1979) and Hales (1978). Precipitation is an effective scavenging process for SO<sub>2</sub> in the sub-cloud layer. In several previous experiments (Table 1) significant part of sulfur in the precipitation was found to be in the oxidation state S(IV). Clarke and Radojevic (1987) have argued that the importance of free S(IV) in rainwater was seldom reported because free S(IV) is easily oxidized after sampling. The lack of precaution to prevent the oxidation during storage may have influenced the results. The falling time of a raindrop is too short to form the HMS adduct and hence the SO<sub>2</sub>, which is scavenged by rainwater mainly remains in the form of free S(IV). According to the hypothesis of Möller (1995a), the amount of SO<sub>2</sub>, which is emitted into the sub-cloud layer and subsequently scavenged by rainwater in the form of S(IV) can be significant in regions with high SO<sub>2</sub> emission and a low mixing ratio of oxidants.

In a summary, only the part of HMS and sulfate which remain in aerosol particles after cloud cycling contribute to the direct negative climate forcing.

The produced sulfate aerosols can subsequently enhance the formation of the clouds. The higher concentration of sulfate aerosol particulates can cause the increase of the number of small clouddrops which can efficiently reflect solar radiation within the cloud layer. Therefore, the increase of the number of clouddrops in one cloud event as well as the increase of the occurrence frequency of cloud events can also have the effect of negative climate forcing. This indirect negative climate forcing of sulfur is a subject of time and space.

The ratio of S(IV)/S(VI) is an important parameter to model cloud processes. Ignorance of the wet deposition of S(IV) results in an overestimation of the yield of sulfate aerosols and therefore causes overestimation of negative climate forcing.

It is known that the formation of sulfate acid is one major cause of the acidity in precipitation. In a precipitating cloud, sulfate will be removed by precipitation to the ground and cause acid deposition. Especially in highly polluted regions, S(IV) to S(VI) transformation is of great interest. Therefore, S(IV)/S(VI) ratio is also an important parameter with respect to the problem of acid rain.

The S(IV) levels listed in Tab. 1 have been determined by different measuring methods which can be divided into three basic analytical methods: West and Gaeke method (West and Gaeke, 1956); Ion Chromatography (IC) (Dasgupta, 1982) and Continuous flow chemiluminescence method (CFCL) (Jaeschke, 1990). In most measurements Tetrachloromercurate and formaldehyde solutions were used to stabilize free S(IV). A detailed comparison of the three methods (detection limit, sensibility, reproductivity etc.) was made by Schmidt (1995). We used Ion Chromatography and CFCL methods for samples with (IC) and without (CFCL) formaldehyde stabilization.

The aim of this work is to get a better understanding of the partitioning of total sulfur concentrations in the forms of S(IV) and S(VI) as well as the factors that especially influence the ratio of S(IV) to S(VI) in the aqueous phase. Several weeks of field experiments were carried out and the data were applied to model calculations. Since our research focusses on local transformation and vertical scavenging of sulfur dioxide rather than remote transportation, we use a one dimensional stratiform physical-chemical cloud model to discuss our experimental findings.

In Chapter 1, a brief summary of the pathways of S(IV) transformation to S(VI) and the influence of sulfate aerosols on negative climate forcing is given. A schematical fate of emitted SO<sub>2</sub> in the troposphere is also shown in Chapter 1.

In Chapter 2, characteristics of sub-cloud scavenging processes of SO<sub>2</sub> and the ratio of S(IV) and S(VI) in rainwater is discussed based on two weeks of experiment in Berlin-Frohnau. The experiment took the advantage of a 324m high telecommunication tower to collect rainwater simultaneously from two different levels, and is ideal for the measurement of vertical profiles of S(IV) and S(VI) as well as the concentrations of other components in rainwater.

In Chapter 3, the ratio of S(IV) to S(VI) in cloudwater is discussed in detail for four cloud events we observed during field experiment at our cloud chemical station at the Mt. Brocken (Harz). The ratio of S(IV) to S(VI) was discussed together with

meteorological conditions, the mixing ratio of various oxidants and gas phase chemical species.

In Chapter 4, we present a one-dimensional time-dependant physical-chemical model and various calculations made with this model to evaluate the factors which influence the wet deposition of free sulfite in rainwater.

In Chapter 5, a summary and outlook is given.

Table 1. Reported measurements of S(IV) in cloud, fog and rainwater.

	Site and time	S(IV) $\mu\text{mol l}^{-1}$	S(IV)/ total Sulfur %	Re.
Cloud	Los Angeles, USA (1981-1982)	5-365 (total S(IV))	3-47	(1)
	Los Angeles Basin, USA (1983-1985)	Under detection limit (free S(IV))		(2)
	California USA (1982-1983)	1-365 (total S(IV))		(3)
	North sea	4-23 (free S(IV))	3-14	(4)
	Le Donon/Vosges Mtn. France (1990)	1.2-90 (1/3 is free S(IV))	1-17	(5)
	Kleiner Feldberg Germany (1990)	5-39 (free S(IV))		(6)
	South Germany (1992)	0.1-4 (free S(IV))	<3	(7)
	Great Dun Fell UK (1993)	0.04-17.5 (free S(IV))	<25	(8)
	Brocken, Germany (1994)	0.34-1.02 (free S(IV))		(9)
	Several sites in USA (1993-1994)	0-31 (free S(IV))	< 3.3	(10)
		<37.8 (HMS)	<4.1	
	Brocken Germany (1998)	<17.3 (free S(IV))	<20	(11)
		<40 (total S(IV))	<30	
Fog	Marine fog California USA (1982)	3.5-18 (total S(IV))		(3)
	Urban fog California USA (1981-1983)	8-2980 (total S(IV))		(3)
	Urban fog, Switzerland (1985)	60-270 (total S(IV))	24-253	(12)
	Stuttgart, Germany (1991)	6-290 (free S(IV))	0.6-77	(13)
		140-1020 (HMS)	19-123	
	Po Valley, Italy (1989)	8-820 (HMS)		(14)
	Frankfurt(M) Germany (1990)	1.5-30 (free S(IV))	< 30	(15)
Rain	Rural UK (1975-1976)	~ 12.5 (free S(IV))	~ 14	(16)
	Urban and	~ 13.7 (total S(IV))	~ 22	(17)
	Rural UK (1977-1978)	~ 6.2 (total S(IV))	~ 14	
	Frankfurt/M Germany	6.9 (total S(IV))	7	(18)
	Rural Minnesota USA (1982)	0-9.5 (HMS)	3.24	(19)
	Urban England (1980-1981)	3.4-61.5 (total S(IV))	16.8-93.6	(20)
	Frankfurt(M) Germany (1990)	1.56-7.81 (free S(IV))	<60.0	(15)
	Berlin-Frohnau Germany (1997)	1.4-27.4 (total S(IV))	13-51	(11)

Both of S(IV) and total Sulfur are presented in the units of  $\mu\text{mol l}^{-1}$ .

(1) Richards et al., 1983; (2) Richards, 1995; (3) Munger et al., 1984; (4) Jaeschke, 1989; (5) Lammel and Metzger, 1991; (6) Wobrock et al., 1994; (7) Preiss et al., 1994; (8) Laj et al., 1997; (9) Möller, 1996c; (10) Rao et al., 1995; (11) This work; (12) Johnson et al., 1987; (13) Lammel et al., 1998; (14) Fuzzi et al., 1992; (15) Otto et al., 1992; (16) Martin et al., 1978; (17) Davies, 1979; (18) Gravenhorst et al., 1980; (19) Guiang et al., 1984; (20) Clarke and Radojevic, 1987.



# Chapter 1

## SO<sub>2</sub>--Sulfate aerosol--Cloud--Climate

### 1.1 Atmospheric precursors of sulfate aerosols

Sulfate aerosols have natural as well as anthropogenic precursors. Marine dimethylsulfide (DMS) and sulfur dioxide (SO<sub>2</sub>) are the most important natural and anthropogenic sources of particulate sulfate in the atmosphere.

The sources and sinks of DMS have been the main topic of many works (Charlson et al, 1987; Andreae, 1990; Chin et al., 1993; Lovelock 1997). It is now widely accepted that DMS is the major sulfur gas emitted from oceans into the atmosphere. Vegetation and tropical forests make minor contributions to the global emission budget of DMS. The recent estimation of DMS global emission to the atmosphere is  $24.45 \pm 5.30 \text{ Tg a}^{-1}$  (Watts, 2000), whereof 85% stem from the oceans. The main sinks of DMS are chemical reactions which restrict the average residence time of DMS to the range of one day (Warneck, 1988). The oxidation pathways of DMS to build H<sub>2</sub>SO<sub>4</sub> are reactions with OH radicals during the daytime and with NO<sub>3</sub> during the nighttime. Despite its importance for atmospheric sulfate aerosols, the yield of H<sub>2</sub>SO<sub>4</sub> converted from DMS is not exactly known.

SO<sub>2</sub> enters the atmosphere directly via volcanic emissions and from anthropogenic sources. The estimations of volcanic emissions of SO<sub>2</sub> range between 2-20 Tg S a<sup>-1</sup>, with an average of around 10 Tg S a<sup>-1</sup> (Möller, 1995a). The most important anthropogenic source of sulfur dioxide is fossil fuel combustion. Lelieveld et al. (1997) estimated the global anthropogenic emission of sulfur dioxide to be about 70 Tg S a<sup>-1</sup> ( $\pm 30\%$ , which is a relatively small uncertainty). According to the recent study of human impact on the atmospheric sulfur balance by Rodhe (1999), anthropogenic sulfur emissions (mainly SO<sub>2</sub>) are two to three times as large as the natural emissions. About

90% of the man-made emissions of SO<sub>2</sub> occur in the Northern Hemisphere (Langner and Rodhe, 1991). Facing the evidence of the problems caused by sulfur pollutions, for example London smog in 1952, many methods and technologies to reduce sulfur emissions were developed, e.g. flue gas desulfurization which is dominantly used. Consequently it was possible to reduce emissions of anthropogenic sulfur compounds in Europe and in North America (see Tab. 1.1). For example, Husain et al. (1998) reported a continuous reduction of sulfur dioxide emissions in midwest USA and a continuous decrease of particulate sulfate in Whiteface Mountain, which lies downwind of the emission sources. Hence, reduction of SO<sub>2</sub> emission can efficiently reduce the production of sulfate aerosols. A second example is the drastic reduction of SO<sub>2</sub> emission in east Germany after 1990 (Acker et al., 1998a). However, SO<sub>2</sub> emissions are still a serious problem in Asia (Lelieveld and Crutzen, 1999; Streets et al., 2000), eastern Europe (some east european countries like Poland and Czech have also recent success in reducing sulfur emissions (see Tab. 1.1)) and South America because of the combustion of sulfur-containing fossil fuels.

Table 1.1. Anthropogenic sulfur dioxide emissions around the world (thousand tons)

	1989	1990	1991	1992	1993	1994	1995	1996	1997	1998	Re.
Germany	6196	5262	4173	3429	3082	2587	2094	1477	1359	1290	(3)
East Germany	5254	4441	3264	2558	2283	2121					(3)
Czech	2000	1876	1776	1538	1419	1270	1091	946	1000		(2)
Poland	3896	3273	3014	2830	2725	2605	2376	2368	2180		(2)
China		23,011					25,178				(4)
USA	23,308	23,678	23,056	22,818	22,476	21,879	19,189	19,812	20,369		(1)

(1) EPA (Environmental Protection Agency, USA), National air pollutant emission trend report

(2) EMEP (co-operative programme for monitoring and evaluation of the long range transmission of air pollutants in Europe), website:www.emep.int

(3) UBA (Umweltbundesamt)

(4) Streets, et al., 2000

Oxidation of other reduced sulfur species (hydrogen sulfide (H<sub>2</sub>S), carbonyl sulfide (OCS) and carbon disulfide (CS<sub>2</sub>)) can also form SO<sub>2</sub> in the atmosphere. All sulfides except COS react rapidly with OH radicals to form SO<sub>2</sub> in the atmosphere. The sources

of H<sub>2</sub>S, OCS and CS<sub>2</sub> were estimated to be  $7.72 \pm 1.25 \text{Tg a}^{-1}$ ,  $1.31 \pm 0.25 \text{Tg a}^{-1}$  and  $0.66 \pm 0.19 \text{Tg a}^{-1}$  respectively (Watts, 2000). H<sub>2</sub>S is an abundant natural sulfur compound from marshlands, estuaries and oceans. Volcanoes also emit H<sub>2</sub>S. OCS is a quite stable gas mainly from oceans as well as DMS and CS<sub>2</sub> oxidations (Chin and Davies, 1993). Anthropogenic direct emission makes a minor contribution to the sources of OCS. OCS can be transported over tropopause and is the source of sulfate aerosol layer in stratosphere. Oceans and anthropogenic emissions are the main sources of CS<sub>2</sub>. The emission of CS<sub>2</sub> is so low that its influence on sulfate aerosols can be neglected.

The global distribution of SO<sub>2</sub> varies horizontally and vertically. The highest concentration of SO<sub>2</sub> was observed near industrial areas especially in the northern hemisphere (Lelieveld, 1997). Despite its short life time of less than one week, SO<sub>2</sub> can be horizontally transported and distributed over regional areas. Thus sulfur dioxide pollution is not only a local but also an interregional problem. SO<sub>2</sub> has different vertical distributions in continental and marine atmosphere. In continental atmosphere SO<sub>2</sub> decreases exponentially with height up to about 6 km, whereas in marine atmosphere SO<sub>2</sub> is vertically constant (Warneck, 1988).

An important pathway of SO<sub>2</sub> in the atmosphere is the oxidation to produce sulfate aerosols. As a complex gas-liquid-solid system, the atmosphere offers different media where chemical oxidation of SO<sub>2</sub> can take place. A small part of SO<sub>2</sub> (less than 20%) is oxidized in the gas phase by photochemical reactions. After being built from SO<sub>2</sub>, sulfuric acid forms hydrated clusters which condense or coagulate to form aerosol particles. More important than gas phase processes are the aqueous phase SO<sub>2</sub> oxidations. The aqueous phase chemical processes are considered to be significantly faster than those in the gas phase (Calvert et al., 1985; Pitts, 1986). Liquid water in rain, clouds, and fog provides a medium in which aqueous phase reactions can occur. It is believed that more than 80% of global SO<sub>2</sub> oxidation occur in clouds. Oxidation of SO<sub>2</sub> can also take place in the water film on the surface of solid, e.g. aerosol particles.

There are two mechanisms which remove SO<sub>2</sub> from the atmosphere. The first one is dry deposition. Dry deposition is the uptake of SO<sub>2</sub> at earth's surface by soil, water or vegetation. In periods without precipitation, dry deposition is the dominant removal

process of air pollutants from the atmosphere. The dry deposition process is a complex mechanism which is regulated not only by the physical, chemical and biological characteristics of the earth surface, but also by the physical and chemical characteristics of the atmospheric surface layer and the solubility and absorptivity of the species (Gravenhorst et al., 2000). The second one is wet deposition. SO<sub>2</sub> is dissolved into cloud or rain droplets and removed from the atmosphere by precipitation. The scavenging process by clouds and precipitation can be divided into in-cloud (rainout) and sub-cloud scavenging (washout) (Qin et al., 1992; Jensen and Asman, 1995).

The transformation and deposition processes of emitted SO<sub>2</sub> in the troposphere are shown schematically in Fig. 1.1. Möller (1995a) presented a roughly assessed fate of

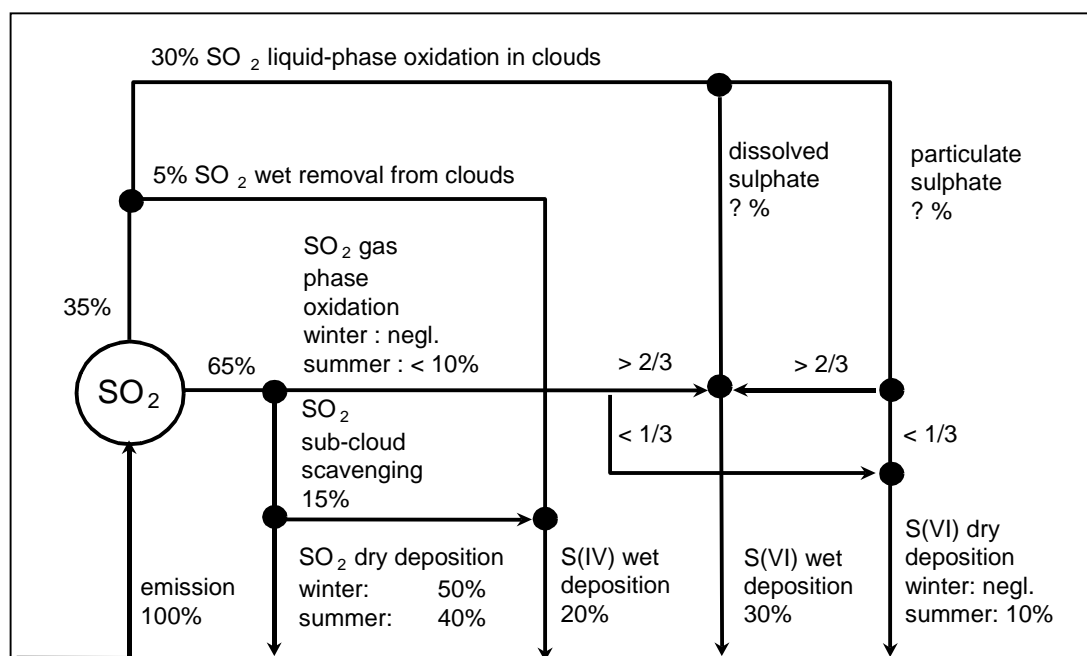


Fig. 1.1. The fate of emitted SO<sub>2</sub> in the troposphere (Möller, 1995a).

anthropogenic SO<sub>2</sub> based on published kinetic processes and cloud statistic data. According to his estimation, About 35% of all emitted SO<sub>2</sub> is emitted or transported into the cloud layer where 30% get oxidized into sulfate in the liquid phase and 5% are removed from clouds without oxidation. The rest of 65% which remains in the sub-cloud layer is partly oxidized in the gas phase (less than 10% in the summer, in winter a negligible amount), partly scavenged by precipitation (15%) and to the largest part dry

deposited (in winter 50%, in summer 40%). Thus, about 40% of wet deposited sulfur could be S(IV). Hence, sub-cloud scavenged S(IV) (15%) is three times that of in-cloud scavenged S(IV) (5%). The estimation of Warneck (1989) (about 30% of wet deposited sulfur was in the oxidation state S(IV)) is very similar to that of Möller (1995a).

## 1.2 Transformation of SO<sub>2</sub> to sulfate in the troposphere

### 1.2.1 Gas phase oxidation of SO<sub>2</sub>

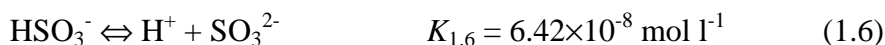
The reaction scheme and the associated rate of gas phase SO<sub>2</sub> oxidation by OH is well known. It is also considered as the only efficient process for the formation of sulfuric acid aerosols in the gas phase (Pitts, 1986). The following three reactions (1.1-1.3) represent the mechanism leading to sulfuric acid formation from SO<sub>2</sub>. The first (1.1) is the rate determining step (Eisele, 1997):



M is the atmospheric substance which carries energy during the reactions. The oxidation rates depend on the OH radical concentration. The residence time of SO<sub>2</sub> due to this pathway is between 1 and 2 weeks. Since the production of OH is highly dependent on photochemistry, the residence time is shorter in the bright sunlight (at midday and in summer time).

### 1.2.2 Mass transfer of SO<sub>2</sub> into liquid phase

When sulfur dioxide dissolves into water, an equilibrium between hydrated sulfur dioxide (SO<sub>2</sub>·H<sub>2</sub>O), the bisulfite ion (HSO<sub>3</sub><sup>-</sup>), and the sulfite ion (SO<sub>3</sub><sup>2-</sup>) will be established in a time scale of a few seconds. The Henry coefficient and reaction rates are according to Maahs (1982).



We refer to the sum of these three forms as free S(IV). The oxidized form of sulfur, e.g. sulfate, is commonly referred to as S(VI).

A modified Henry's law coefficient ( $H_{S(IV)}^*$ ) was defined to describe the balance between free S(IV) and the partial pressure of SO<sub>2</sub>:

$$[S(IV)] = H_{S(IV)}^* P_{SO_2}$$

where

$$H_{S(IV)}^* = H_{SO_2} \left[ 1 + \frac{K_{1.5}}{[H^+]} + \frac{K_{1.5}K_{1.6}}{[H^+]^2} \right]$$

The solubility of SO<sub>2</sub> is highly dependent on the pH value of the aqueous phase. The amount of S(IV) increases drastically with increasing pH due to the pH-dependence of reactions (1.5) and (1.6). Over the pH range 2—6 (typical range for atmospheric droplets), most of S(IV) is in the form of the bisulfite ion (HSO<sub>3</sub><sup>-</sup>) (Gravenhost, 1980). The equilibrium between S(IV) and the gas phase partial pressure of SO<sub>2</sub> is additionally a function of temperature. At lower temperature more S(IV) can be found at the same pH (Seinfeld, 1986).

The scavenging of SO<sub>2</sub> by hydrometeors is a sequence of processes involving diffusion of the gas to the surface of water, transfer of the gas through the gas-water interface, formation of the equilibrium of the dissolved gas, diffusion within the droplet and the aqueous phase reactions of SO<sub>2</sub>. The residence time of SO<sub>2</sub> for each step was calculated by Schwartz and Freiberg (1981). For SO<sub>2</sub>, chemical reaction in aqueous phase is considered to be the rate determining step. The mass transfer coefficient (see Chapter 4) according to Schwartz (1986) is widely used in cloud chemistry modelling.

### 1.2.3 Formation of hydroxymethanesulfonate (HMS)

When SO<sub>2</sub> is absorbed into the aqueous phase, S(IV) is found to be in two different forms: free S(IV) (see Chapter 1.2.2) and HMS (adduct of S(IV) with formaldehyde). There are various aldehydes which may form hydroxyalkylsulfonic acids in solution by the addition of bisulfite or sulfite ions to aldehydes (Munger 1986; Facchini et al., 1992). The reaction between free S(IV) and formaldehyde can be described as follows:





The Henry coefficient and rate coefficients of reactions (1.8-1.10) are taken from Möller and Mauersberger (1995).

Formaldehyde is a highly soluble gas which is often abundant in urban atmosphere. It is directly emitted from combustion sources or produced via photochemical oxidation of hydrocarbons. The background level of gas phase formaldehyde is reported to be in the range of 0.5-2 ppb, while in the urban area the value can be up to 10 times higher (Munger et al., 1984). The reaction between formaldehyde and S(IV) is quite slow in acid conditions. According to Munger et al. (1986), at pH 7 the rate of formation of HMS (for a gas-phase concentration of 1ppb HCHO) restricts the lifetime of S(IV) to about 5 min, however, at pH 5 the lifetime prolongs to be 35 days. Thus the question of whether the addition of free S(IV) to formadehyde can compete with the oxidation of free S(IV) with hydroxy peroxide, ozone and O<sub>2</sub> (with catalyse) depends strongly on the concentration of the oxidants in the liquid phase, the concentration of gas phase formaldehyde and the pH value of the hydrometeors. Although HMS is stable against O<sub>3</sub> and H<sub>2</sub>O<sub>2</sub>, it can be oxidized by OH to build formic acid (Olson and Hoffmann, 1989). The reaction rate is expected to be reasonably fast (Warneck, 1989). The formation of HMS is found to be partially responsible for the high concentrations of observed S(IV) in fog and cloudwater (Munger et al., 1984; 1986, Warneck, 1989; Rao et al., 1995).

When a droplet evaporates, the concentrated HMS in aerosol particle can be slowly oxidized to SO<sub>4</sub><sup>2-</sup> and thus influence the concentration of sulfate in the aerosol particles.

#### 1.2.4 Aqueous phase oxidation of SO<sub>2</sub>

In the aqueous phase free S(IV) will be oxidized into S(VI) mainly by reaction with hydrogen peroxide, ozone and oxygen catalyzed by trace metals (Penkett et al., 1979; Maahs, 1983; Martin, 1984; Hoffmann, 1986; Warneck, 1991; Radojevic, M., 1992; Radojevic, M. et al., 1995; Brandt et al., 1995; Lagrange et al., 1996; Warneck et al., 1996; Sedlak et al., 1997; Möller, 2000). The oxidation mechanisms are discussed in the following subsections.

#### 1.2.4.1 Oxidation with H<sub>2</sub>O<sub>2</sub>

Hydrogen peroxide is a highly soluble gas. Because of its high solubility, even low concentrations (of a few ppb) of H<sub>2</sub>O<sub>2</sub> in the gas phase can contribute significantly to the H<sub>2</sub>O<sub>2</sub> concentrations in the liquid phase. H<sub>2</sub>O<sub>2</sub> is considered to be the main oxidant of S(IV) in the liquid phase at low pH values (Penkett et al., 1979; Lee et al., 1986; Radojevic et al., 1990; Möller and Mauersberger, 1995). The reaction rate between S(IV) and H<sub>2</sub>O<sub>2</sub> is dependent on the pH value of the aqueous phase and is decreasing strongly with increasing pH (at pH>1.5). At pH of less than 1.5 the reaction rate increases with increasing pH. Since the solubility of SO<sub>2</sub> increases with increasing pH, the production of S(VI) from the reaction with H<sub>2</sub>O<sub>2</sub> does not change with pH in the range of 1-7 (Martin, 1984). The oxidation of S(IV) by H<sub>2</sub>O<sub>2</sub> can be written as



The kinetics of this reaction was thoroughly investigated by a number of researchers and the results agree quite well with each other. The oxidation rate can be defined as

$$\frac{d[\text{S(VI)}]}{dt} = k[\text{H}^+][\text{H}_2\text{O}_2][\text{S(IV)}]$$

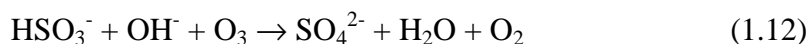
where  $k$  is  $(5.3 \pm 2.7) \times 10^7 \text{ mol}^{-1} \text{ l s}^{-1}$  at 298K (Möller and Mauersberger, 1995).

Organic peroxide also can oxidize S(IV) in a similar mechanism as H<sub>2</sub>O<sub>2</sub>. But as the concentration of organic peroxides in the atmosphere are much smaller than that of H<sub>2</sub>O<sub>2</sub>, the production of sulfate via this pathway contributes only 5% to the total sulfate production in the aqueous phase (Möller 2000).

#### 1.2.4.2 Oxidation with ozone

Ozone is a moderately soluble gas. With the gas phase concentration of 40 ppb (mean background concentration in the troposphere) and a Henry coefficient of  $0.013 \text{ mol l}^{-1} \text{ atm}^{-1}$  at 298K (Martin, 1984), the equilibrium concentration of ozone in solution is only  $5 \times 10^{-10} \text{ mol l}^{-1}$ . However, as in the liquid phase the reaction between ozone and S(IV) is rapid, the sulfate production via the reaction of ozone and S(IV) is important especially for the solutions with  $\text{pH} \geq 4.5$  because the rate of the reaction and the solubility of SO<sub>2</sub> increase with increasing pH value. There are two different mechanisms of S(IV) oxidation by ozone. One is an ionic mechanism which can be described as





The reaction rate is given by

$$k = (k_a + k_b[\text{OH}^-])[\text{HSO}_3^-][\text{O}_3]$$

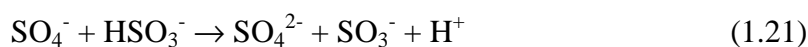
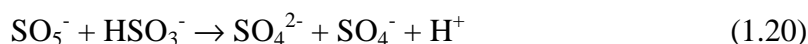
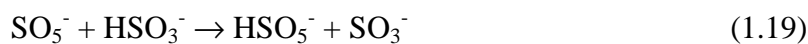
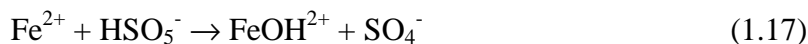
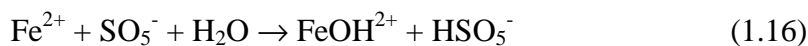
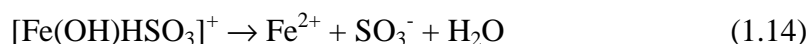
where  $k_a = 3.8 \times 10^5 \text{ mol}^{-1} \text{ s}^{-1}$  and  $k_b = 1.05 \times 10^{16} \text{ mol}^{-2} \text{ l}^2 \text{ s}^{-1}$  at 298K (Pitts, 1986).

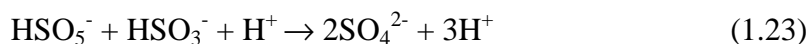
The other mechanism is free radical mechanism (Botha et al., 1994; Warneck, 1996; Möller, 2000). Ozone reacts with the hydroxyl ion and produces HO<sub>2</sub>/O<sub>2</sub><sup>-</sup> radicals which subsequently form OH radicals. The hydroxyl radicals react with S(IV) species initiating chain reactions.

### 1.2.4.3 Oxidation with O<sub>2</sub> catalyzed by trace metals

In the absence of any catalyst, the autoxidation of S(IV) to S(VI) in the liquid phase is negligible. However, the rate of autoxidation of S(IV) can be significantly catalyzed by trace metals like dissolved iron, manganese and copper (Brimblecombe et al., 1974; Hoffmann and Jacob, 1984; Hoffmann and Calvert, 1985; Clark and Radojevic, 1987; Warneck, 1991; Radojevic, 1992; Radojevic et al., 1995; Brandt and van Eldik, 1995; Warneck, 1996; Sedleck et al., 1997; Grgic et al., 1999).

Iron is a transition metal which is abundant in rural and urban atmosphere. To catalyse the autoxidation of S(IV) to S(VI) oxidation state Fe(II) should be first oxidized to oxidation state Fe(III). The mechanism of the redox cycling of Fe(II/III) in the presence of bisulfite and oxygen can be described as follows (Warneck, 1996):





The reaction rate of the S(IV) autoxidation catalyzed by iron is found to be proportional to the Fe(III) concentration. However, the values of the reaction rates published in the papers are quite different from one another.

Manganese and Copper catalyze the autoxidation of S(IV) in the aqueous solution in a similar mechanism as iron does. The manganese catalyzed reaction rate can be described as

$$-\frac{d[S(IV)]}{dt} = k[Mn(II)][S(IV)]$$

where  $k = 1.4 \times 10^3 \text{ l mol}^{-1} \text{ s}^{-1}$  in the pH range of 2.5-5.

Interestingly, when Fe<sup>3+</sup> and Mn<sup>2+</sup> are both present in the solution, an enhancement of the reaction rate to a value higher than the sum of the individual catalyzed rates has been observed (Martin, 1984).

### 1.3 Sulfate aerosols and climate forcing

The role of sulfate in the formation of acid rain is well known (Möller, 2000). Since the last decade, the influence of sulfate aerosols on climate negative forcing has drawn more and more notice. The life time of sulfate aerosol in the troposphere is relatively short (in humid regions a few days and in dry subtropics a few weeks), however, because of its abundance in polluted atmosphere, sulfate aerosols are considered to be an important factor in negative climate forcing competing with the global warming effect of greenhouse trace gases (Charlson et al., 1987; Anderson et al., 1992; Möller, 1995a; Choularton et al., 1997; Cox, 1997). Sulfate aerosols scatter short-wave solar radiation and thus increase the amount of sunlight reflected into space. Consequently, the earth's surface will be cooled down due to increase of sulfate aerosols. This is the direct negative climate forcing of sulfate aerosols. On the other side, sulfate aerosols can influence climate via their role in cloud formation. Sulfate particles are the predominant source of cloud condensation nuclei (CCN). Non sea-salt sulfate particles exist predominantly in the accumulation mode of aerosols which can be effectively nucleated into cloud droplets when the relative humidity of atmosphere exceeds 100%. Increase of aerosols which can act as CCN results in increase of the number of cloud droplets and decrease of cloud droplet size provided that the liquid water content is

constant. Increase of small sized cloud droplets is favorable for the scattering of incoming sunlight (shortwave) because of the greater surface area on which the light will be reflected or refracted. Also the deliquescent particles which will grow to a few micrometers without activated into CCN will increase the amount of solar radiation reflected from the cloud into space. The earth's albedo is 0.3, however, if the earth had no clouds, the albedo would reduce to about 0.15. Production of higher number of small droplets can also prolong the lifetime of clouds, which increase the fraction of the earth covered by cloud and thus further increase earth's albedo. Both of these effects cause indirect negative climate forcing.



## Chapter 2

# Experimental observations of Atmospheric S(IV)/S(VI) Ratio in Rainwater

### 2.1 Introduction

The harmful effect of acid rain on plants, lakes and buildings is well known since the last hundred years. Sulfate and nitrate concentrations and the pH value of rainwater have been measured worldwide and in many countries regular monitoring programs were established. However, the concentration of S(IV) in rainwater drew first notice in the beginning of the 1970s.

Since that time, significant amounts of S(IV) have been observed in rainwater (Davies 1974; 1976; 1979; Hales, 1979; Martin et al.1978; Radojevic, 1985; Otto et al. 1992). Davies (1979) pointed out that S(IV) levels in rainwater do not reflect sulfur dioxide rainout (in-cloud scavenging) but mainly the washout (sub-cloud scavenging) of sulfur dioxide. Since the falling time of raindrops from the cloud base to the earth surface is too short for a quantitative oxidation of the absorbed SO<sub>2</sub> in rainwater, it is assumed, that the largest part of the sub-cloud scavenged SO<sub>2</sub> will remain in the oxidation state S(IV) during the removal from the atmosphere. However, most of the measurements of S(IV) in rainwater were carried out on the ground level. It would be helpful to check the assumption that S(IV) is an indicator of the sub-cloud scavenging of sulfur dioxide by an experiment where rainwater is collected simultaneously at different vertical levels to observe an enrichment of SO<sub>2</sub>. The early measurements of the 1970s have not separated S(IV) into free S(IV) and HMS. Due to the slow reaction rate of sulfite ions with formaldehyde (Munger et al., 1986), HMS in rainwater is very likely from in-cloud processes whereas free S(IV) is mainly from sub-cloud scavenging

processes. Therefore, separate analysis of free S(IV) and HMS is needed for a better understanding of the in-cloud and sub-cloud processes.

In heavily polluted areas where high SO<sub>2</sub> concentrations are observed, sub-cloud scavenging of SO<sub>2</sub> is found to be more important than in-cloud scavenging (Huang et al., 1995; Lei et al., 1997). Davies (1976) found from a one-year observation program that precipitation removed only a small fraction of the emitted SO<sub>2</sub> in an industrial area. However, the percentage of S(IV) in total sulfur in heavily-industrialized areas was much higher than in rural sites. In Chapter 4 the ratio of S(IV)/S(VI) will be discussed under different emission situations of SO<sub>2</sub> with the help of one-dimensional cloud model.

The aim of this chapter is to study the S(IV)/S(VI) ratio in precipitation at different altitudes and hence to estimate the increase of S(IV) in rainwater via sub-cloud scavenging. A radio tower at the north-west border of Berlin is well suited for this purpose.

## **2.2 Measurement site**

A field experiment was carried out in Berlin-Frohnau (51.80° N; 10.67° E) from November 3<sup>rd</sup> to November 15<sup>th</sup>, 1997. Berlin-Frohnau is located on the north-west part of Berlin. Around the site is a forest. Measurements were done on the ground and additionally on a telecommunication tower with a platform at 324 m height. The two sites with different levels (one on the platform of the tower and the other on the ground direct near the tower) were used to collect rain samples. 10 km southly from Frohnau tower is a busy airport. Heavy traffics can be found in the direction of east and west (in each direction with 5 km distance from the Frohnau tower). The ground site (50m a.s.l.) is lower than the tree around it and hence isolated from local air flow.

## **2.3 Experimental**

Two different rain samplers were used, one at the ground and the other on the platform of the tower. The first has a surface of 1 m<sup>2</sup>, while the other one has a surface of 0.5 m<sup>2</sup>. It is necessary to install a smaller one on the tower because the space on the platform is not sufficient for a larger one. The surface of the rain sampler on the tower formed about 20 degree angle with respect to the horizontal line, with the collecting surface

facing the main wind direction (predominantly SW and SE) to increase the impaction collecting efficiency in case of strong wind. The surface of the rain sampler on the ground is installed horizontally.

Aerosol particles were collected only on the tower every two hours with a TSP (Total Suspended Particulate) High Volume Sampler “Digitel“. Cloud base was monitored by a ceilometer CT25K (Vaisalla) from the ground.

Conductivity (measured with WTW LF196 plus Philips PW 9513 electrode) and pH (measured with WTW pH 196 plus Mettler Toledo InLab 422 electrode) of the rain samples were measured in the field soon after sampling. A H<sub>2</sub>O<sub>2</sub> analyser (AL-1002) was used to measure the concentration of H<sub>2</sub>O<sub>2</sub> in the liquid phase in the field. S(IV) concentration in rainwater was measured in the field according to CFCL method (Jaeschke, 1990). This measurement was performed only on November 6<sup>th</sup> from 13:00 to 14:00. During other periods due to unfavorable sampling time (mostly in the evening, midnight or early morning) we collected the rain samples with bottles containing 10 ml formaldehyde (6.5 mmol l<sup>-1</sup>) as preservation reactant. In these samples free S(IV) was stabilized to HMS during collection and HMS was measured with ion chromatography (IC) instead of the concentrations of free S(IV). The different measurement methods to determine S(IV) provide different information about the S(IV) content. While the results from the CFCL method give the concentration of free sulfite (SO<sub>2</sub>·H<sub>2</sub>O, HSO<sub>3</sub><sup>-</sup> and SO<sub>3</sub><sup>2-</sup>), the results from IC show the sum of free sulfite (which is stabilized by formaldehyde during sampling) and original HMS (which exists already in rainwater before collecting). After field site analysis the rainwater samples were stored in a refrigerator (4°C) until they were analyzed for main cations and anions with ion chromatography in the laboratory. All analytical data were validated by check of the ion balance between cations and anions (< ± 10%) and by comparison of the measured with the theoretically calculated conductivity (the required accuracy is < ± 20%). The quality of our laboratory analysis was validated by WMO (World Meteorological Organization) and EPA (Environmental Protection Agency) intercomparison studies (Acker et al., 1998b; WMO 1992; WMO 1994).

Gas species ( $\text{SO}_2$ ,  $\text{O}_3$ ,  $\text{NO}_x$ ) and meteorological parameters (wind direction and velocity, temperature and humidity) were measured continuously by the Berlin Environmental Agency at both height levels.

Detailed descriptions of individual measuring methods and instruments can be found in Appendix.

## 2.4 Results and discussions

During the experiment we observed four rain periods, in which more than 70 samples were collected. 17 samples from each level could be collected simultaneously from both levels within the four different time periods. The results of these four events will be discussed in the following.

### Weather situation

Cloud base heights, cloud type, rain intensity and a short description of air mass transport are listed in Table 2.1 for each of the four events. The back trajectories of the rain events, calculated using a three dimensional model (Naumann, 1996) are shown in Fig. 2.1.

Event #1 and #2 took place both on November 6<sup>th</sup>, the earlier one at midnight (1:00-5:00) and the later one in the afternoon (13:00-14:00). During those time periods Berlin lay just behind a warm front. The raise of warm air mass built large scale stratocumulus clouds and caused showers in Berlin. The air mass transport in both events shows similar trajectories, characterized as continental air mass. In event #3 (November 9<sup>th</sup>, 1997), Berlin lay in front of an occlusive front, a weak shower was observed at Berlin-Frohnau. The trajectories are not homogeneous during the whole period of event #3, therefore the trajectories were calculated for two separate time spans. One from November 9<sup>th</sup> 17:00 to 19:00, the other from November 9<sup>th</sup> 20:00 to 21:00. From 19:00 to 20:00 due to inhomogeneity no trajectories were calculated. During event #4 (November 15<sup>th</sup>, 1997), fog is observed. Berlin lay in the middle of a low pressure area. The falling raindrops evaporated into water vapor and increased the water vapor pressure of the air. As the air near the ground is saturated, a fog formed. Consequently in event #4 the collected samples were a mixture of rain and fog water. The air mass from event #4 reached the measuring site from southwest direction, however, from the



trajectories we can see that the transport of air mass was from west crossing Hannover and Magdeburg. The air mass was also continental.

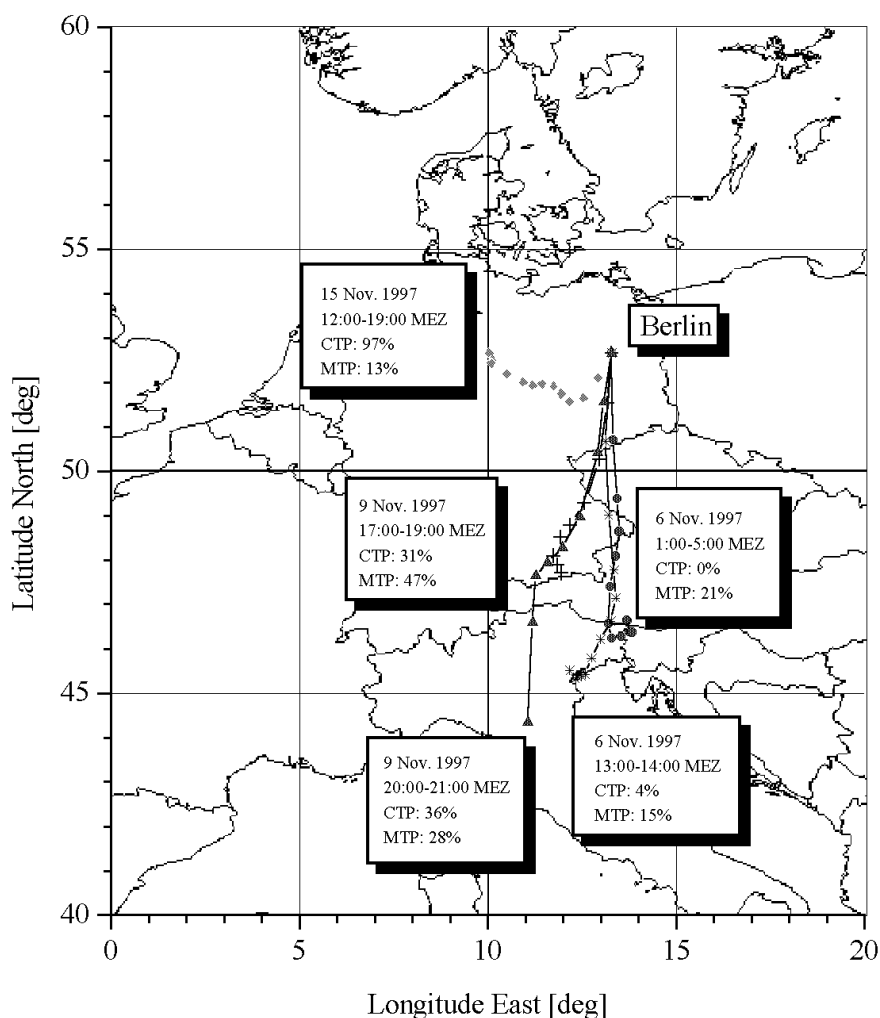


Fig. 2.1. The trajectories from Berlin-Frohnau experiment, November, 1997. CTP: the percentage of air mass transport inside clouds. MTP: the percentage of air mass transport inside mixing layer.

The average rain intensities of all four rain events were lower than  $1\text{mm hr}^{-1}$ . Rain intensities from both levels (calculated from rain volume collected by rain samplers on both levels) are slightly different. During the most sampling periods, we measured higher rain intensity on the ground than on the tower except at the beginning of each rain event. When rain began, rain sampler on the ground reacts more slowly because of

its larger surface. According to the model simulation, the evaporation of raindrops during falling period from the tower to the ground (about 300m) is found to be negligible. That means that the difference of rain intensity from both levels is not due to the evaporation of raindrops.

Table 2.1. Cloud base height, rain intensity and short descriptions of air mass transport during four rain events in November, 1997 at Berlin-Frohnau

Event #	date	time [MEZ]	Cloud base Height [m]	Cloud type	Rain intensity [mm hr <sup>-1</sup> ]	Description of air mass transport
1	06/11	01:00-05:00	1500-2500	Stra.cu.	0.43	South, <i>via</i> Czech and industrial areas of East Germany; continental air mass.
2	06/11	13:00-14:00	2000-2500	Stra.cu.	0.45	Similar to that of event 1
3	09/11	17:00-21:00	1000-1500	Stra.cu.	0.20	SSW, <i>via</i> Bavaria, west part of Czech republic and industrial areas of East Germany.
4	15/11	12:00-19:00	0-1500 (fog)	Stra.cu.	0.74	West, <i>via</i> Hannover, Magdeburg, reaching the experimental site from southwest direction, continental air mass.

### Trace gases and trajectories

The measured mean concentrations of the trace gases O<sub>3</sub>, SO<sub>2</sub> and NO<sub>x</sub> during each event are listed in Table 2.2. With respect to the fact that on the ground site the air flow may be influenced by the surrounding trees, we only list the trace gas concentrations measured on the tower level. The air mass from southern and southwestern trajectories (#1, #2 and #3) show average ozone concentrations of 28 ppb which are near to the background ozone concentration. Nevertheless, very low ozone concentrations (~10 ppb) were measured in air masses from western trajectories (#4). In these western trajectories at the same time high concentrations of NO<sub>2</sub> were observed. The busy freeway between Berlin and Hannover, which lies on the route of the western trajectories, can cause high NO emission which can be oxidized by ozone into NO<sub>2</sub>. Hence we find a reduced ozone

content and increased NO<sub>2</sub> concentration in the air mass. Moreover, in this event the percentage of cloud occurrence on the route of the trajectories was as high as 97%. This means the air mass in event #4 was transported mostly inside clouds. It is well known that clouds can be a sink for oxidants like ozone (Acker et al., 1995b).

The comparison of main wind direction and resulting SO<sub>2</sub> concentrations shows that SO<sub>2</sub> concentrations are influenced by different factors. For example, air masses in event #1 and #2 stem from similar trajectories, but in event #1 much more SO<sub>2</sub> was measured than in event #2. It can be seen that local emission sources are another important factor determining the content of the SO<sub>2</sub>. In event #1 the wind was from south (city center of Berlin), while in event #2 the wind was from southwest (forest). Apparently, in these cases the SO<sub>2</sub> concentration was more strongly influenced by local sources than by remote transportation.

Table 2.2. SO<sub>2</sub>, NO<sub>2</sub> and O<sub>3</sub> concentrations at tower level

Event	SO <sub>2</sub> (ppb)			NO <sub>2</sub> (ppb)			O <sub>3</sub> (ppb)		
	Min.	Mean	Max.	Min.	Mean	Max.	Min.	Mean	Max.
1	1.7	8.8	16.5	1.9	6.1	8.3	22.0	28.3	46.2
2	1.7	2.5	4.2	8.3	10.1	12.2	20.1	23.1	28.5
3	0.3	1.2	2.1	1.0	3.2	6.3	26.1	33.3	38.3
4	1.4	4.5	10.2	7.3	14.6	22.9	1.4	9.8	32.2

### Ion distributions

The main anions of rainwater were NO<sub>3</sub><sup>-</sup>, SO<sub>4</sub><sup>2-</sup> and Cl<sup>-</sup>, whereas the main cations were Na<sup>+</sup>, NH<sub>4</sub><sup>+</sup> and Ca<sup>2+</sup>. In all events, the fractions of SO<sub>4</sub><sup>2-</sup> in total ion concentrations in rainwater on the ground were greater than those on the tower.

In event #1, #2 and #3 the concentration of sulfate (µeq l<sup>-1</sup>) was in the same order with that of nitrate (µeq l<sup>-1</sup>) in rainwater collected on the tower, but in rainwater collected on the ground sulfate concentration was almost double of nitrate concentration (Tab. 2.3). The concentrations of other ions (excluding sulfate and sulfite) were lower in the ground samples than in the tower samples. Only for event #4 (fog) no significant difference in ion concentrations in rainwater between tower and ground was found. Due to the mixing of fogwater in the rain samples, in event #4 the ion concentrations on the

ground were generally higher than those in other rain events (Tab. 2.3). It is well known that in general fogwater contains much higher concentrations of ions than rainwater. In event #4, the overwhelming fraction of equivalents was represented by  $\text{NO}_3^-$ . The high  $\text{NO}_3^-$  concentration can be traced to high concentration of gas phase  $\text{NO}_x$  in this event which will be discussed in the subsection of **NO<sub>x</sub> and nitrate**.

Table 2.3. Rainwater mean concentrations of main ions (precipitation weighted) (in  $\mu\text{eq l}^{-1}$ ).

Event	S(IV)		S(VI)		$\text{NO}_3^-$		$\text{NH}_4^+$		$\text{Na}^+$		$\text{Cl}^-$	
	T*	G*	T	G	T	G	T	G	T	G	T	G
1	6.2	9.8	49.6	51.6	44.0	27.6	20.8	18.0	9.7	5.3	9.1	4.2
2	3.9	10.5	29.4	21.8	24.7	11.2	18.6	11.7	8.7	2.5	7.3	2.2
3	5.5	6.7	33.0	28.0	39.6	17.4	46.2	22.7	52.1	9.1	58.4	13.9
4	4.9	4.7	43.8	48.0	93.4	73.9	56.1	45.5	9.0	6.9	7.0	6.8

\*: G: ground; T: Tower

Only the concentration of the S(IV) ion increased in samples taken from the ground compared to the samples taken from the tower. In contrast we measured about the same concentrations of S(VI) from both levels. Because the component ratios (e.g.  $\text{Na}^+/\text{Cl}^-$  and  $\text{NO}_3^-/\text{NH}_4^+$ ) were nearly identical at ground level and tower level, we argue that there is a dilution effect between the two levels. There are two different mechanisms which can cause dilution between the two height levels: One is an increasing amount of rainwater content via water vapor condensation on the falling raindrops. But as the humidity in the layer between both levels was approximately 90 %, rainwater will rather evaporate than increase and thus this explanation is rather unlikely. The other way is the evaporation of rainwater and consequently a loss of small raindrops. But our modeling study in chapter 4 shows that evaporation of rainwater during the falling time of raindrops from the tower to the ground is negligible. Therefore, we can only conclude that the sampling efficiency of the rain sampler on the tower to collect small raindrops was higher than that on the ground (via its correlation with wind speed and wind direction). Because small raindrops generally have much higher concentrations of ions than larger ones, the samples collected on the ground have a dilution effect because of the higher fraction of larger droplets. As small drops contribute only little to the mass of

rainwater, there is no significant change in rain intensity. Hence we assume that at the tower level we just sampled more smaller raindrops with higher ion concentrations. The different concentration ratios of different ions may express their different droplet size depending concentrations. Only during event #4 (foggy situation), the concentration ratio was around one for all species, i.e., the collected drop spectrum in both samplers was nearly identical. The result that S(VI) concentration is nearly similar at both levels can hence only be explained by a formation of S(VI) during the rain fall via SO<sub>2</sub> scavenging and subsequent oxidation.

At the end of each rain event, almost all of the main ion concentrations have a slight increase, which can be explained by evaporation of raindrops due to entrainment of dry ambient air.

### **SO<sub>2</sub> and sub-cloud scavenging**

During event #2, a decrease of SO<sub>2</sub> concentration with the evolution of rain was observed (Fig. 2.2a). This can be well explained by sub-cloud scavenging of SO<sub>2</sub> by raindrops. However, we also observed periods in which SO<sub>2</sub> concentration decreased only very slowly (event #3 and #4) or even increased during a short period of a rain event (event #1). During event #1, between 3:00-4:00 the SO<sub>2</sub> concentration increased after an initial washout of SO<sub>2</sub> by rainwater (Fig 2.2a). This indicates an entrainment of a new air mass into the sub-cloud layer. In event #2, the washout effect of SO<sub>2</sub> by rainwater is very obvious. Comparing the concentrations of SO<sub>2</sub> on the tower before and after rain event #2, we can figure out that approximately 80% of SO<sub>2</sub> was scavenged by rainwater. However in event #3 the SO<sub>2</sub> concentration has only slight decrease throughout the rain period, indicating that the scavenging efficiency of SO<sub>2</sub> by rainwater is influenced by different factors. The factors will be discussed in detail in Chapter 4 with model simulation. In event #4, in the period in which only fogwater was collected (Fig. 2.4a), SO<sub>2</sub> gas phase concentration had no observable increase or decrease, demonstrating the balance between fogwater and gas phase SO<sub>2</sub> concentration.

### **Free S(IV)**

Free S(IV) was measured only during event #2. The rain samples were collected every

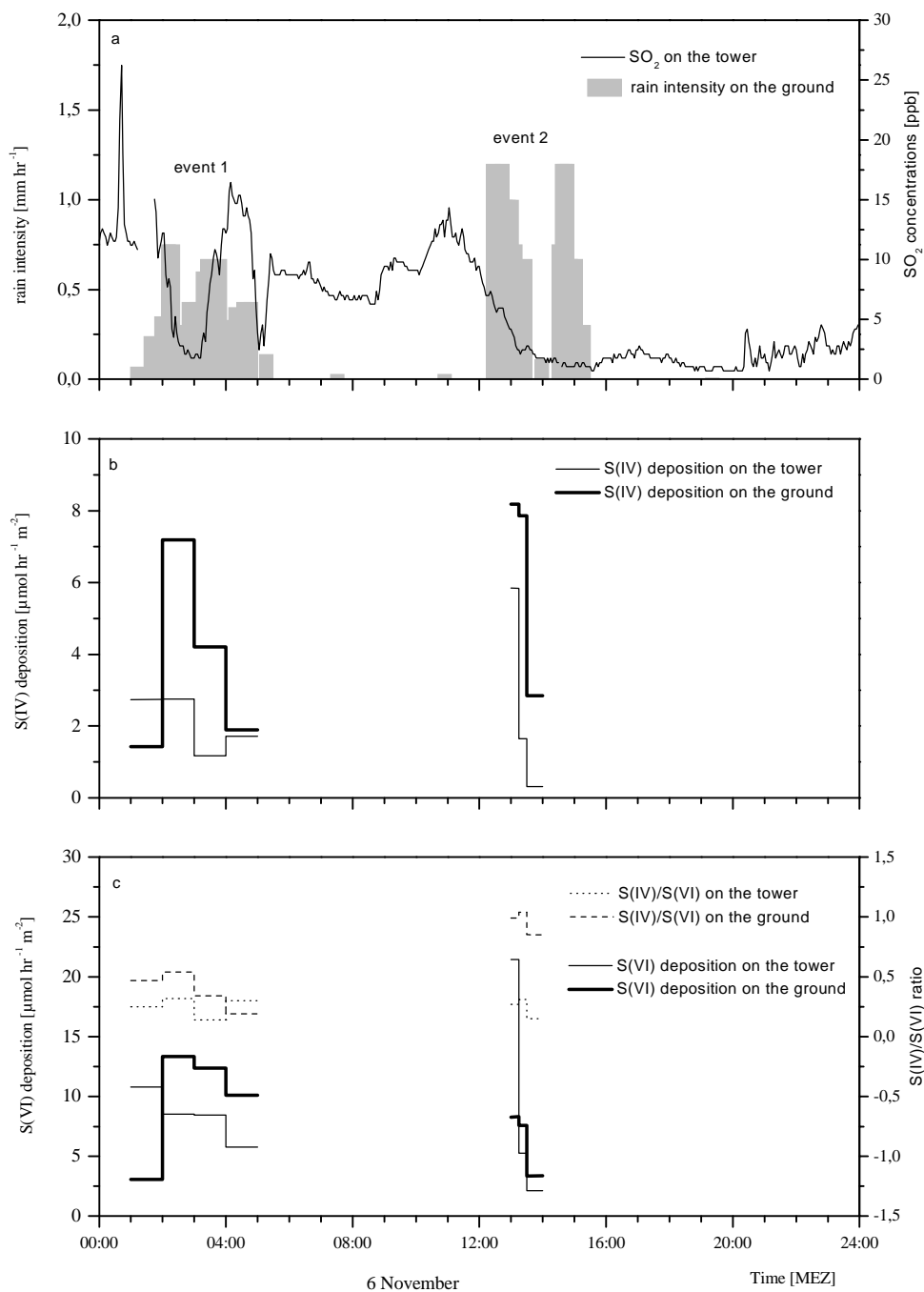


Fig. 2.2. (a) Rain intensity and SO<sub>2</sub>; (b) S(IV) depositions at both levels; (c) S(VI) depositions and S(IV)/S(VI) ratios at both levels during event #1 and #2 at Berlin-Frohnau in November, 1997.

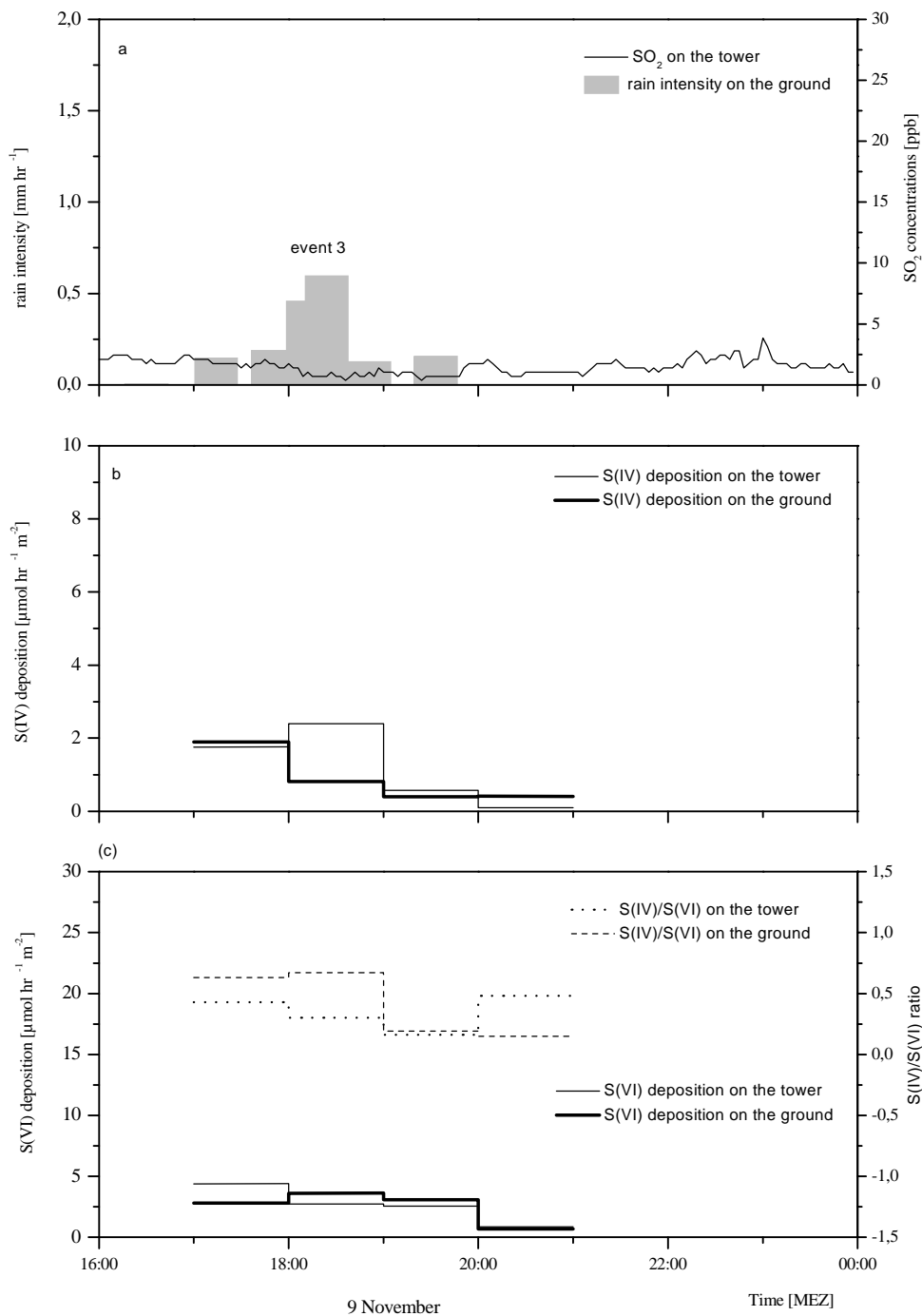


Fig. 2.3. As for Fig. 2.2 but for event #3.

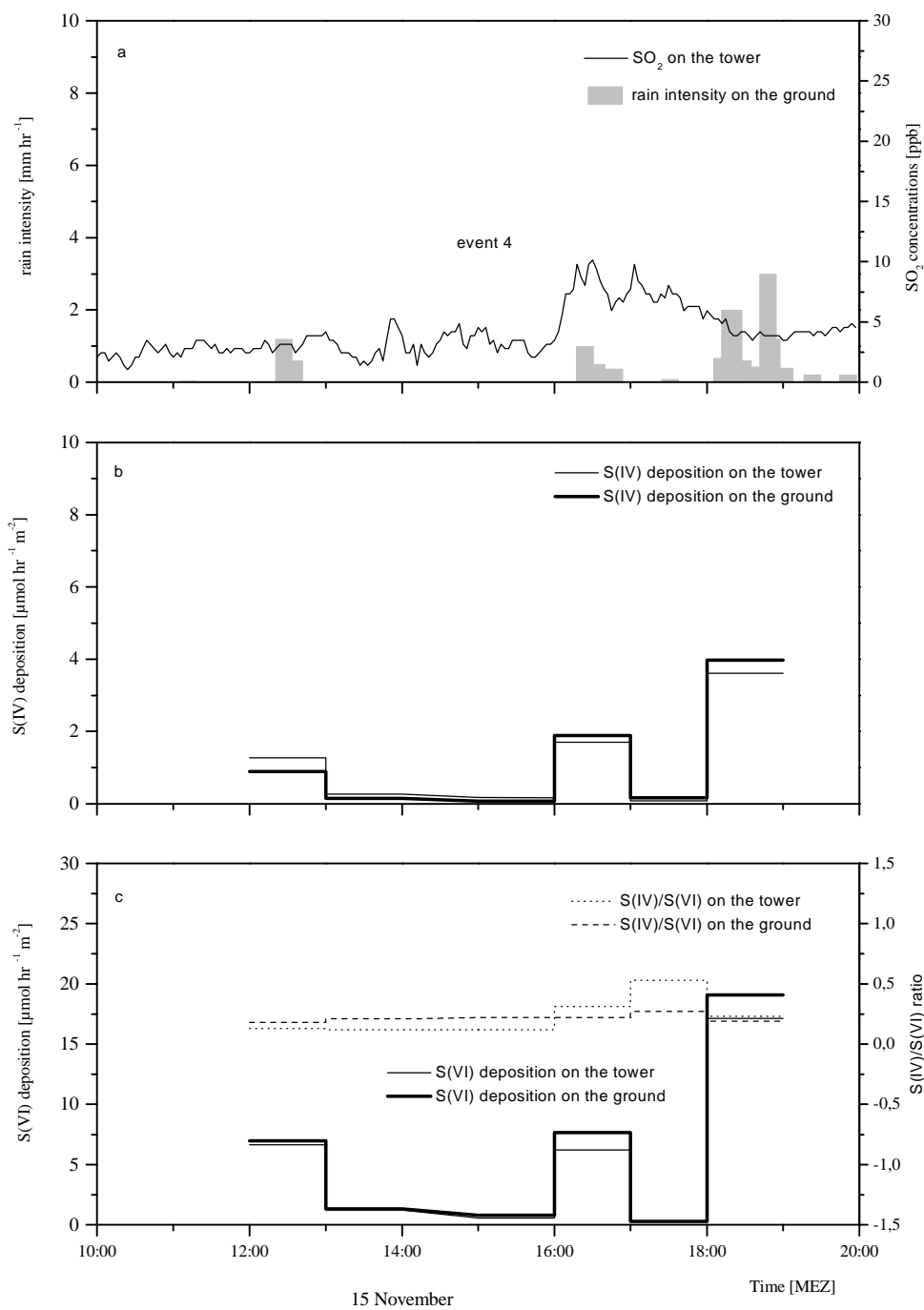


Fig. 2.4. As for Fig. 2.2 but for event #4.



15 or 30 min (depending on rain intensity) between 13:00-14:00 on November 6<sup>th</sup>, 1997 without formaldehyde stabilization. In other periods due to unfavorable sampling time, only automatical collecting of rainwater with stabilization was conducted. The samples we collected in event #2 were measured for free S(IV) with CFCL method just after sampling in the field. Later in our laboratory in Berlin total HMS was measured with IC in those samples. Total HMS is the sum of the original HMS and free S(IV). As original HMS we describe the amount of HMS which can be found in rainwater just before sampling.

Free S(IV) and original HMS in rainwater may stem from in-cloud scavenging as well as sub-cloud scavenging. As mentioned in Chapter 1.2.3, the formation rate of HMS at low pH is very slow and decreases with decreasing pH value. Assuming a gas phase concentration of 1ppb HCHO and a pH value of 5, the lifetime of free S(IV) ions in rainwater is regulated by the rate of HMS formation to be in the order of several hours. Since the falling time of raindrops from cloud base to the ground is normally in the order of several minutes, the formation of HMS in the falling raindrops is negligible at the pH of 5 or less than 5, which is typical of these rain events. With respect to this fact, we can assume that the original HMS found in rainwater mostly came from in-cloud scavenging. On the contrary, free S(IV) is found to be to a large extent originated from sub-cloud scavenging. This may be explained by the following arguments: As the life time of a cloud is relatively long compared with the rate of liquid phase oxidation reactions of SO<sub>2</sub>, and additionally oxidants like H<sub>2</sub>O<sub>2</sub>, ozone and oxygen (with catalyzing metal ions) are always present in the cloud layer (Cape et al., 1999), most of the free S(IV) will be oxidized to sulfate or can react to HMS in the cloud layer before the raindrops fall out of the cloud base. However, the dissolved SO<sub>2</sub> in the falling raindrops will remain mainly as free S(IV) because neither liquid phase oxidation reactions of free S(IV) nor the adduct reaction between free S(IV) and formaldehyde is fast enough to consume free S(IV) in rainwater during the falling period of raindrops.

The concentrations of HMS and free S(IV) in the three rainwater samples from both levels collected in this event are listed in Table 2.4. Original HMS was calculated from the difference between total S(IV) and free S(IV). Original HMS contributes 40%~60% to the total S(IV) in the samples collected on the tower, but only 10~20% in the samples taken on the ground. We do not observe (within the uncertainties) a difference in HMS

for the samples from the ground and the tower levels, whereas the free S(IV) concentration strongly increased with decreasing height. These results suggest that sub-cloud scavenging may be a source of free S(IV) in rainwater on the ground.

Table 2.4. Concentrations of free S(IV) and original HMS in rainwater in event #2

S(IV) ( $\mu\text{mol l}^{-1}$ )		13:00-13:15	13:15-13:30	13:30-14:00
Ground	Free S(IV)	9.29	9.44	8.13
	Total S(IV)	10.83	11.23	9.32
	Original HMS	1.54	1.79	1.19
Tower	Free S(IV)	3.58	1.15	0.62
	Total S(IV)	5.62	2.75	1.44
	Original HMS	2.04	1.60	0.82

### The ratio of S(IV) and total sulfur

Tab. 2.5 shows average values of  $\text{SO}_2$  concentration, pH, rain intensity, concentrations of S(IV) and S(VI) as well as the ratio between S(IV) and total sulfur in the samples taken at the ground level. Cloud base heights, pH of rainwater and raindrop spectrum may all influence the ratio of S(IV) to total sulfur. For example, in event #2 the concentration of  $\text{SO}_2$  was only 2.5ppb, but 49% of sulfur was deposited as S(IV). A possible explanation for this finding is the high cloud base. If the cloud base is higher, the falling distance of raindrops is also higher and raindrops have more time to exchange sulfur compounds with surrounding  $\text{SO}_2$  in the gas phase. If it is true, it supports the idea that washout can significantly contribute to the deposition of sulfite in rainwater.

A higher sulfite content was found in rainwater samples with higher pH values. For example, in event #2 and #3, where very low  $\text{SO}_2$  concentrations were found, the average pH is 4.9, higher than the pH in event #1 and #4 (pH about 4.3). We found that the ratio of S(IV) and total sulfur is also higher in event #2 (49%) and #3 (32%) than in the other two events (27% and 16% respectively). The reason for this difference is the solubility of sulfur dioxide, which increases with increasing pH. Hence, more sulfur dioxide can be dissolved into rainwater at higher pH (see reactions 1.5 and 1.6).

Table 2.5. Gas phase SO<sub>2</sub>, pH, rain intensity, SO<sub>4</sub><sup>2-</sup>, S(IV) and ratio of S(IV)/total sulfur at the ground site (G) during each event.

Event	SO <sub>2</sub> [ppb]	pH tower	Rain intensity [mm hr <sup>-1</sup> ]	S(VI)-G [μmol l <sup>-1</sup> ]	S(IV)-G [μmol l <sup>-1</sup> ]	S(IV)/total Sulfur-G [%]
1	8.8	4.4	0.43	26	10	27
2	2.5	4.9	0.45	11	11	49
3	1.2	4.9	0.20	14	7	32
4	4.5	4.3	0.74	24	5	16

In event #4 (fog), the ratio of S(IV) to total sulfur is only 16%, much lower than that in other events. The most probable reason for the low ratio is the small size of fogdrops. Fog normally has much smaller sizes of droplets than rain droplets and thus also much longer residence time in the air than rain droplets. Therefore, dissolved SO<sub>2</sub> in fog water has enough time to underlie oxidation reactions before the deposition of droplets occur.

#### Gas phase SO<sub>2</sub>, S(IV) deposition and the ratio of S(IV)/total sulfur

From the results presented in Tab. 2.5, we can not draw a direct relationship between SO<sub>2</sub> concentrations and the fractions of S(IV) of total sulfur in rainwater taken on the ground. According to Henry balance, higher SO<sub>2</sub> concentration cause higher S(IV) concentration in the liquid phase. However, the ratio of S(IV) to total sulfur is influenced not only by the concentration of S(IV) but also by the concentration of S(VI). As mentioned above, this ratio is determined by several microphysical and chemical parameters. More data are needed to figure out the relationship between SO<sub>2</sub> and S(IV)/total sulfur ratio statistically. Later in Chapter 4, several tests will be made to discuss the relationship of SO<sub>2</sub> and the ratio between S(IV) and S(VI) with the help of model changing the gas phase concentration of SO<sub>2</sub>.

Sulfite concentration (in μeq l<sup>-1</sup>) is multiplied with rain intensity to show the deposition of sulfite. The difference of sulfite deposition from the tower to the ground is the removal rate of SO<sub>2</sub>. Sulfite depositions in event #1 and #2 have increase from the tower to the ground in most of raining periods (Fig. 2.2b). However, in event #3, the sulfite deposition has less increase or even decrease from the tower to the ground, showing negligible SO<sub>2</sub> removal by raindrops from the tower to the ground (Fig. 2.3b). The possible reasons are the low SO<sub>2</sub> concentration (1.2 ppb in average) and the high

H<sub>2</sub>O<sub>2</sub> concentration on the tower level (about 3 μmol l<sup>-1</sup> in average) in this event. In other events very low H<sub>2</sub>O<sub>2</sub> concentrations (in the order of 0.1 μmol l<sup>-1</sup>) have been found. The excess oxidant (H<sub>2</sub>O<sub>2</sub>) in event #3 compared to SO<sub>2</sub> in the rainwater hinder the accumulation of S(IV). In fogwater (event #4) sulfite deposition has negligible difference vertically (Fig. 2.4b).

In all events sulfate deposition (in μeqhr<sup>-1</sup>m<sup>-2</sup>) on the ground was greater than that on the tower. The increase of sulfate deposition indicates the production of sulfate in the falling period of raindrops from the tower to the ground.

### Aerosol

The washout of aerosol particles by raindrops in the beginning of each event can be clearly observed (Tab. 2.6). All ions in the aerosol samples decreased to different extents. In event #2 and #3 less amounts of ions were measured in the aerosol samples

Table 2.6. Ionic aerosol concentration at tower level (in neq m<sup>-3</sup>)

Event	Rain event *	TSP [μg m <sup>-3</sup> ]	Cl	NO <sub>3</sub> <sup>-</sup>	SO <sub>4</sub> <sup>2-</sup>	Na <sup>+</sup>	NH <sub>4</sub> <sup>+</sup>	K <sup>+</sup>	Ca <sup>2+</sup>	Mg <sup>2+</sup>
1	Before	61.9	10.4	227.6	173.3	200.4	165.6	34.9	6.0	1.7
	During	35.8	8.9	130.3	136.4	233.3	17.5	22.5	2.5	0.8
	After	59.4	11.0	200.2	200.4	206.1	173.9	37.7	8.5	1.7
2	Before	77.8	18.3	216.8	262.7	203.5	231.1	45.1	12.0	2.6
	During	30.2	7.0	101.5	97.5	190.9	3.9	20.8	1.5	0.0
	After	---	13.0	79.7	111.0	163.0	0	11.0	1.5	12.5
3	Before	8.9	13.0	30.5	54.0	77.8	0	3.6	0	0
	During	10.0	9.9	18.5	40.2	52.7	0.0	2.6	0.0	0.0
	After	10.9	12.1	23.4	44.0	56.5	0	2.3	0	0
4	Before	31.1	14.9	223.1	117.6	287.0	0	19.2	3.6	0.8
	During	23.9	20.3	153.6	118.4	232.8	0.0	16.5	---	0.0
	After	22.1	31.3	92.6	109.8	170.4	0	11.5	2.0	0

\* During the rain event we collected only interstitial aerosol particulates.

after rain event than before rain event. This is a sign for the lack of entrainment of new aerosol particles after their washout by rainwater. However after rain event #1, the aerosol ion contents are approximately in the same level of those before rain event began. It means, there was an entrainment of new aerosol particulates after rain event #1. In event #4, Na<sup>+</sup> and NO<sub>3</sub><sup>-</sup> decreased significantly after the rain event, while the

concentrations of  $\text{SO}_4^{2-}$  remained the same. This indicates that sulfate was produced during the fog event and hence could compensate the scavenged sulfate in aerosols.

### Seasalt characteristics

The molar ratio of  $\text{Na}^+/\text{Cl}^-$  in rainwater on the ground varies between 0.7 and 1.3 (average  $1.0 \pm 0.1$ ), in good agreement with the same ratio found in remote European continental sites (Möller, 1990). It is somewhat larger than that in bulk seawater (0.86) as a result of a separation process between  $\text{Na}^+$  and  $\text{Cl}^-$  during the transport from ocean to continent. In contrast to rainwater, particulate matter shows an  $\text{Na}^+/\text{Cl}^-$  ratio between 3.5 and 16.8 (average  $12 \pm 5$ ). Assuming that there was no excess sodium, this figure suggests a strong loss of  $\text{Cl}^-$  ion (evaporated as gaseous HCl) similar to that found in marine fine aerosols. Since the concentrations of neutralizing ions like  $\text{NH}_4^+$  and  $\text{Ca}^{2+}$  were extremely low in particulates, we argue that the “pure” man-made particulate matter must be very acid, i.e. the missing cation in free electroneutrality budget is  $\text{H}^+$ . If we put the lost  $\text{Cl}^-$  (expressed as  $\Delta = [\text{NO}_3^-] + [\text{SO}_4^{2-}]_{\text{excess}} - [\text{NH}_4^+] - [\text{Ca}^{2+}] - [\text{K}^+]$ ) into consideration, we get almost identical ratios of  $\text{Na}^+/\text{Cl}^-$  in rainwater and aerosol (Tab. 2.7). Excess sulfate has been calculated based on the seawater  $\text{Na}^+/\text{SO}_4^{2-}$  ratio (seawater sulfate contributes around 20% to total sulfate in total suspended particle).

Table 2.7.  $\text{Na}^+/\text{Cl}^-$  ratio in rainwater and in aerosol particles

Ratio/Event	1	2	3	4
$\text{Na}^+ / (\Delta + \text{Cl}^-)$ in aerosol	1.15	1.23	0.86	0.98
$\text{Na}^+/\text{Cl}^-$ in rainwater	1.27	1.14	0.65	1.02

In contrast to the particulate phase, seasalt sulfate only plays a minor role in rainwater on the ground (0.6-2%). This suggests that the origin of sulfate in rainwater might be droplet phase itself via  $\text{SO}_2$  scavenging and subsequent oxidation.

### Ammonium

Ammonium shows the largest difference in concentration between rainwater (15% of all ion measured) and particulate matter (1% of all ion measured). This suggests that  $\text{NH}_4^+$

in rain- and cloudwater predominantly stems from in-cloud scavenging ( $(\text{NH}_4)_x\text{H}_y\text{SO}_4$ ) from long-range transport. On the other hand,  $\text{NH}_4^+$  in particulate matter is the only ion, which is almost completely removed during rain. The molar concentration ratio between aerosol collected during the rain event and before the rain event is 0.06 (note that for event #3 and #4 no detectable amounts of ammonium have been found in particulate matter). This ratio is about 0.6 for  $\text{NO}_3^-$  and  $\text{SO}_4^{2-}$  whereas for seasalt it is close to unit ( $\text{Na}^+$ : 0.92;  $\text{Cl}^-$ : 0.81).

### **NO<sub>x</sub> and Nitrate**

Similar to sulfate, nitrate is the final oxidation product from primary emitted NO. In contrast to  $\text{SO}_2$ , which is oxidized mainly within the aqueous phase, NO is only oxidized in the gas phase, finally into  $\text{HNO}_3$  via different pathways. Nitrate also can be formed heterogeneously via scavenging of  $\text{NO}_3$  and  $\text{N}_2\text{O}_5$ . Recently it has been shown that  $\text{NO}_2$  react on aqueous surface forming  $\text{HNO}_2$  and  $\text{HNO}_3$  (Acker et al., 1999). The significantly high concentration of nitrate in event #4 (fog) related to other ions (the molar ratio  $\text{NO}_3^-/\text{SO}_4^{2-}$  is 3.1 compared to 1.0-1.2 in other rain events, whereas during event #4 the ratio in the particulate matter is 0.9 compared to 0.3-0.6 in other events) might support the idea of heterogeneous nitrate formation during the urban fog and rain period. Also the gaseous  $\text{NO}_2$  concentration was the highest (14.6 ppb) during event #4 (3.2-10.7 ppb for other events).

### **Sulfite and sulfate**

As already shown, the concentrations of S(IV) increase from in the samples taken on the tower to in the samples taken on the ground. With respect to a “dilution factor” of about 1.8 from the tower to the ground (based on nitrate and ammonium), the “true” S(IV) increase might be even higher if we assume that the dissolution of  $\text{SO}_2$  into different raindrops of different sizes is the same. From Tab. 2.8 and Tab. 2.3 it follows (again excluding event #4) that the S(IV) ground to tower ratio is 1.7 on average (1.2-2.7) and this may be “corrected” by the dilution factor 1.8 into 3 ( $1.7 \times 1.8$ ). Sulfate concentration in rainwater on the ground is the sum of sulfate in rainwater on the tower divided by the dilution factor of 1.8 (on average  $10.5 \mu\text{mol l}^{-1}$  sulfate on the ground) and sulfate produced by S(IV) oxidation in raindrops from the tower to the ground (on average

6.5  $\mu\text{mol l}^{-1}$ ). The ozone concentration was between 23 and 33 ppb during the events #1, #2 and #3. 30 ppb  $\text{O}_3$  leads to a S(IV) oxidation rate  $R/[\text{S(IV)}]$  of  $2.2 \times 10^{-3} \text{ s}^{-1}$  for pH 4.7 (mean pH of rainwater during the experiment) using the rate law by Maahs (1983). Assuming 1 min for falling raindrops from tower to ground, 13% of S(IV) can be transformed into S(VI) via ozone at pH 4.7. Additionally we have to regard the catalytic (via metal ions) S(IV) oxidation and the oxidation via  $\text{H}_2\text{O}_2$  (despite its very low aqueous concentration in the order of 0.1  $\mu\text{mol l}^{-1}$ ). Assuming that on average 40% of S(IV) may be oxidized before reaching the ground, this can compensate for the sulfate production of about 6.5  $\mu\text{mol l}^{-1}$  we mentioned above.

Based on analytical figures (Tab. 2.5) the fraction of S(IV) in total sulfur in rainwater on the ground is between 13 % and 51 % with an average (excluding event #4) of 36%. Taking into account the argumentation that S(IV) is partly oxidized during rain fall, this figure increases up to 60% and represents the percentage of sulfur in wet deposition that has never transformed into sulfate aerosol in the atmosphere. In summary, we argue that  $\text{SO}_2$  emitted into the sub-cloud layer will be mainly wet scavenged in the form of S(IV) and that the rate depends on frequency of precipitation occurrence.

Table 2.8. Molar concentration ratios in rainwater

Event	S(IV)/ G/T	S(IV)/ S(VI) G	S(IV)/ S(VI) T	S(IV)/ $\text{NO}_3^-$ G	S(IV)/ $\text{NO}_3^-$ T	$\text{NO}_3^-$ / S(VI) G	$\text{NO}_3^-$ / S(VI) T	$\text{NO}_3^-$ / $\text{NH}_4^+$ G	$\text{NO}_3^-$ / $\text{NH}_4^+$ T
1	1.6	0.38	0.25	0.35	0.14	1.1	1.8	1.5	2.1
2	2.7	0.96	0.26	0.94	0.16	1.0	1.6	1.0	1.3
3	1.2	0.48	0.33	0.38	0.14	1.2	2.4	0.8	0.9
4	1.0	0.20	0.22	0.06	0.05	3.1	4.2	1.6	1.7

T:tower      G:ground

## 2.5 Conclusion

S(IV) was measured simultaneously in rainwater on a tower at the 324 m level and on the ground. Measured S(IV) concentrations in rainwater were in the range of 1.44 to 27.36  $\mu\text{mol l}^{-1}$ . This measurement suggests that S(IV) is an important form of sulfur in fresh rainwater. On average about 36 % (13-51 %) of total sulfur in rainwater on the ground was in the form of S(IV). Taking into account the dilution effect, about 60% of wet deposited S(IV) came from sub-cloud scavenging below the 324m level. This is

fully consistent with the theoretical figures (Fig. 1.1) suggesting a 40% share of S(IV) to total wet sulfur deposition.

As the average cloud base height was about 1500m, we can estimate that the raindrops falling out of the cloud base would pass through a 4 times longer distance than the height of the tower. This means, that the efficiency of sub-cloud scavenging must be even greater than our estimation from the measurement from the two levels.

Our findings support the idea that the transformation of SO<sub>2</sub> to sulfate in rainwater is very limited. Moreover, the question how reduced sulfur in the form S(IV) may influence the redox potential and acidity budget in soils and water might be a question again.



## Chapter 3

# Case studies of S(IV) to S(VI) ratio in cloud events from Brocken experiment

### 3.1 Introduction

According to satellite observations, about 50% of the earth are covered by clouds. Most of them are in the troposphere. Consequently cloud processes play an important role in the tropospheric sulfur cycle. The lifetime of clouds is much longer than that of precipitation. Therefore the available time for chemical reactions in cloud droplets and for mass transfer between gas and liquid phase within the cloud layer is much longer than in falling raindrops. Earlier measurements of S(IV) (Tab. 1) have shown that the concentration of S(IV) in cloudwater is much more variable than in rainwater. In Chapter 2 we explained that S(IV) in rainwater dominantly stems from sub-cloud scavenging of SO<sub>2</sub> and preferentially is in form of free sulfite. In contrast, S(IV) in cloudwater is mainly found to be in form of HMS (Munger, 1984, 1986; Rao et al., 1995; Lammel, 1996).

Like precipitation, clouds are a sink for gas phase SO<sub>2</sub>. While precipitation removes SO<sub>2</sub> out of the atmosphere, nonprecipitating clouds act as a medium for the conversion of SO<sub>2</sub> to sulfate aerosols. The sulfur chemistry in cloudwater is strongly influenced by different factors like meteorology, microphysical parameters, the pH value and other chemical species. Different weather situations and air mass transport can vary significantly the concentrations of the trace species at the same measuring site (Acker et al., 1998a). Many measurements have shown that microphysical parameters of cloud droplets are spatially and temporally different during a cloud event (Pruppacher and Klett, 1997). For example, the liquid water content (LWC), which is a key indicator of cloud processes varies with height above cloud base and has strong temporal variation

during a cloud event (Möller et al., 1996b). Additionally, the concentrations of metal ions in cloudwater (which catalyze the oxidation reactions of S(IV)) and other trace gases (like  $\text{NH}_3$ , which buffers the acidity of cloudwater) also may influence the sulfate formation in cloudwater.

The aim of this chapter is to study the ratio of S(IV)/S(VI) in clouds in consideration of other chemical components (e.g.  $\text{SO}_2$ ,  $\text{H}_2\text{O}_2$ , ozone and  $\text{H}^+$ ) and cloud microphysical and meteorological parameters (e.g. LWC, cloud base ). Additionally, the origin of the air masses is included into the analysis (72h back trajectories calculated according to the model from the Free University of Berlin).

### **3.2 Measurement site**

The measurement site Mt. Brocken ( $51.80^\circ\text{N}$ ;  $10.67^\circ\text{E}$ ) lies 1142m above sea level and is located northeastly in the Harz mountains. It is the highest mountain in the north of Germany. Surrounded by lowlands Mt. Brocken is mainly covered by forest, with a tree free plateau (diameter about 500m) on the summit. As early as in 1895, a meteorological station was built on the Brocken summit and has been in operation until now. Since around Brocken mountain are nature parks, there is no industrial source of pollutants except for some fossil fuel combustion of household in villages around the site. The influence of this kind of local sources on Brocken summit is quite low except for some orographical transportation cases which will be discussed in chapter 3.4.

As touristic attractions, a regular steamtrain (which has been in operation since 1899) comes up to the summit every hour on the daytime. The influence of coal combustion from steamtrain on our trace gas measurements is already known from earlier experiments and will be discussed in chapter 3.4 together with  $\text{SO}_2$  gas phase concentrations.

The nearest large cities to Harz mountains are Magdeburg (80 km northeastly from Brocken) and Hannover (100 km northwesterly from Brocken). Northerly from Brocken (in 50 km distance) is a busy freeway from Berlin to Hannover, westerly from Brocken (in 35 km distance) is a freeway between Hannover and Frankfurt.

A climatological statistic was made on the Brocken station based on the meteorological data from DWD (Deutscher Wetterdienst) in the time period of 1967-1991 (Östreich, 1995). A part of the result is shown in Tab. 3.1. The meteorological

parameters were measured during the frostfree period (April-October). The station at Mt. Brocken is also characterized by a yearly short sunshine duration (1371 hours per year) and high occurrence of cloud (40%-50% station in cloud in frostfree periods) (Acker et al., 1995a). The duration of cloud events range from less than half an hour to several days. The yearly average (only during frost free period) liquid water content ranges between 250 and 360 mg m<sup>-3</sup> (1991-1998). In summary, Mt. Brocken is ideal for air and cloud chemical measurements.

Tab. 3.1. Average values of the temperature, pressure, cloud coverage and amount of precipitation based on the statistics from 1967-1991 (April-October)

	Temperature °C	Pressure hpa	Cloud coverage degree (eighths)	Yearly amount of precipitation (min→max) mm
1967-1991	6.9±0.7	884.7±1.0	6.1±0.3	888.0 (686.1→1089.9)

The set up of a long-time measurement station on the Brocken summit began in 1990 and a long-time cloud chemistry program has been in operation since 1991 by our institute (Wieprecht et al., 1995; Möller et al., 1996b; Acker et al., 1998a, 1998b). Several cloud chemistry campaigns were carried out on Brocken station, e.g. EUROTRAC-GCE (Ground-based Cloud Experiments as part of the large-scale European research effort EUROTRAC), SANA (Scientific Accompanying Program for Clean-up the Atmosphere over the New Federal countries). The aim of SANA program is to investigate cloud chemistry in the background of drastic decrease of sulfur emission in the former East Germany.

According to the statistical studies mentioned above, the dominant winds on the Brocken summit in frostfree periods are southwest and west winds, the dominant cloud types on Mt. Brocken are stratocumulus (37.9%) and stratocumulus with cumulus clouds (31.6%). The data are based on hourly performed cloud observations from DWD at Mt. Brocken and at Braunlage (Braunlage (610m a.s.l.) lies 8km southerly from Mt. Brocken). Statistics from April 3<sup>rd</sup> to November 6<sup>th</sup>, 1996 show that 60% of all cloud samples (representing more than 90% of all cloud events that occurred in this period) are from non-precipitating clouds (Acker et al., 1998b). Although the surface

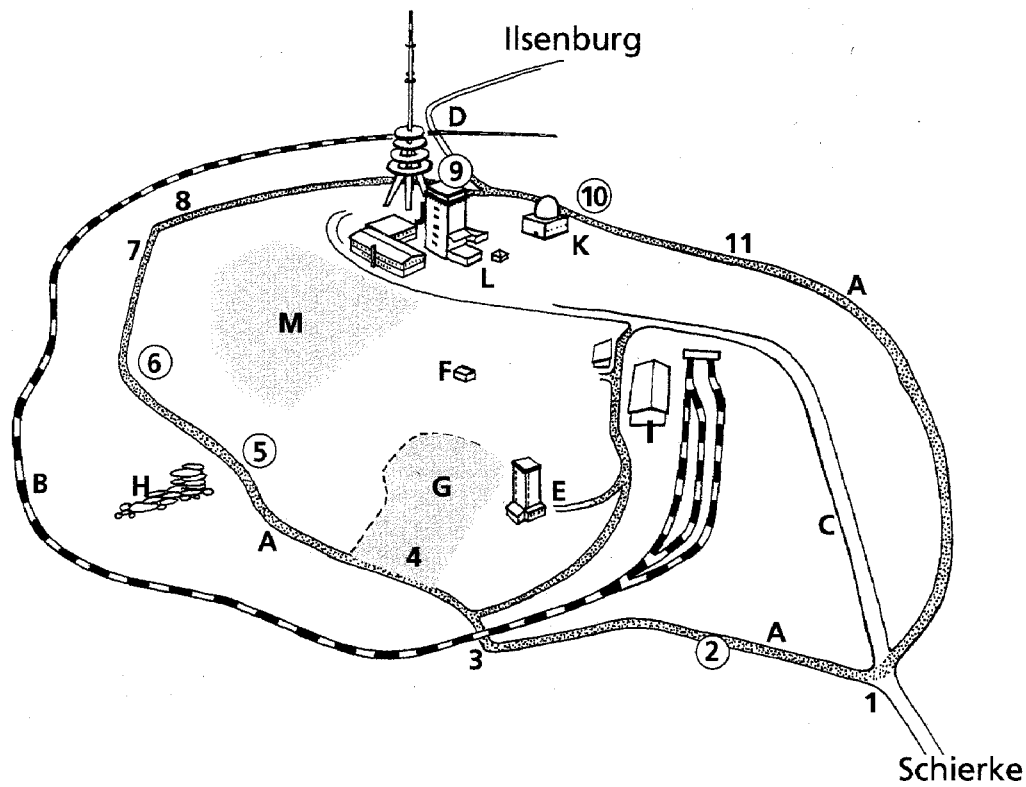


Fig. 3.1a. A schematical description of the plateau on the summit of Mt. Brocken.  
F: our measurement station.  
E: meteorological station.  
I: touristical steamtrain station.

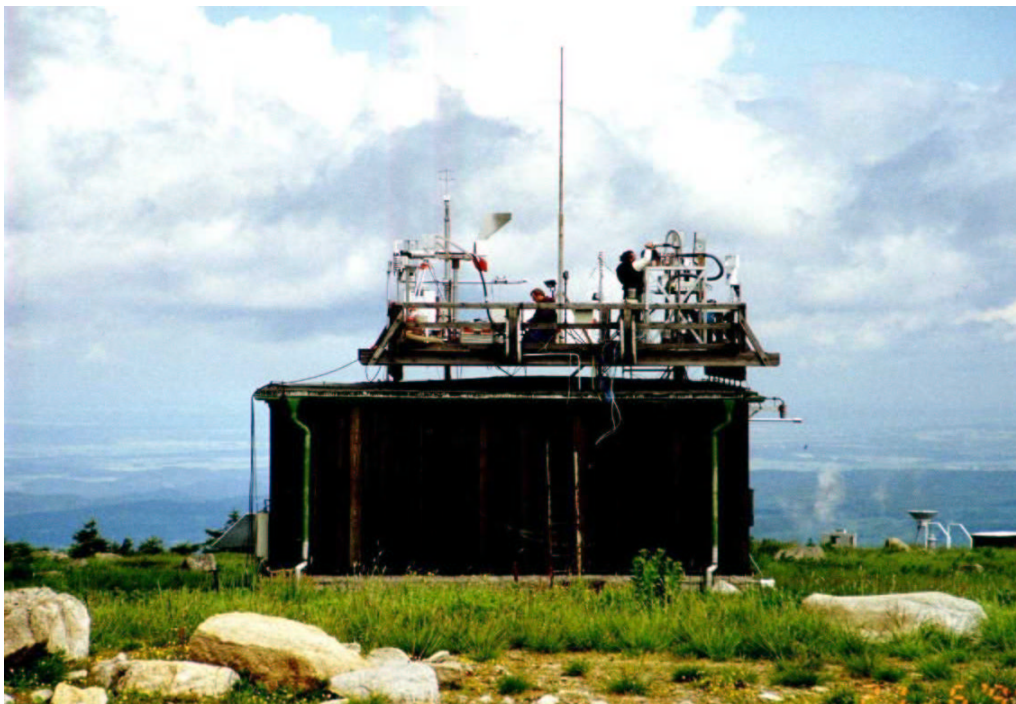


Fig. 3.1b. A view of our measurement station (F in Fig. 3.1a)

wind in the lower Harz region is strongly influenced by the mountains, the wind field at the Brocken summit itself is relatively uninfluenced and represents the predominant low tropospheric wind.

The measurement station consists of a small house with a platform roof about five meter above the ground, where all meteorological, cloud physical and sampling devices are installed. During each campaign an additional mobile system was used for trace gas measurements.

### 3.3 Experimental

During the campaign from September 23<sup>rd</sup> to October 8<sup>th</sup>, 1998 we measured a broad spectrum of meteorological and microphysical parameters and chemical constituents (see Tab. 3.2).

Cloudwater was collected with a passive string collector (ASRC-type). The impact efficiency for this type of passive cloud-water collectors which collects droplets onto 0.4 mm Teflon wires string between two circular disks depends on ambient wind (Mohnen, 1989). One string collector was connected with an automatic sampling unit (ISCO 3700 sampler), which contains 24 polyethylene sample bottles (1liter). In each bottle 10 ml formaldehyde solution ( $6.5 \text{ mmol l}^{-1}$ ) were filled to prevent S(IV) from oxidation. Cloudwater samples were collected every 30 or 60 minutes depending on the LWC of the cloud. The second string collector was used to collect 15 minutes samples (sometimes more than 15min to get enough volume of cloudwater) without stabilization by formaldehyde. All these samples were stored in a refrigerator for further analysis in the laboratory in Berlin after the measurement period.

A gas-sampling system was developed for the continuous measurement of gas phase  $\text{HNO}_2$  and  $\text{HNO}_3$ . The gas-sampling system used a wet denuder technique and was connected with an ionchromatograph to monitor nitrite and nitrate in the field (Acker et al., 1999). During cloud events cloudwater was separated from interstitial air by a one-stage active cloudwater collector (winkler type) in front of the wet denuder system. The interstitial air passed the denuder and all soluble gases were absorbed into the water film. At the end of the denuder a filter was attached which collected aerosol particles in the air (interstitial aerosols). The filters were analyzed for chemical compositions later in the laboratory in Berlin. On October 8<sup>th</sup> a two level cloudwater sampler (Wieprecht et

al., 1999) was used to collect clouddrops in the ranges of 5-10 $\mu$ m and >10 $\mu$ m. In combination with impactors interstitial aerosol particles were also collected.

Table 3.2. Summary of the parameters measured in the experiment at Mt. Brocken from September 23<sup>rd</sup> to October 8<sup>th</sup>, 1998.

Parameters	Instrumentation	Measurement frequency and notes
wind speed, wind direction, temperature, pressure, relative humidity	Thies-system	Continuously (5s)
Cloud type, cloud coverage and cloud base	Observer in Schierke (day-time)	Hourly
Cloud base	Ceilometer CT25K	Continuously
Liquid water content	Gerber PVM 100/300	Continuously (5s)
Cloud droplet spectrum	FSSP 100	
Chemical constituents of aerosols	Filter pack after wet denuder; analysis with ion chromatography (IC)	4h
Ion concentrations of cloudwater	Passive/active collectors with IC analysis	15min or 1h
pH of cloudwater	WTW pH 196 plus Mettler Toledo InLab 422 Electrode	Measured shortly after sampling
Conductivity of cloudwater	WTW LF 196 plus Philips PW 9513 electrode	
Free S(IV) in cloudwater	CFCL	
H <sub>2</sub> O <sub>2</sub> in cloudwater	AL-1002	
HMS in cloudwater	IC	30min or 1h
SO <sub>2</sub>	TEI 43S	Continuously (5s)
O <sub>3</sub>	Dasibi 1108 RS	
Nox	Tecan CLD 770Alpppt	
H <sub>2</sub> O <sub>2</sub>	AL-1002	
Gaseous HNO <sub>3</sub> and HNO <sub>2</sub>	Wetdenuder in combination with IC	
72-h backward trajectories	every 10 min from the station level	FU Berlin

Direct optical cloud base measurements were carried out with a Ceilometer located at Schierke (613 a.s.l.), 4.5 km in horizontal direction southeasterly from Brocken summit. Visual cloud observations were also done every hour from Schierke (by Max Nitschke, private communication). Continuous cloud base height data from Ceilometer

measurements were available from September 29<sup>th</sup> 10:00. Visual optical observation of cloud base height from Schierke was used for the period between September 28<sup>th</sup>, 14:00 and 29<sup>th</sup>, 10:00, but only in day time. To measure the droplet size and number distribution, a FSSP was used. The FSSP was running from September 30<sup>th</sup> to October 8<sup>th</sup>, however, the data is available only for October 8<sup>th</sup>.

More information for the individual principles of measurement methods and instruments can be found in Appendix.

### **3.4 Results and discussions**

153 unstabilized cloudwater samples and 128 stabilized cloudwater samples were collected. In addition to the data set from the campaign, a long-time continuously running cloud chemistry program (see in chapter 3.2) provides us measurements of ion concentrations, pH and conductivity of 1h cloudwater samples also during the period of the campaign.

A continuous cloud coverage at Mt. Brocken was observed from September 28<sup>th</sup> 14:00 to October 8<sup>th</sup> 18:00 with a short break in the afternoon of September 29<sup>th</sup>. Weather conditions changed several times during this period. For example, for the time period from October 2<sup>nd</sup> to October 4<sup>th</sup> and on October 6<sup>th</sup> we had to interrupt our measurements because temperatures fell below frost point. So we divided the whole cloudy period into four cloud events for detailed result discussion:

Event 1: September 28<sup>th</sup>, 1998, 14:00 to September 29<sup>th</sup>, 1998, 14:00;

Event 2: September 29<sup>th</sup>, 1998, 22:00 to October 01<sup>st</sup>, 1998, 18:00;

Event 3: October 05<sup>th</sup>, 1998, 10:00 to October 05<sup>th</sup>, 1998, 24:00;

Event 4: October 07<sup>th</sup>, 1998 8:00 to October 08<sup>th</sup>, 1998, 18:00.

In each event cloud base height varies with the evolution of the cloud event. By means of Ceilometer measurements, we can follow the variation of cloud base height in 15s time step. Caused by the ascending and descending of the cloud base in each event, our measurement site can be found in different heights above cloud base which we can calculate according to Ceilometer or observation data. This is very helpful for us to discuss vertical profiles of LWC, ion concentrations and S(IV)/S(VI) ratio in cloudwater.

**Event #1**

Time: September 28<sup>th</sup>, 1998, 14:00 — September 29<sup>th</sup>, 1998, 14:00

**Weather situation and back trajectories**

The first cloud event of our campaign on the Brocken station started in the afternoon of September 28<sup>th</sup>. A week of sunny days ended. On September 28<sup>th</sup> a region of low pressure over middle-europe had shifted in the eastern direction during the last 24h.

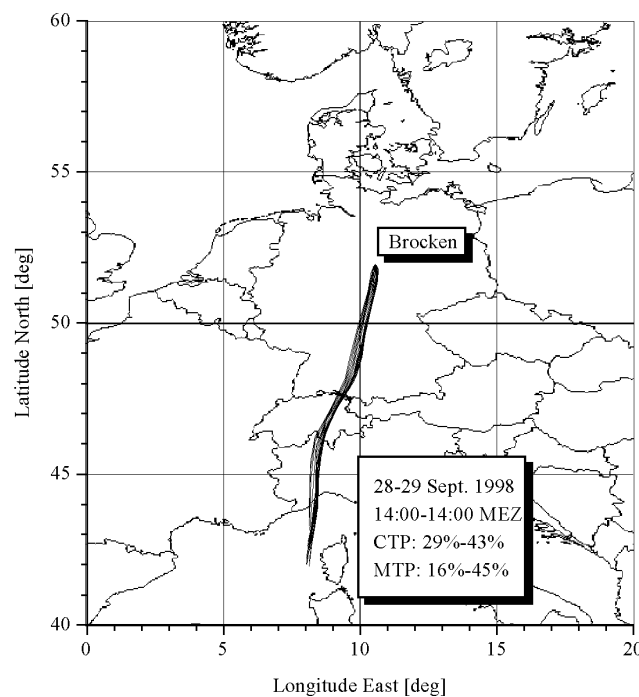


Fig. 3.2. 72h back trajectories during event #1.

CTP: the percentage of air mass transport inside clouds.

MTP: the percentage of air mass transport in side mixing layer.

The occlusion separated dry and warm continental air in the northeast from cool maritime air in the other parts of Germany. Mt. Brocken was located in the region of warm and humid maritime air. On September 29<sup>th</sup> Germany was situated under a weak high trough (from 500hpa map), which brought rain and storm to the northern half of Germany. However, at Mt. Brocken no measurable rain was observed. Middle-Europe was still under control of relatively moderate maritime air, the temperature on the Brocken was almost constant, about 8°C. The observed cloud types were cumulus congestus, cumulus mediocris and cumulus humilis.



Back trajectories from September 28<sup>th</sup>, 14:00 to September 29<sup>th</sup>, 14:00 showed that the air mass stemmed from Mediterranean sea and was transported to Brocken station from SSW direction, traversing over Northwest Italy, Alps in Switzerland and Southwest part of Germany (Fig. 3.2). Because of the relative long transport distance in the past 72 hours and of the small deviation of the single trajectories (1h mean) from the mean transport pathway of the whole event, we can conclude that the air mass was transported relatively fast. No special industrial areas were on the way of air mass transportation.

### **LWC and cloud base height**

Fig. 3.3a shows the temporal variation of LWC (in  $\text{mg m}^{-3}$ ) together with cloud base height and the height of Brocken summit above sea level. In the first 6 hours of the cloud event LWC increased continuously from 0 to  $800\text{mg m}^{-3}$ . In the same period cloud base descended from 1300m to 900m. The anti-correlation of LWC and cloud base height can be clearly observed. LWC increases with increasing position of the measurement station relative to the cloud base. During the night of September 28<sup>th</sup> (after 20:00) a continuous decrease of LWC was observed. Because neither Ceilometer measurement nor optical observation data of cloud base are available during the period from September 28<sup>th</sup>, 20:00 to September 29<sup>th</sup>, 5:00, the cloud base height during this period is not known. We can only assume, based on cloud statistical investigations over longer time (Möller et al., 1995b), that at an LWC of about  $300\text{ mg m}^{-3}$  and cumulous cloud type the altitude of measurement station above cloud base is  $200\pm 50\text{m}$ . On September 29<sup>th</sup>, as the cloud slowly dissipated, LWC decreased but varied strongly. Cloud base height changed from about 900m to more than 1200m.

### **ion concentrations**

Fig. 3.3b and 3.3c present the temporal variation of the main ions of the cloudwater samples. We listed the measured ion concentrations into the unit  $\mu\text{eq m}^{-3}$ , which means that the ion concentrations were multiplied with LWC. So we got the variation of soluted ion amounts in cubic meter air volume. Thus the concentrations are independent of LWC. The main ions  $\text{NH}_4^+$ ,  $\text{NO}_3^-$  and  $\text{SO}_4^{2-}$  increased slightly from 14:50 to 16:30 on September 28<sup>th</sup> and then decreased with increasing LWC. During a

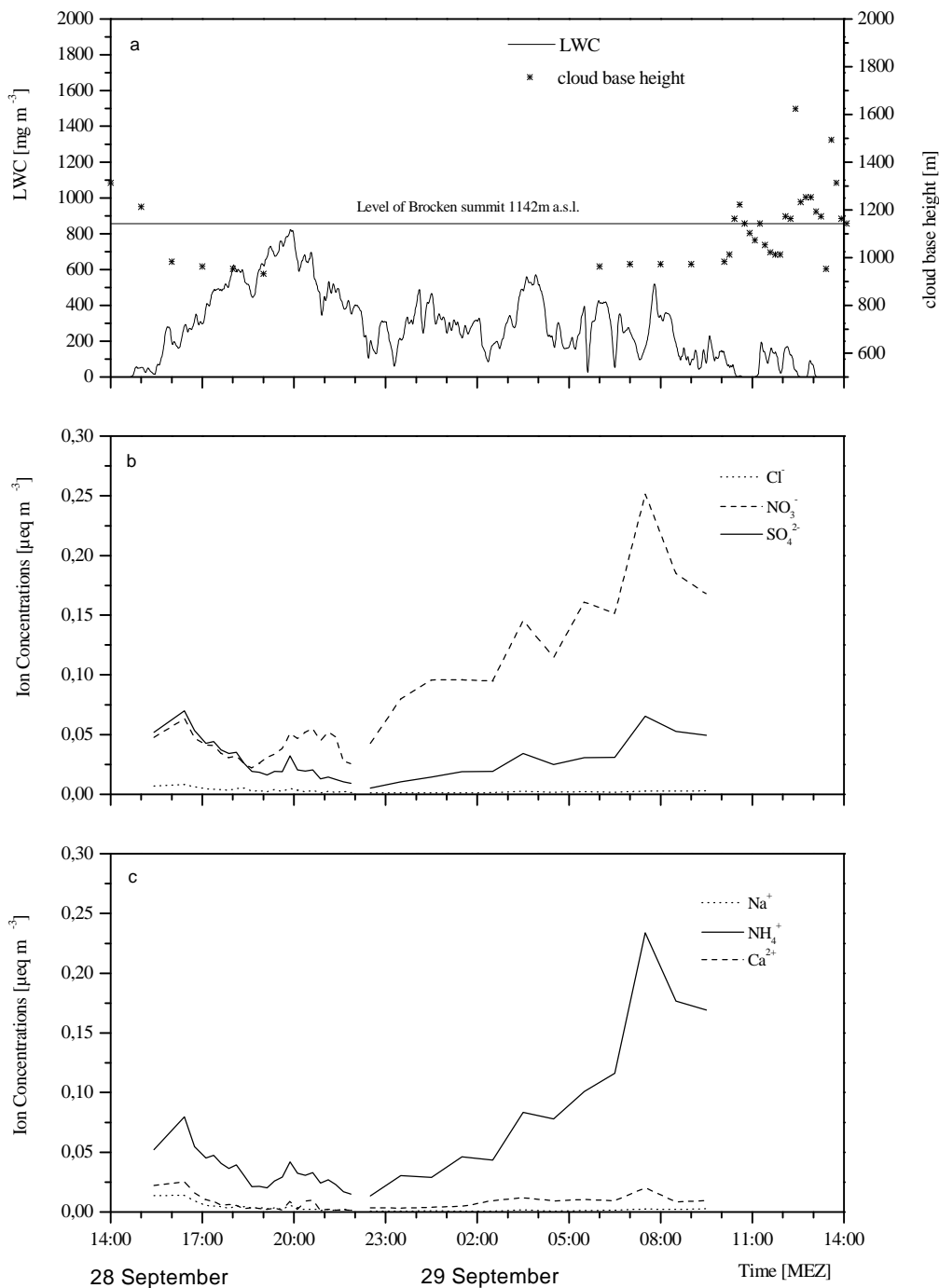


Fig. 3.3. (a) the variation of LWC and cloud base height; (b) main cations and (c) anions of sampled cloudwater during event #1 at the Brocken station. All ions are multiplied with LWC.

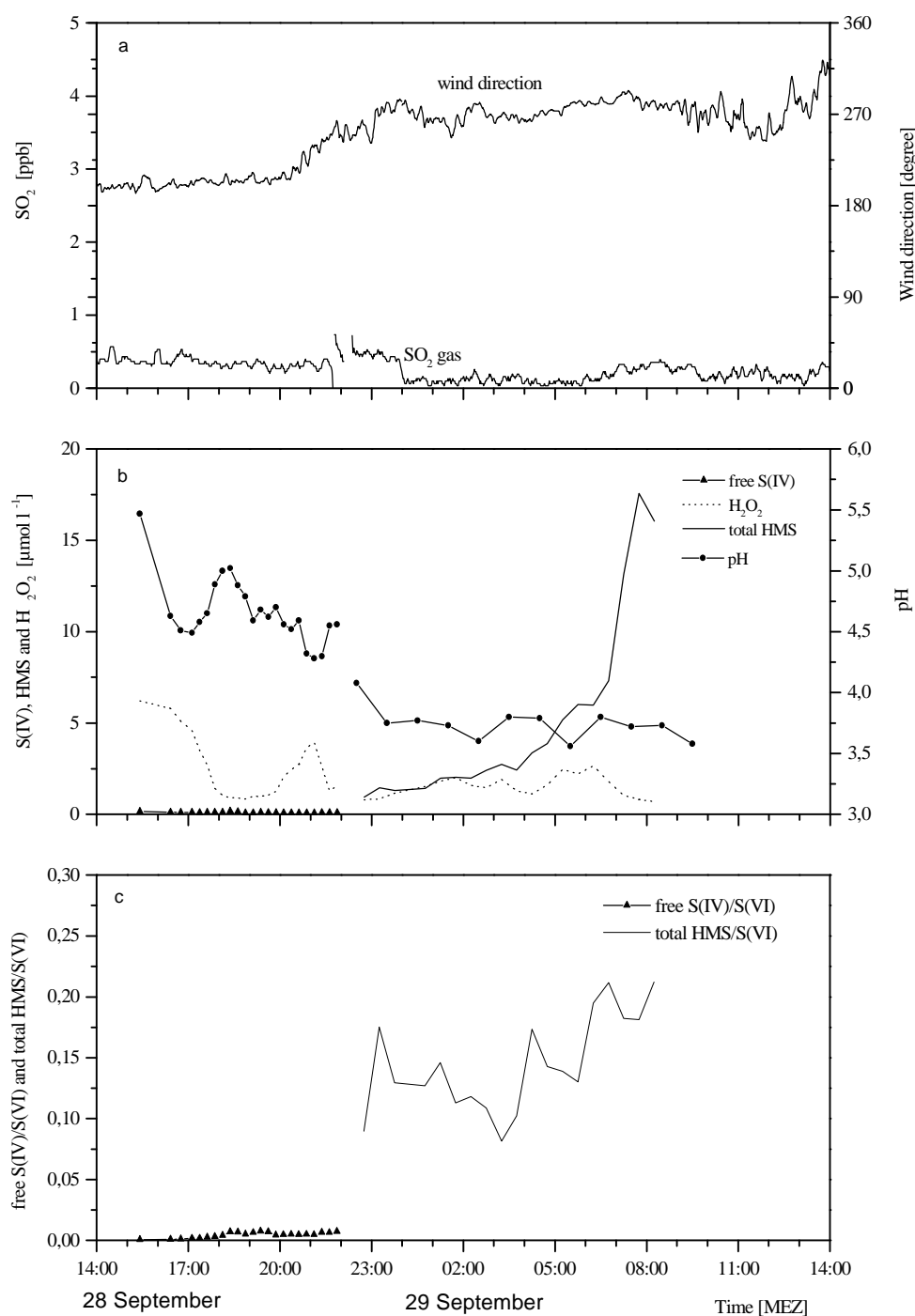


Fig. 3.4. (a) the variation of gas-phase  $\text{SO}_2$  with wind direction; (b) concentrations of free S(IV),  $\text{H}_2\text{O}_2$ , total HMS and pH value in cloudwater; (c) ratios of free S(IV)/S(VI) and total HMS/S(VI) in cloudwater during event #1 at the Brocken station.

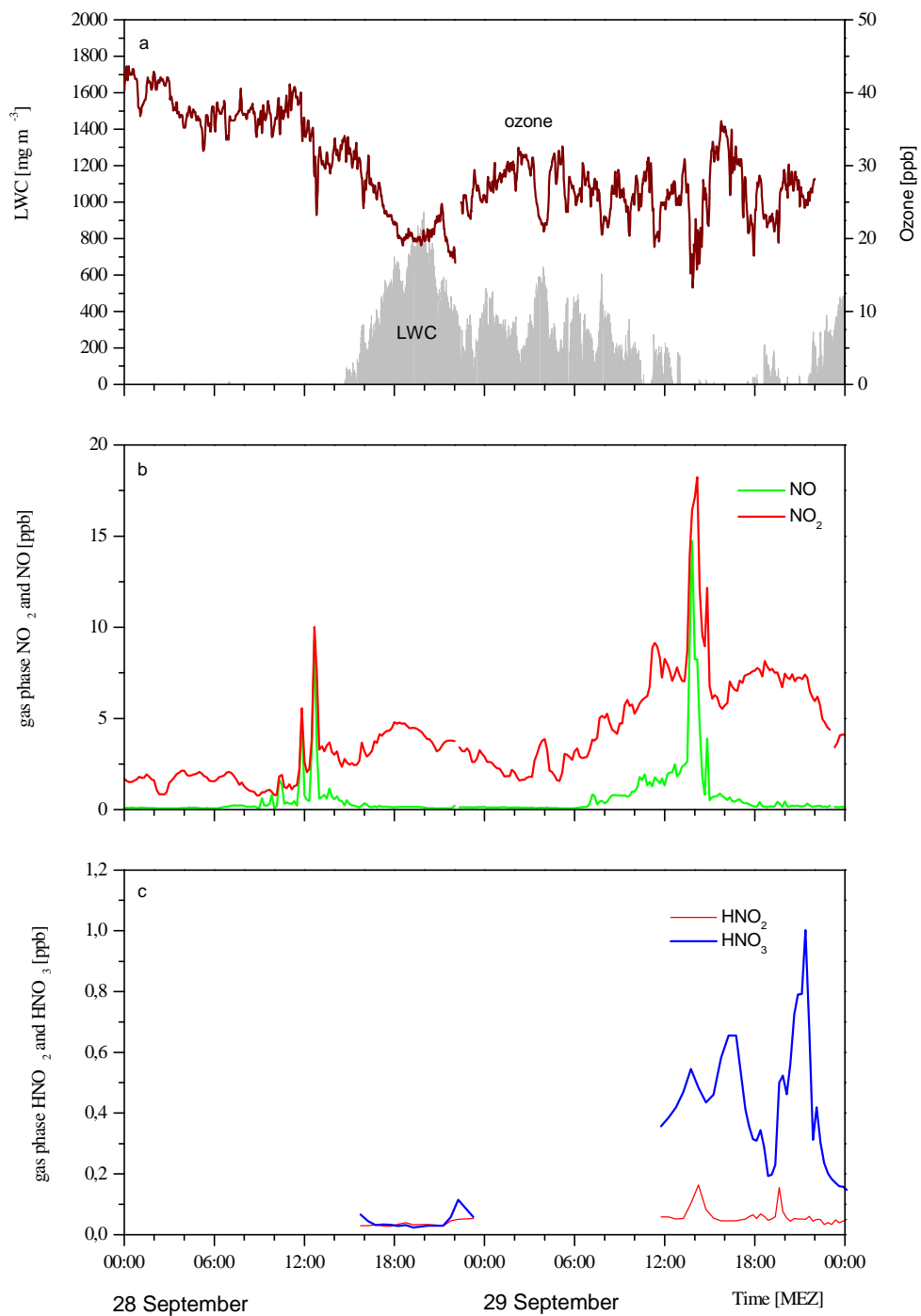


Fig. 3.5. (a) the variation of LWC and ozone; (b) NOx; (c) HNO<sub>2</sub> and HNO<sub>3</sub> during event #1 at the Brocken station.

single cloud event,  $\text{NH}_4^+$ ,  $\text{NO}_3^-$  and  $\text{SO}_4^{2-}$  ions in cloudwater mainly come from the activation of ammoniumnitrate and ammoniumsulfate aerosols as well as from dissolution and oxidation of trace gases in cloudwater. Droplet number density in cumulus clouds is known to be very high near cloud base despite low LWC. Additionally, the mean droplet diameter was much smaller near cloud base than that in deeper cloud layer (Pruppacher and Klett, 1997). This is caused by the entrainment of fresh air from the layer below cloud base, which brings more activable aerosol particles and trace gases into the cloud. As a result, ion concentrations in cloudwater reach a maximum slightly above cloud base height. It is in coincidence with our early observations on the Brocken (Möller et al., 1996b).

On September 29<sup>th</sup>,  $\text{NH}_4^+$ ,  $\text{NO}_3^-$  and  $\text{SO}_4^{2-}$  concentrations in cloudwater strongly increase with nitrate and ammonium being the dominant anion and cation. The concentration of nitrate was about 5 times more than that of sulfate and had a strong correlation with ammonium. There was an accumulation of ammoniumnitrate aerosols or an increasing loading of  $\text{NH}_3$  and  $\text{HNO}_3$  gases on September 29<sup>th</sup>. Back trajectories have remained unchanged throughout the cloud event. Nevertheless, wind direction changed from south to west from September 28<sup>th</sup> to September 29<sup>th</sup> (Fig. 3.4a). Therefore we can estimate that west wind on September 29<sup>th</sup> brought an air mass with significant high nitrate concentration. The high concentration of nitrate in cloudwater on September 29<sup>th</sup> will be discussed with gas phase  $\text{HNO}_3$  and  $\text{NO}_x$  concentrations later in subchapter **Other trace gases**. Ammonium is an abundant cation in non-industrialized areas as it is in this case.

#### **pH, gas phase $\text{SO}_2$ , free S(IV), HMS, $\text{H}_2\text{O}_2$ and S(VI)**

On September 29<sup>th</sup>, the pH value of the measured cloudwater samples was in average 3.7 and thus about 0.9 unit lower than the average pH value of cloudwater samples on 28<sup>th</sup> (4.6). The difference between the average pH values from September 28<sup>th</sup> and 29<sup>th</sup> suggests that the increase of the nitrate concentration which we observed in the samples on September 29<sup>th</sup> caused the stronger acidity of the cloudwater. The protons were produced as more nitrate ions were formed in cloudwater. Gas phase  $\text{SO}_2$  concentration was mainly lower than 1ppb (Fig. 3.4a). On September 29<sup>th</sup>, when west wind dominated, even lower concentrations of  $\text{SO}_2$  than on September 28<sup>th</sup> were observed.

On September 28<sup>th</sup> from 15:00 to 22:00, sampling without formaldehyde stabilization was conducted. Free S(IV) was measured with CFCL method in-situ. The sulfate concentration in these samples was analyzed later in our laboratory in Berlin. According to Radojevic (1985) free S(IV) is readily oxidized by different oxidants during storage without stabilization. To check if all free S(IV) is oxidized into sulfate during the storage period, we performed the following test: The concentration of free S(IV) was measured in cloudwater samples on the Brocken shortly after sampling. The samples were stored at a temperature of 4°C for two days. After two days, we measured the concentration of free S(IV) in the samples again. The measured concentration of free S(IV) in these samples was below detection limit (10 nmol l<sup>-1</sup>) even in the samples, in which significant amount of free S(IV) was measured just after sampling. Therefore, the assumption that free S(IV) was totally oxidized into S(VI) during 2 weeks of storage was acceptable. Since S(VI) in these samples was also measured after two weeks of storage, a part of the amount of S(VI) in these samples was from the oxidation of free S(IV). Hence, the ratio of free S(IV) to S(VI) here represents rather the ratio between free S(IV) and the sum of free S(IV) and sulfate. According to our measurement, free S(IV) concentrations were in the range of 100 nanomol and the ratio of free S(IV)/S(VI) was as low as 0.008 in this event, which means that the contribution of free S(IV) to total sulfur is negligible. These low concentrations of free S(IV) and the free S(IV)/S(VI) ratio were expected because the gas phase SO<sub>2</sub> in this period was extremely low and excess amounts of H<sub>2</sub>O<sub>2</sub> (in average 2 μmol l<sup>-1</sup>, with a span from 0.7 to 6.2 μmol l<sup>-1</sup>) were measured in cloudwater. In the aqueous phase H<sub>2</sub>O<sub>2</sub> can efficiently oxidize free S(IV) into sulfate under pH lower than 5 (see Chapter 1.2.4.1).

At midnight and in the early morning, the collection of cloud samples with formaldehyde stabilization was conducted. From September 28<sup>th</sup>, 22:30 to September 29<sup>th</sup>, 8:30 we sampled cloudwater in bottles containing 10 ml of a 6.5 mmol l<sup>-1</sup> formaldehyde solution. An excess amount of formaldehyde in the sampling bottles is necessary to stabilize free S(IV) to HMS in the short sampling period. Thus the concentration of HMS was the sum of free S(IV) and original HMS (which exists already in cloudwater before sampling). S(VI) was measured later in our laboratory in Berlin. Since HMS is stable against oxidants like H<sub>2</sub>O<sub>2</sub> or O<sub>3</sub>, the ratio between HMS and S(VI) represents the ratio between total S(IV) and S(VI). In contrast to the extreme

low concentration of free S(IV) on September 28<sup>th</sup>, significant amounts of total S(IV) were found in the stabilized samples. The ratio of HMS/S(VI) was up to 0.20, the average being 0.15. HMS in cloudwater has two sources: one is HMS in aerosol particles which comes into cloudwater via nucleation scavenging; the other is the combination of dissolved SO<sub>2</sub> with formaldehyde in clouds and during sampling period in the sampling bottles. Dixon et al. (1999) measured HMS in atmospheric aerosols. According to their measurement, the contribution of HMS to total aerosol sulfur is as low as 0.2% and thus negligible. If we transfer this result to the aerosol particles at Mt. Brocken, we can conclude from our data that even under low concentration of SO<sub>2</sub> considerable amounts of SO<sub>2</sub> can dissolve into cloudwater and adduct with formaldehyde to form HMS and accumulate in cloudwater. We have not measured free S(IV) concentration on September 29<sup>th</sup>, however, based on the low concentration of SO<sub>2</sub> and low pH value in the cloudwater samples we can assume that free S(IV) concentration should be also very low. That means, the main part of the total S(IV) we measured was original HMS. Our results agree well with that of Warneck (1989) and Munger (1986) who have shown that in slightly acid situations the formation of HMS is a very effective pathway for SO<sub>2</sub> scavenging. Due to the lack of measurement instruments, we could not measure gas phase and liquid phase formaldehyde during this experiment. Like SO<sub>4</sub><sup>2-</sup>, NO<sub>3</sub><sup>-</sup> and NH<sub>4</sub><sup>+</sup>, HMS increased drastically on September 29<sup>th</sup>, especially after 6:00. SO<sub>2</sub> showed a slight increase after 6:00. The reason for the increase of HMS concentration is the entrainment of a new air mass from below the cloud base with higher concentration of formaldehyde into the cloud layer and thus an enhanced production of HMS in cloudwater.

Fig 3.6 shows the relationship between gas phase H<sub>2</sub>O<sub>2</sub> with relative humidity from September 26<sup>th</sup> to 28<sup>th</sup>, together with LWC from September 28<sup>th</sup> 14:00-24:00. On September 26<sup>th</sup>, two days before the observed cloud events began, the concentration of gas phase H<sub>2</sub>O<sub>2</sub> was as high as 2ppb, caused by strong solar radiation during the whole week. However, on September 27<sup>th</sup> after a short rain event (9:00-9:15), the concentration of gas phase H<sub>2</sub>O<sub>2</sub> dropped to 0.1ppb. An anti-correlation of gas phase H<sub>2</sub>O<sub>2</sub> and relative humidity can be observed. Under high relative humidity, the soluble part of aerosol particles builds an aqueous film around them. As H<sub>2</sub>O<sub>2</sub> is a highly soluble gas, it can be dissolved into this aqueous film around the aerosol particles and

participate in further reactions with other chemical substances. Radicals like  $\text{HO}_2$  which are essential for  $\text{H}_2\text{O}_2$  formation were produced less in interstitial air of cloud, and the produced radicals are mainly dissolved into cloudwater. Therefore the production of  $\text{H}_2\text{O}_2$  is very limited in the interstitial air of clouds. At the beginning of the cloud event, up to  $6.2\mu\text{mol l}^{-1}$   $\text{H}_2\text{O}_2$  were measured in the cloudwater samples. The concentrations decreased quickly as the gas phase  $\text{H}_2\text{O}_2$  in the interstitial air decreased (Fig. 3.4b). Product of the oxidation reaction between S(IV) and  $\text{H}_2\text{O}_2$  is not only sulfate, but also  $\text{H}^+$  ions. Thus this reaction is an important factor leading to the acidification of cloudwater. An anti-correlation of  $\text{H}_2\text{O}_2$  and pH was observed in the samples. The higher the concentration of  $\text{H}_2\text{O}_2$  is, the lower is the pH value of the sample.

Dissolution of  $\text{SO}_2$  and  $\text{H}_2\text{O}_2$  into cloudwater is a dynamic process. Even though we can measure little free S(IV) in our samples, we can not conclude that the transformation of S(IV) to sulfate is negligible. As long as there are sufficient

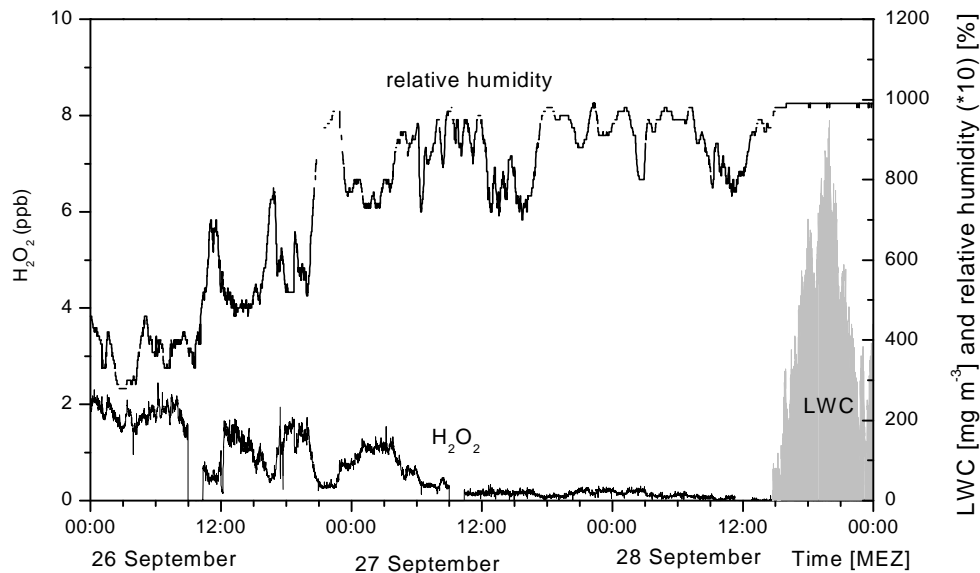


Fig. 3.6. The relationship of gas phase  $\text{H}_2\text{O}_2$  concentration with relative humidity and LWC.



concentration of oxidants, the oxidation reaction of S(IV) with H<sub>2</sub>O<sub>2</sub>, ozone and other oxidants proceed quickly enough to transform S(IV) to S(VI) in cloudwater.

### **Other trace gases**

An obvious depletion of ozone (from 40 ppb to 25 ppb) was observed at the beginning of the cloud event on September 28<sup>th</sup> (Fig. 3.5a). Such kind of rapid decrease of ozone concentration with passing clouds has been also reported elsewhere (Lelieveld et al., 1990; Möller et al., 1992a; Acker et al., 1995b). It is known that clouds can be a sink for ozone due to oxidation reactions with O<sub>2</sub><sup>-</sup> and S(IV) in the aqueous phase and the reduction of ozone formation in the gas phase resulting from the separation of peroxy radicals and NO.

During the night NO<sub>x</sub> is present mainly as NO<sub>2</sub> as a result from the reaction between NO and ozone. NO<sub>x</sub> concentration in periods of clouds is not lower compared to cloud free periods, on the contrary, even a slight increase can be observed on 28<sup>th</sup> September at the beginning of the cloud event (Fig. 3.5b). As a poorly soluble gas, NO<sub>2</sub> will accumulate in the interstitial air via the reaction of NO with ozone. The sink of NO<sub>2</sub> via photolysis is limited due to reduction of penetrating shortwave radiation and lack of radicals which convert NO<sub>2</sub> into HNO<sub>3</sub>. On September 29<sup>th</sup> significantly higher amount of NO<sub>2</sub> was measured than on September 28<sup>th</sup>. Gas phase HNO<sub>3</sub> increased up to 1ppb with the dissipation of the cloud (Fig. 3.5c). This confirms us again that the air mass which reached the Brocken station on September 29<sup>th</sup>, is characterized with high nitric acid and that the dissolution of HNO<sub>3</sub> gas is a main cause of high nitrate concentration in cloudwater.

### **Aerosols**

With the formation of the cloud, nitrate and sulfate concentration of interstitial aerosols decreased significantly. The reason is that more than half of all nitrate and sulfate particles will be activated into cloud droplets in the cloud layer. During the cloud event, main ion concentrations of the interstitial aerosols remain relatively constant. Since the position of our measurement site above cloud base changed with the evolution of cloud event, the constant ion concentrations of interstitial aerosols indicates the vertical homogeneity of interstitial aerosols. Sulfate and nitrate concentrations of interstitial

aerosol particulates increase at the end of cloud event, which indicates the entrainment of new air mass into the cloud.

Table 3.3. Aerosol ion concentrations and pH value during Brocken campaign measured from gas sampling system with denuder.

Unit:  $\mu\text{eq m}^{-3}$

Sampling time	Cl <sup>-</sup>	NO <sub>3</sub> <sup>-</sup>	SO <sub>4</sub> <sup>2-</sup>	Na <sup>+</sup>	pH	Remarks
980927 15:10-16:40	0,033	0,0041	0,044	0,056	5,08	Between two rain events
980927 16:45-18:45	0,017	0,0027	0,042	0,033	5,1	Between two rain events
980927 18:45-980928 09:43	0,010	0,0018	0,017	0,011	5,12	Overnight with rain
980928 10:43-12:43	0,033	0,0052	0,042	0,042	5,16	Shortly before cloud event 1
980928 15:30-18:30	0,011	0,0019	0,020	0,017	5,08	In cloud event 1
980928 18:30-21:30	0,011	0,0022	0,020	0,017	5,10	In cloud event 1
980929 10:30-14:30	0,008	0,0062	0,029	0,012	5,12	In cloud event 1
980929 14:30-19:30	0,003	0,0034	0,037	0,010	5,04	after cloud event 1
980929 19:35-980930 09:30	0,001	0,0006	0,011	0,004	5,05	Half time in cloud free period half time in cloud event 2
980930 09:45-15:45	0,006	0,0013	0,017	0,008	5,13	In cloud event 2
980930 15:50-22:00	0,006	0,0008	0,011	0,008	5,13	In cloud event 2
980930 22:10-981001 10:00	0,004	0,0005	0,011	0,010	4,9	In cloud event 2
981001 11:00-18:00	0,007	0,0008	0,007	0,007	5,22	In cloud event 2
981001 18:00-981002 09:00	0,003	0,0008	0,006	0,004	5,44	Half time in cloud event 2
981005 20:45-981006 09:45	0,003	0,0003	0,005	0,004	5,04	In cloud event 3
981006 10:00-12:00	0,008	0,0013	0,025	0,017	5,14	No event
981006 13:00-15:00	0,017	0,0016	0,025	0,025	5,24	No event
981007 09:30-13:30	0,008	0,0009	0,046	0,012	5,12	In cloud event 4
981007 13:35-17:35	0,004	0,0003	0,025	0,008	5,04	In cloud event 4
981007 17:35-981008 09:00	0,001	0,0003	0,006	0,002	5,07	In cloud event 4
981008 09:15-19:15	0,002	5,6E-4	0,005	0,003	5,11	In cloud event 4

Aerosol samples on September 28<sup>th</sup> from 10:43 to 12:43 and from 15:30-18:30 in Tab. 3.3 were collected before the cloud event #1 and during the cloud event #1. From the sulfate concentration of the two samples we can conclude that about  $0.02 \mu\text{eq m}^{-3}$  sulfate was activated into cloudwater. However, the sulfate concentration we measured in cloudwater was about  $0.03 \mu\text{eq m}^{-3}$ , which means that one third of sulfate in cloudwater came from sulfuric gas scavenging. Extremely low concentration of nitrate was measured in aerosol samples even in cloud-free periods. The nitrate concentration in aerosol is 10 orders of magnitude lower than that in cloudwater. A loss of nitrate and  $\text{NH}_4^+$  in aerosol during sampling can be explained by the volatilizing escape of  $\text{NH}_4\text{NO}_3$  in the form of  $\text{NH}_3$  and  $\text{HNO}_3$  gas on the surface of the filter which is located at the end of a denuder to collect aerosol particulates (Kames and Schmidt, 1992).

### **Short summary**

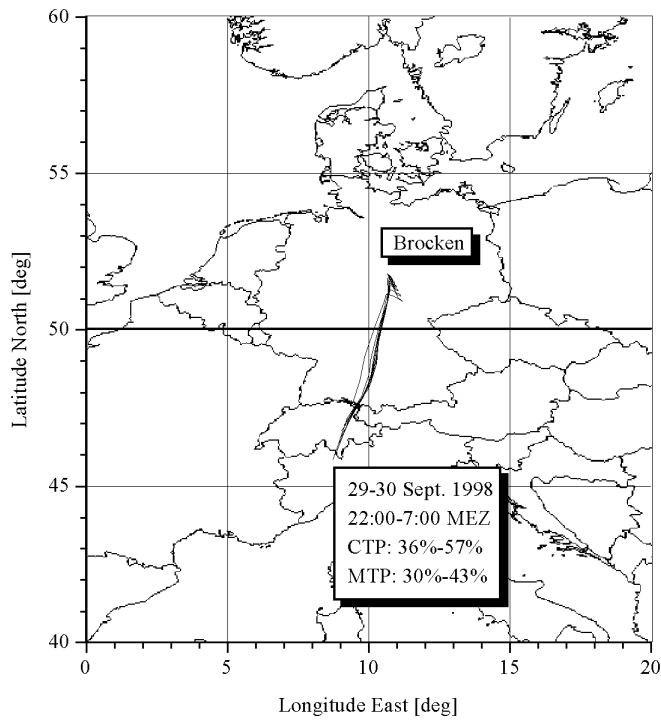
In this event, we observed a cloud from its arrival to dissipation due to the ascending and descending of the cloud base. During the period  $\text{SO}_2$  concentration remained quite low. Consequently the concentration of free S(IV) in cloudwater is negligibly low. In contrast to free S(IV), HMS was found to contribute significantly to the amount of total sulfur in cloudwater. The concentration of  $\text{H}_2\text{O}_2$  was in anti-correlation with the pH value, which explains well the oxidation of S(IV) by  $\text{H}_2\text{O}_2$  to produce sulfuric acid.

### **Event #2**

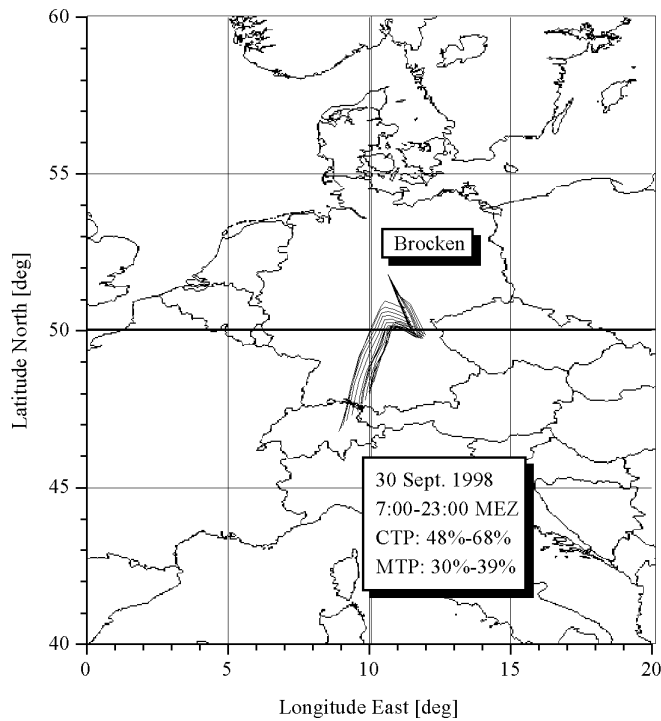
Time: September 29<sup>th</sup>, 1998, 22:00 — October 01<sup>st</sup>, 1998, 18:00

#### **Weather situations and back trajectories**

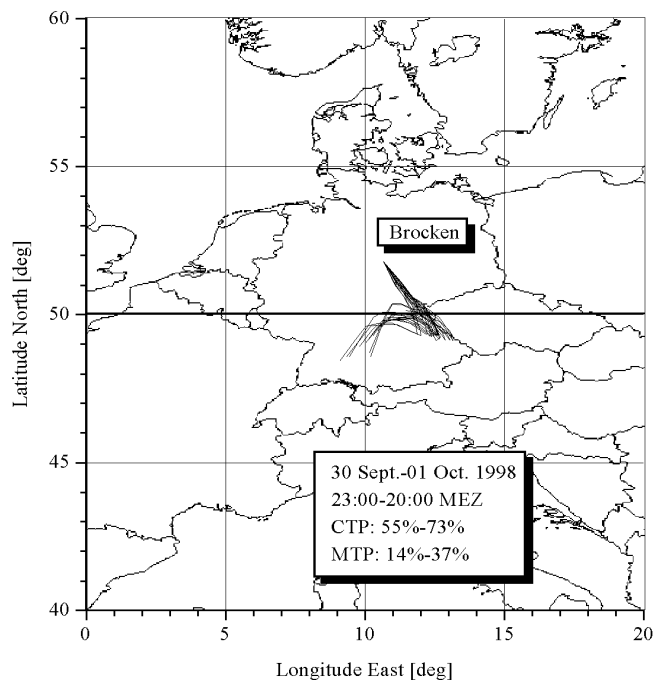
On September 29<sup>th</sup> at about 22:00, a new cloud occurred at the Mt. Brocken. The wind direction changed from West to Southeast about 19:00 on September 29<sup>th</sup>. On the next day (30<sup>th</sup>) Germany laid between two low pressure systems. The western one located across the channel between England and France, the eastern one located over Ukraine. The latter low was responsible for the advection of North-European sub-polar air with easterly winds in Germany. An occlusion of westerly low which crossed France on September 29<sup>th</sup> intruded West and Southwest Germany at noon of September 30<sup>th</sup>. On October 1<sup>st</sup>, the West-European low pressure system intensified and stretched to Middle-Europe. An occlusion laid accross Germany and caused regional precipitation. North Germany was controlled by the air mass imported from Scandinavia whereas southerly from the air mass border relatively high temperatures were measured. The trajectories show SSW route in the evening of September 29<sup>th</sup> (Fig. 3.7). However, on September 30<sup>th</sup> the SSW route turned to east direction shortly before reaching Mt. Brocken and reached the station from Southeast direction. On October 1<sup>st</sup>, the trajectories show obvious SE routes. On the Brocken summit, the temperature decreased slowly from 8°C to 2°C. On October 2<sup>nd</sup>, the temperature on the Mt. Brocken dropped under the freezing point. Wind direction shifted very slowly from south at the beginning of the cloud event to east at the end of the cloud event (Fig. 3.9a). The observed cloud type during the period was Stratus nebulosus.



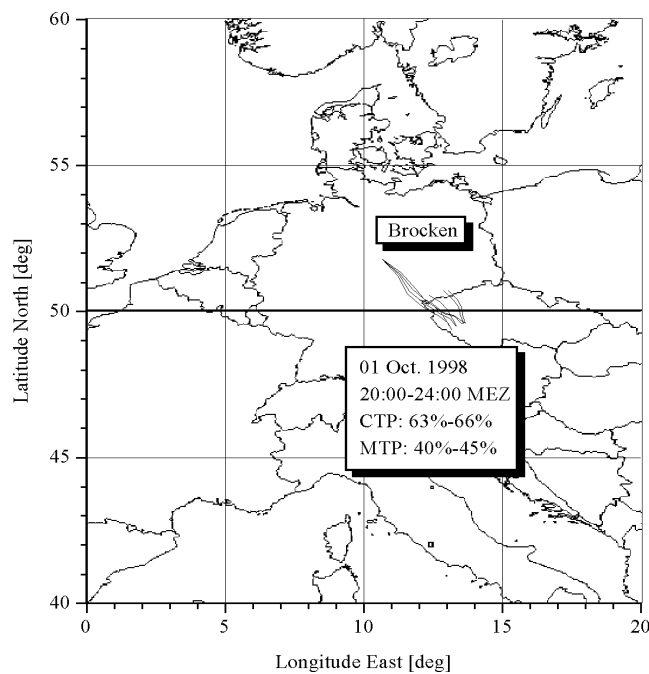
(a)



(b)



(c)



(d)

Fig. 3.7 (a,b,c,d). 72h back trajectories during event #2.

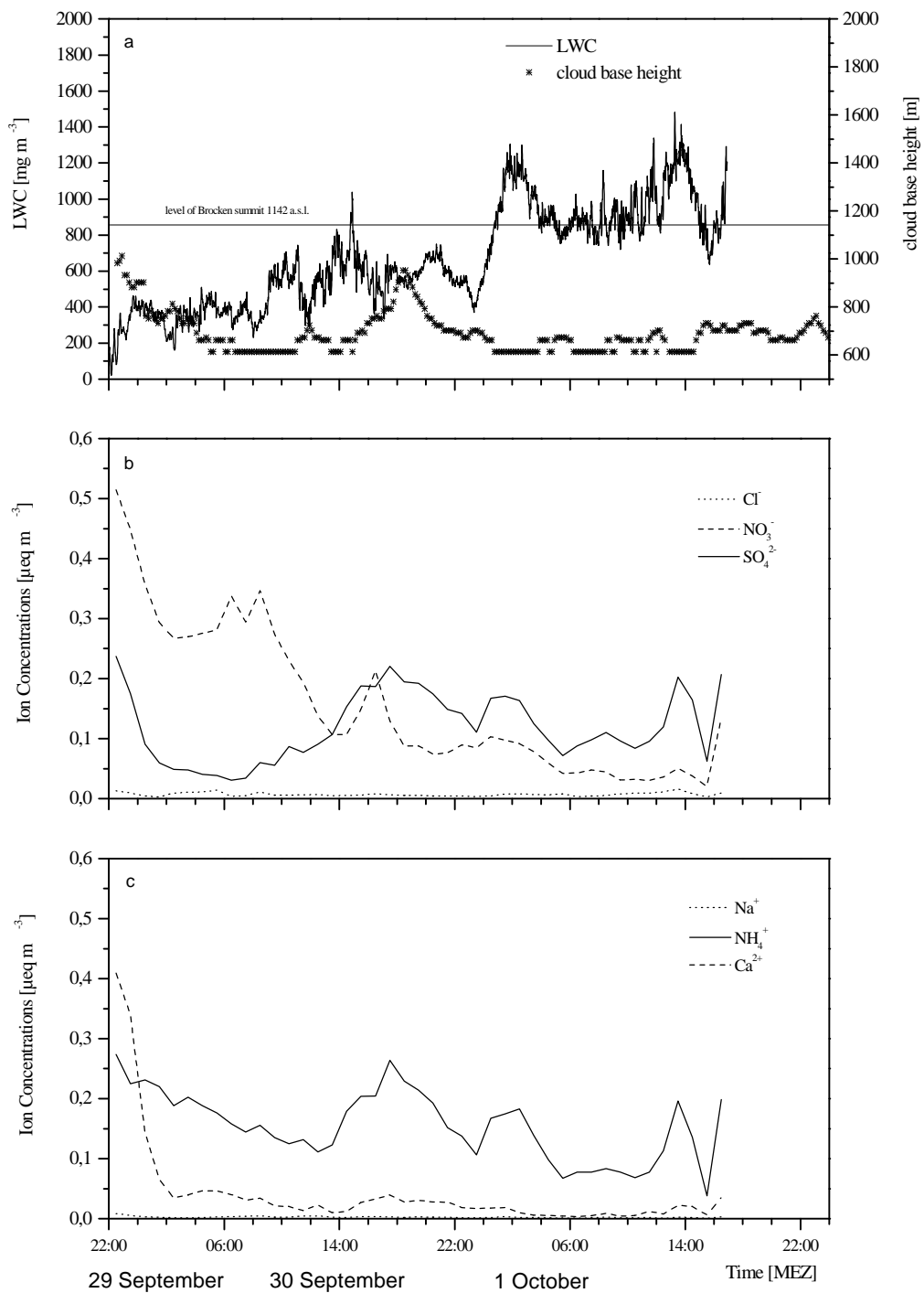


Fig. 3.8. As for Fig. 3.3 but for event #2.

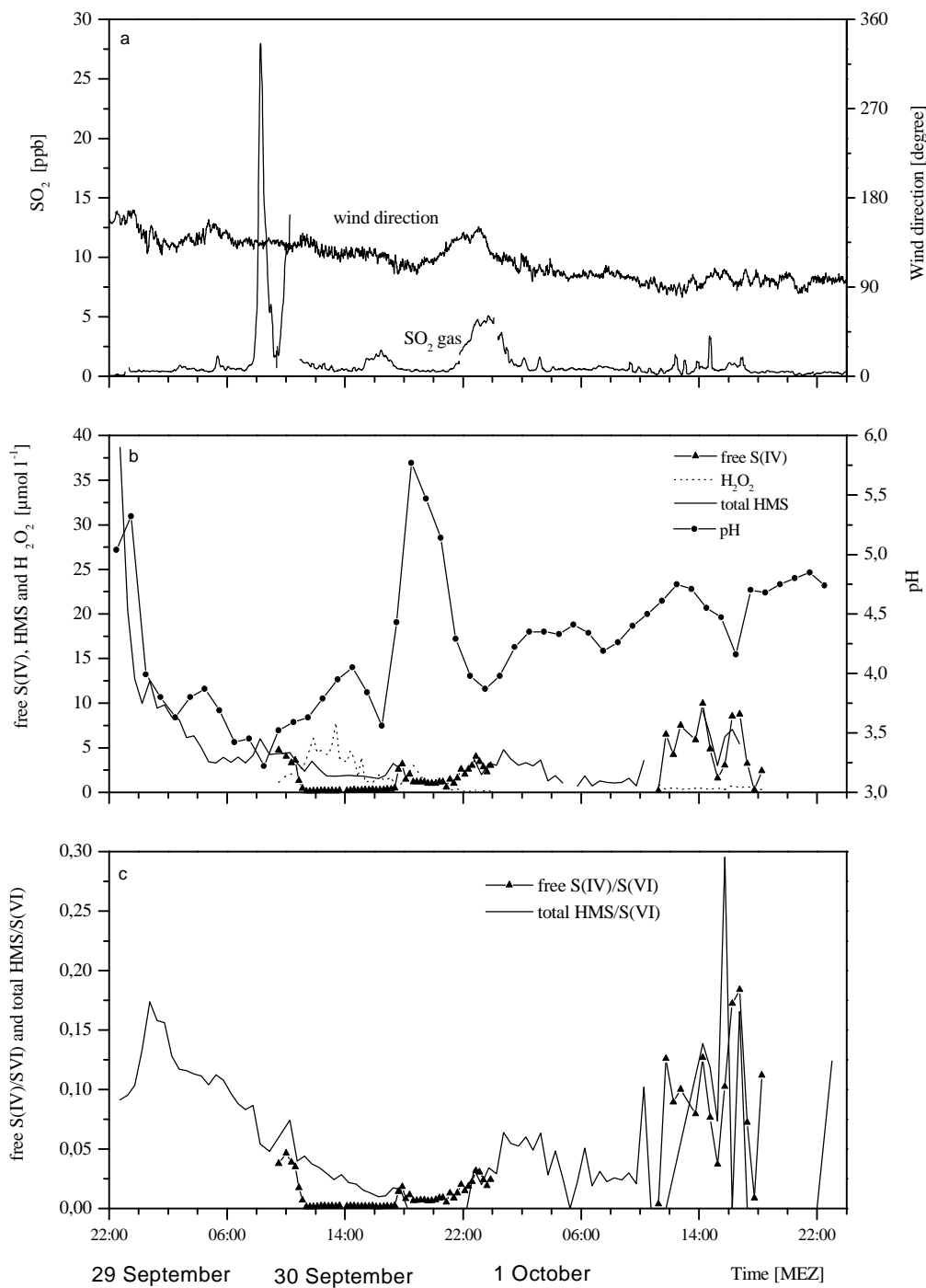


Fig. 3.9. As for Fig. 3.4 but for event #2.

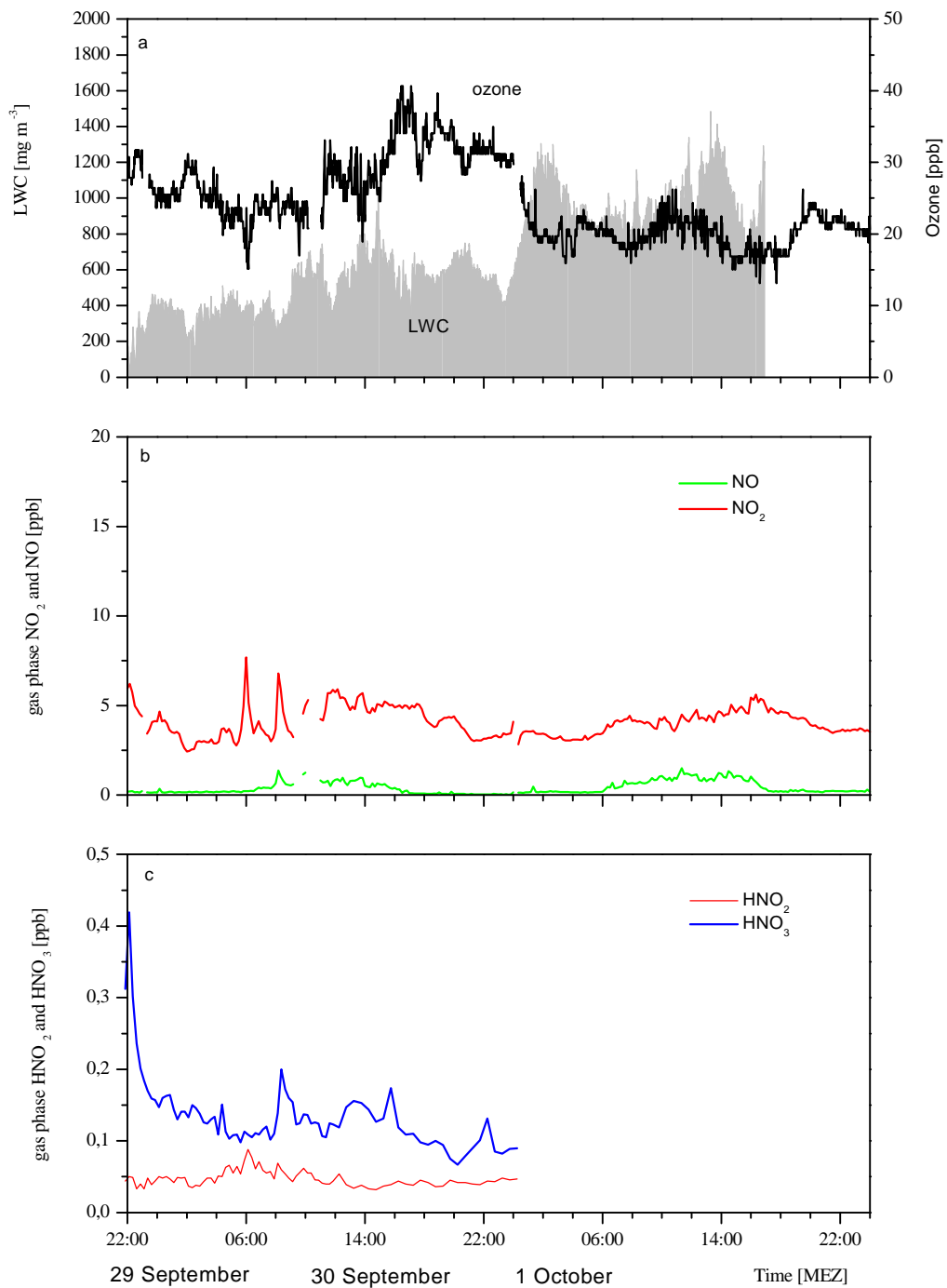


Fig. 3.10. As for Fig. 3.5 but for event #2.



### **LWC and cloud base height**

The cloud event lasted about 50 hours. During this period LWC increased from below  $100 \text{ mg m}^{-3}$  to more than  $1200 \text{ mg m}^{-3}$  (Fig. 3.8a). Cloud base was mostly more than 400 m lower than the summit of Mt. Brocken. Our measurement station was located in the deeper layer of the cloud.

### **Ion concentrations**

Similar to event #1, concentrations of  $\text{Na}^+$  and  $\text{Cl}^-$  were very low, indicating the continental characteristics of the cloud. At the beginning of event #2, the nitrate concentration was about 5 times higher than the sulfate concentration (Fig. 3.8b). Additionally, the  $\text{HNO}_3$  gas phase concentration was up to 1 ppb before the cloud event and then decreased to less than 0.2 ppb during the cloud event (Fig. 3.10c). Obviously the high concentration of  $\text{HNO}_3$  in the gas phase caused the high concentration of nitrate in cloudwater. At about 14:00 on September 30<sup>th</sup>, sulfate became the dominant anion.  $\text{NH}_4^+$  and  $\text{SO}_4^{2-}$  showed a positive correlation in the following period. When we compare the temporal variations of ion concentrations with the trajectories, we find that sulfate is the dominant anion in clouds with SE trajectories, while nitrate is the dominant anion in clouds with SSW trajectories. During this event, with an obvious change of trajectories from SSW to SE, the change of characteristic ion content for clouds from different regions can be well observed.

### **pH, gas phase $\text{SO}_2$ , $\text{H}_2\text{O}_2$ , free S(IV), total HMS and S(VI)**

The pH values of the measured cloud samples followed the same trend as LWC and increased with the progress of the cloud event. An exception was observed between September 30<sup>th</sup>, 16:00 and 22:00. Higher LWC leads to a higher dilution of cloudwater. A lack of soluble acid gases in the interstitial air of the cloud layer may thus restrict the acidification and pH will increase due to dilution effect. Although the routes of the back trajectories show a continuous change from SSW to SE,  $\text{SO}_2$  gas phase concentration remained quite low except for some short periods. There is no relationship between trajectories and gas phase  $\text{SO}_2$  concentration. Consequently, the high concentration of sulfate in cloudwater reflect the sulfate aerosol burden in SE trajectories.

Sampling with formaldehyde stabilization was conducted throughout the cloud event. Additionally sampling without stabilization was made during the time span from September 30<sup>th</sup> 9:15 to 24:00 and from October 1<sup>st</sup> 11:00 to 18:30. The ratio of free S(IV)/S(VI) ranges from 0.001 to 0.18, with a mean value of 0.021 (Fig. 3.9c). The ratio of total S(IV)/S(VI) ranged from zero to 0.3, with a mean value of 0.03. However, the ratio of total S(IV)/S(VI) in the first three hours of the cloud event was much higher than during other periods, ranging from 0.1 to 0.17. That means that a significant amount of total S(IV) can be found in the lower layers of cloud. It is in coincidence with the result of event #1, where up to 0.2 of this ratio was measured near cloud base (Fig. 3.4c).

Due to orographically induced vertical transport of air masses we observed in some periods significantly high concentrations of gas phase SO<sub>2</sub>. For example during September 30<sup>th</sup> from 8:00-10:00, SO<sub>2</sub> gas phase concentration increased to a maximum of 30 ppb. Another example is the time period from September 30<sup>th</sup>, 22:00 to October 1<sup>st</sup>, 2:00 when up to 5 ppb SO<sub>2</sub> was measured in the gas phase. Since during those periods back trajectories and wind direction remained the same, the only source for the high concentrations of SO<sub>2</sub> is the orographically induced air mass transport along the mountain valley. According to our cloud base measurements, the position of our station above the cloud base was higher than 530 m. That means that the village of Schierke, which lies southeastly from Brocken, was also in the cloud. The upward advection of air in the cloud between Schierke and the summit of Mt. Brocken can efficiently transport the locally produced SO<sub>2</sub> (mostly from heating) from Schierke to the summit of Mt. Brocken.

The increase of gas phase SO<sub>2</sub> concentration caused relatively high concentration of free S(IV) in cloudwater. We measured concentrations of up to 4.7 μmol l<sup>-1</sup> of free S(IV) were in cloudwater in these periods. In contrast, H<sub>2</sub>O<sub>2</sub> concentrations in cloudwater were much lower than in other periods. This indicates that in the deep cloud layer, the dissolved part of SO<sub>2</sub> can not be totally consumed and remain relatively high amounts as free S(IV). The pH value dropped with the increase of SO<sub>2</sub>.

From October 1<sup>st</sup>, 10:00 to 18:00, the influence of the steamtrain on the SO<sub>2</sub> gas phase can be seen very clearly. The peaks have different maxima but occur almost hourly. Due to such intermittent change of gas phase SO<sub>2</sub>, we also observed a great

variation in the concentration of free S(IV). The ratio of free S(IV) to S(VI) changed from zero to 0.18, much higher than in other periods in this event. H<sub>2</sub>O<sub>2</sub> concentration was less than 1 μmol l<sup>-1</sup>, which is negligible compared to the content of free S(IV). In contrast to free S(IV), which reflects the increase of gas phase SO<sub>2</sub>, the formation of HMS is more significant near cloud base or when new air mass is entrained. It indicates that the formaldehyde concentration may be the determining factor of HMS formation in cloudwater.

### **Aerosols**

Aerosol samples (September 29<sup>th</sup>, 14:30-19:30 and September 29<sup>th</sup>, 19:35-September 30<sup>th</sup>, 9:30 in Tab. 3.3) were collected before and during cloud event #2. About 2/3 of aerosol sulfate was converted into cloudwater sulfate as the cloud event began. During the cloud event, sulfate amount in aerosol samples remained almost constant except for the period from September 30<sup>th</sup> 9:45 to 15:45. In this period sulfate concentration in interstitial aerosol were about 1.5 factor of that in other periods. Considering that also obvious increase of sulfate in cloudwater was observed in this period, this indicate that there should be an entrainment of new air mass with more activable sulfate aerosols.

### **Short summary**

From the results of this event, we can conclude that an increase of SO<sub>2</sub> will cause an increase of the concentration of free S(IV) in the deeper cloud layer. Moreover, the increase of SO<sub>2</sub> results in an increase of acidity due to its oxidation into sulfate. In the deeper layer of clouds with high LWC, gaseous H<sub>2</sub>O<sub>2</sub> is limited and negligible concentrations of H<sub>2</sub>O<sub>2</sub> were often measured in the liquid phase. Accordingly, relatively high concentrations of free S(IV) can be measured. Comparing the concentrations of total HMS and free S(IV) we can conclude that the concentration of original HMS makes only a small fraction in total S(IV) in the deeper cloud layer. However, HMS can be an important form of sulfur in cloudwater near the cloud base.

### **Event #3**

Time: October 05, 1998, 10:00—24:00

### Weather situation and back trajectories

From October 2<sup>nd</sup> to 4<sup>th</sup>, an air mass border was built by an occluded frontal system, which crossed the North France, Southern Germany, Austria and Slovakia to Russia.

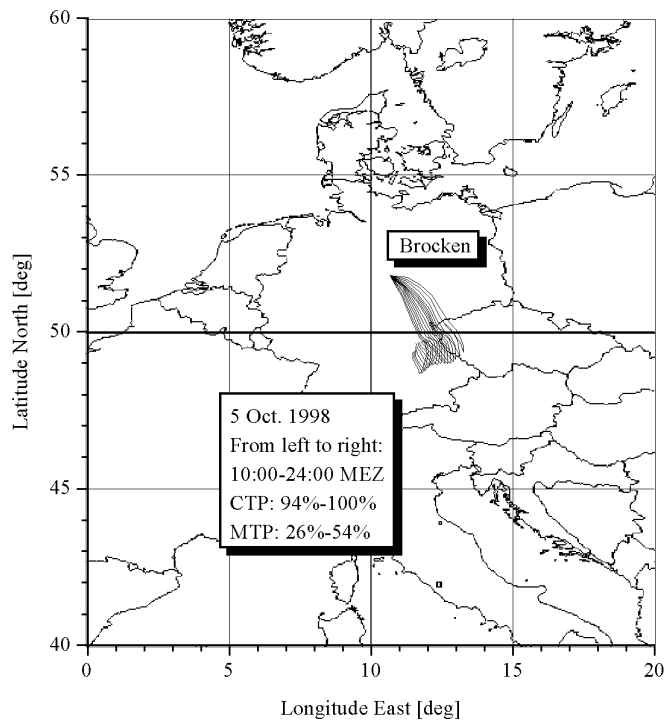


Fig. 3.11. 72h back trajectories during event #3.

From September 30<sup>th</sup> on the station was continually in cloud even during the freezing period from 2<sup>nd</sup> to 4<sup>th</sup> October. The front separated dry and cold continental air mass in North from the warm maritime air in South. Strong east wind brought cold sub-polar continental air to North- and East-Germany. Extremely low temperatures for the season were measured in the regions. At Mt. Brocken a 2cm high snow was observed. Snowfalls were widely observed in Northeast-Germany. On October 5<sup>th</sup> Russian polar air still controlled the northern part of Europe. But from the southwest-Europe a low pressure system initiated the advection of warm humid air. On the Brocken the temperature was above the freezing point. During the event cloud types were mainly stratus nebulosus and stratus fractus. Wind direction was SE during the whole period. From back trajectories (Fig. 3.11) we can see that the air mass made a small circle for

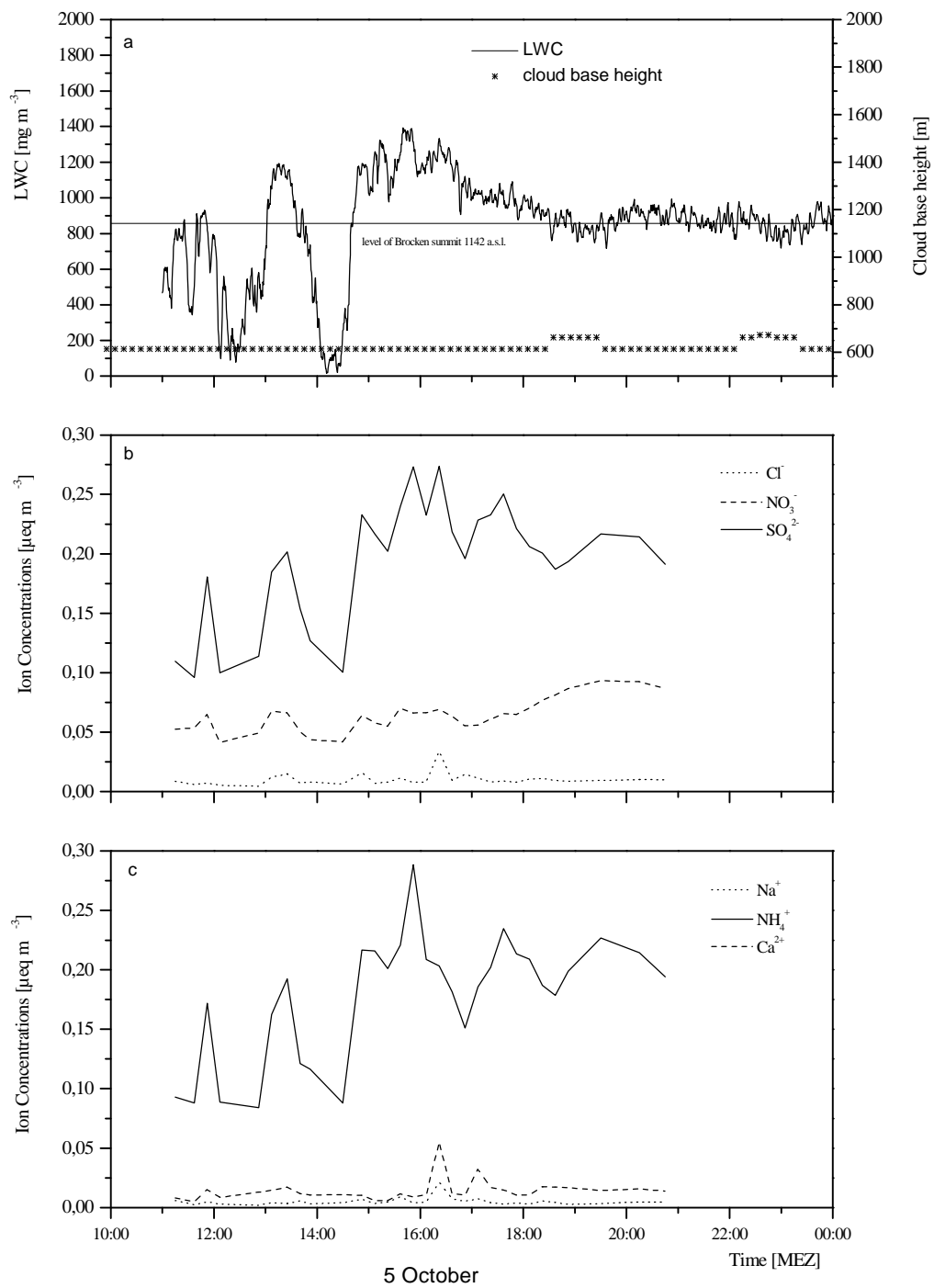


Fig. 3.12 As for Fig. 3.3 but for event #3.

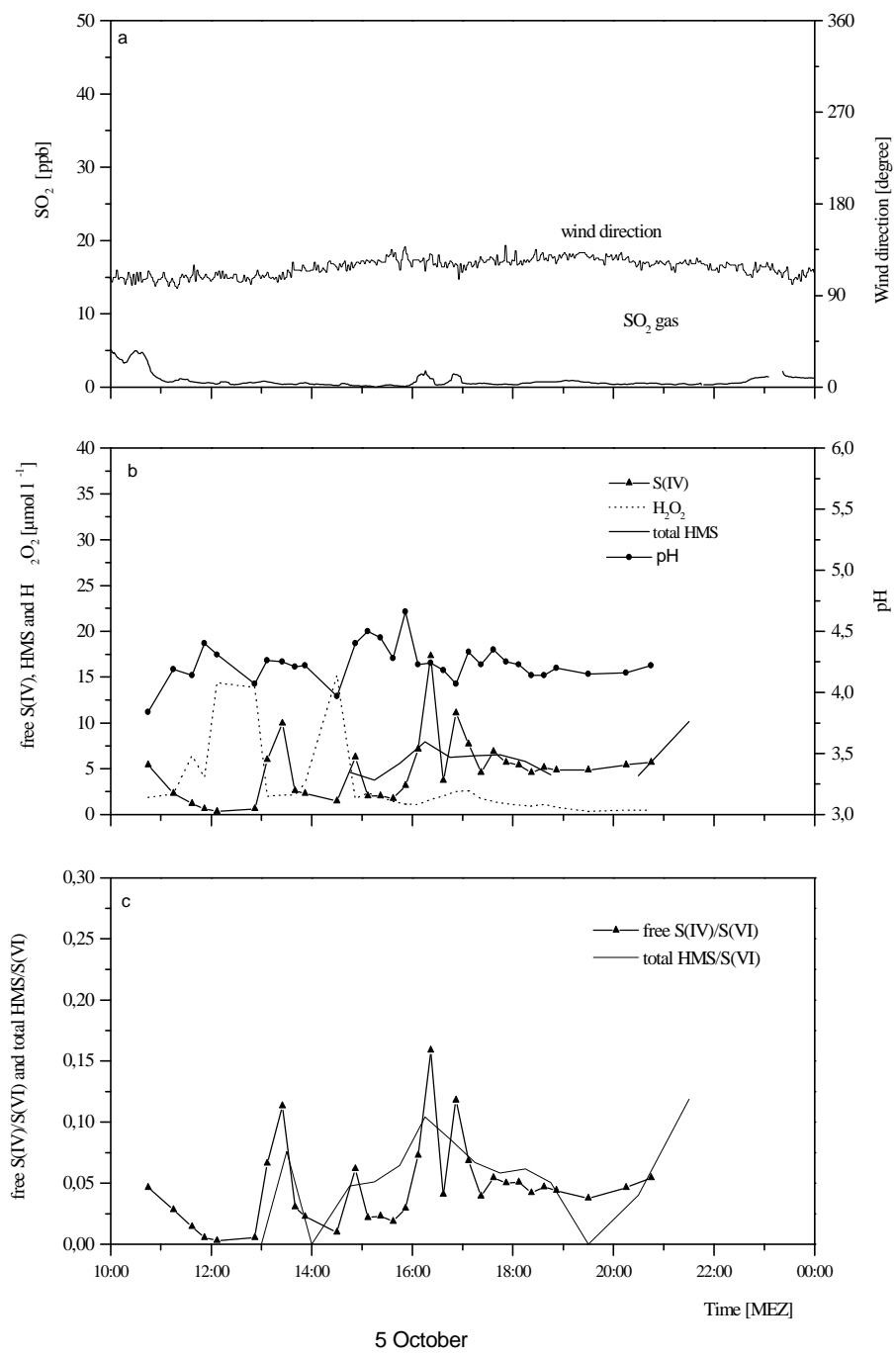


Fig. 3.13. As for Fig. 3.4 but for event #3.

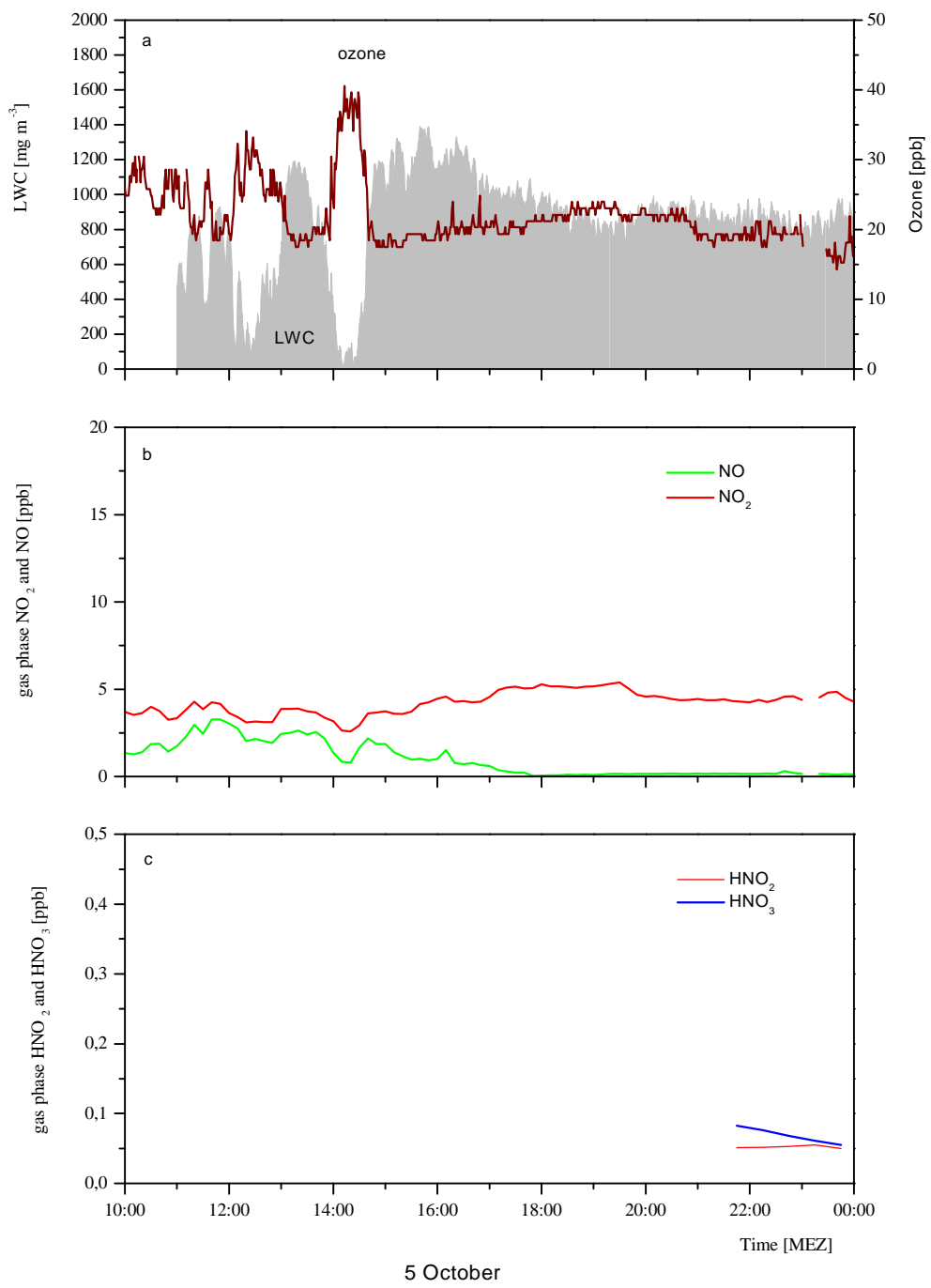


Fig. 3.14. As for Fig. 3.5 but for event #3.

more than 54 hours at the border of south Germany and west part of Czech republic and then was transported from SE to Mt. Brocken. The trajectories shifted slightly from west to east during the whole event.

### **LWC and cloud base height**

LWC varied strongly from 11:00 to 15:00, changing from zero to a maximum of 1400  $\text{mg m}^{-3}$ , but after 17:00 it was stable at about 900  $\text{mg m}^{-3}$  (Fig. 3.12a). LWC data before 11:00 on October 5<sup>th</sup> are not available because of a defect of the Gerber Particulate Volume Monitor. Strong change of LWC in the first part of this cloud event was caused by the different position of the measuring site below cloud top. This can be supported by our ceilometer measurement and optical observation. According to the measurement with the ceilometer, the cloud base height was lower than 600 m. Schierke, where the cloud base height was observed, was also in cloud during the whole period. When LWC decreased sharply, we observed sunshine penetrating through the top of the cloud. It is known that LWC increases with height above cloud base and reaches its maximum about 80-90% of the total cloud depth (Wieprecht et al., 1995). The decreasing gradient of LWC near cloud top is obvious, which can be seen from the strong decrease of LWC in a short period of time.

### **Ion concentrations**

The variation of concentrations of the main anions and cations in the unit air volume follow exactly the same trend as LWC (Fig. 3.12b,c). Similar to cloud base, near cloud top droplet sizes are much smaller and the number concentrations of droplets are higher than in deeper cloud layers (Pruppacher and Klett, 1997). From the cloud top, new fresh air is transported into the cloud layer. As a result, the sizes of cloud droplets will become smaller as they evaporate. Accordingly, the concentrations of chemical constituents in cloudwater will increase. However, in Fig. 3.12b and c the ion concentrations were multiplied with LWC to represent the amount of ions in per cubic meter volume air. The increase of the total ion content in the cloudwater is therefore due to the formation of new small droplets caused by the entrainment of new air masses from the cloud top.



During this event, sulfate is obviously the dominant anion showing a good correlation with ammonium. Thus the composition of new activated aerosol particles mainly consists of  $\text{NH}_4\text{HSO}_4$  or  $(\text{NH}_4)_2\text{SO}_4$ . It confirms us again that SE trajectories are characterized by a higher sulfate load than SSW trajectories.

#### **pH, gas phase $\text{SO}_2$ , $\text{H}_2\text{O}_2$ , free S(IV), HMS and S(VI)**

During the event, the pH value was almost constant, varying slightly between 4.0 and 4.5 (Fig. 3.13b). Gas phase  $\text{SO}_2$  was mainly lower than 1ppb (Fig. 3.13a). Concentrations of up to  $17\mu\text{mol l}^{-1}$  free S(IV) were measured, which were far higher than those in events #1 and #2 (Fig. 3.13b). As mentioned above, near the cloud top the average size of cloud droplets is smaller and the number density of droplets is higher than in the deeper cloud layer. A higher number density of small droplets increases the surface to volume ratio and is consequently favorable for the scavenging of trace gases. Therefore, high concentrations of free S(IV) can be measured in the cloudwater near the cloud top.

During the period from 14:00-14:40, concentrations of up to  $15\mu\text{mol l}^{-1}$   $\text{H}_2\text{O}_2$  were measured in the liquid phase while in the gas phase an average concentration of 0.045 ppb  $\text{H}_2\text{O}_2$  was measured. Assuming an equilibrium and Henry coefficient of  $7.1 \cdot 10^4$  (under  $25^\circ\text{C}$ ), a concentration of 0.045 ppb  $\text{H}_2\text{O}_2$  in the gas phase results in  $17\mu\text{mol l}^{-1}$   $\text{H}_2\text{O}_2$  in the liquid phase. Consequently the high concentration of  $\text{H}_2\text{O}_2$  in the liquid phase can mainly be explained by the photochemical production of  $\text{H}_2\text{O}_2$  in the gas phase. In the deeper cloud layer the  $\text{H}_2\text{O}_2$  concentration in the cloudwater decreased to less  $1\mu\text{mol l}^{-1}$  and in the gas phase  $\text{H}_2\text{O}_2$  was below the detection limit.

The high concentrations of free S(IV) were observed when  $\text{H}_2\text{O}_2$  concentration decreased. Like in event #1 and #2 the pH value measured showed anti-correlation with  $\text{H}_2\text{O}_2$ . As LWC remained stable, which means that our station was in the deeper layer of the cloud, the concentration of free S(IV) was about  $5\mu\text{mol l}^{-1}$ , even though gas phase  $\text{SO}_2$  was below 1 ppb. A possible reason for the accumulation of free S(IV) is the extremely low concentration of  $\text{H}_2\text{O}_2$  in cloudwater.

The ratio of free S(IV)/S(VI) was about 0.05 in the deeper cloud layer and increased up to 0.16 in the samples collected near cloud top with high concentrations of free S(IV). Total HMS concentration was in the same order with that of free S(IV). Low

concentration of original HMS can be caused by the lack of formaldehyde. According to trajectory analysis, the percentage of air mass transport inside cloud was about 100% in this event. As a highly soluble gas, formaldehyde will be efficiently scavenged during the transport of the air mass through clouds.

### **Short summary**

In this event significant amounts of free S(IV) were found in the cloudwater near the cloud top. The ratio of free S(IV)/S(VI) is up to 0.12. This is caused by the high volume to surface ratio of small cloud droplets near cloud top which can significantly enhance the scavenging of SO<sub>2</sub> gas into the cloudwater. In the deeper cloud layer free S(IV) concentrations remained at the level of 5 μmol l<sup>-1</sup> due to low concentrations of H<sub>2</sub>O<sub>2</sub>. However, the concentration of H<sub>2</sub>O<sub>2</sub> in cloudwater increased drastically when low LWC was measured near the cloud top.

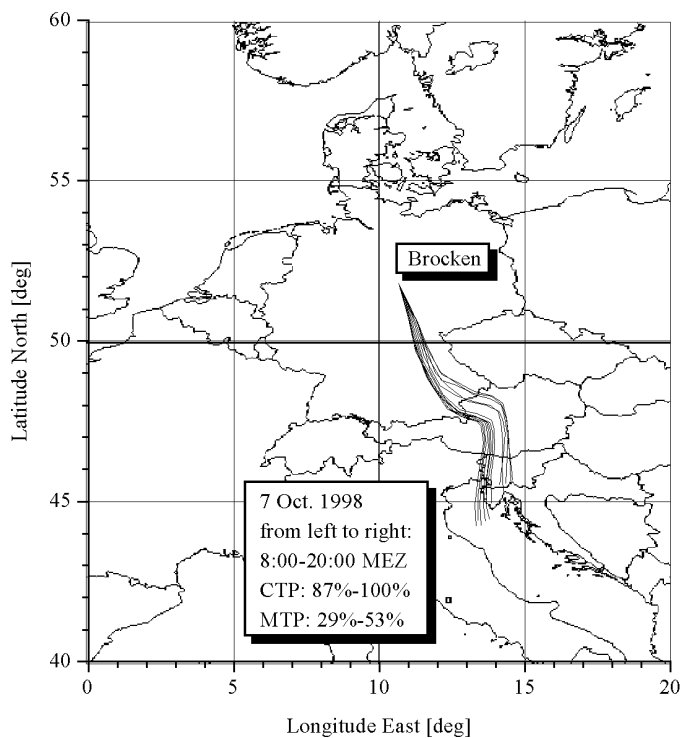
### **Event #4**

Time: October 07<sup>th</sup>, 1998, 8:00 — October 08<sup>th</sup>, 1998, 18:00

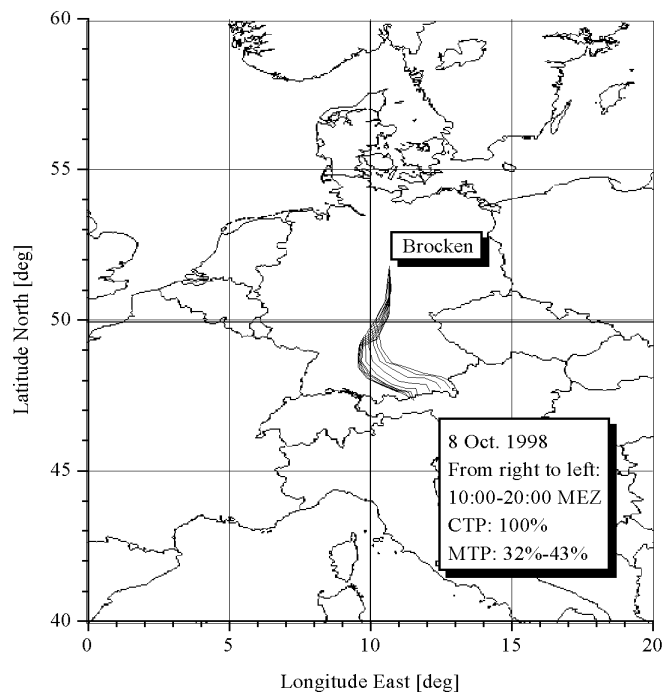
#### **Weather situation and cloud base height**

On October 6<sup>th</sup>, at Mt. Brocken the temperature was below freezing point. On 7<sup>th</sup> an elevated trough laid over France. In front of this trough, a southern to southwestern current in a higher atmospheric level brought warm and humid air mass from the Mediterranean sea via the Alps to Germany. In the same time, a cool airmass from easteurope lifted the upper atmosphere to build clouds and continuous rain. On October 8<sup>th</sup> the core of elevated trough from 7<sup>th</sup> still laid southern of Paris and Germany was under warm maritime subpolar air. An occlusion crossed east Germany from the South. In South and West part of Germany strong precipitation was observed.

On October 7<sup>th</sup> the air mass stemmed from the Italian Adria and crossed Austria, south Germany and arrived at the Brocken station from Southeast (Fig. 3.15). On this way no special polluted industrial areas are located. On 8<sup>th</sup>, the routes of trajectories made a curve in south Germany and turned to south, arriving at Mt. Brocken from South. Again no special pollutant areas are on the way of air mass transport. Compared to the trajectories from 7<sup>th</sup>, the air mass on 8<sup>th</sup> moved relatively slowly. Cloud types



(a)



(b)

Fig. 3.15 (a, b). 72h back trajectories during event #4.

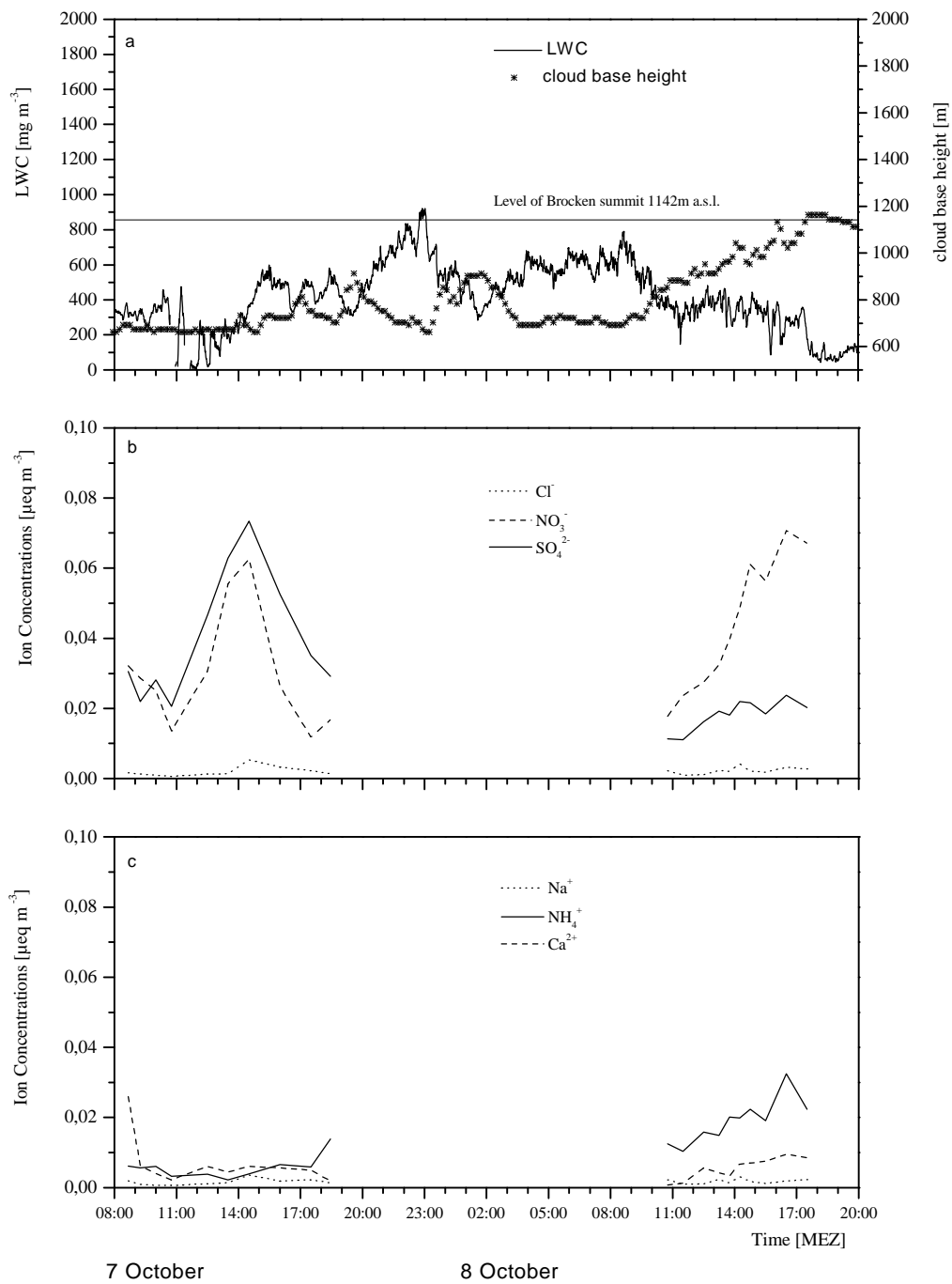


Fig. 3.16. As for Fig. 3.3 but for event #4.

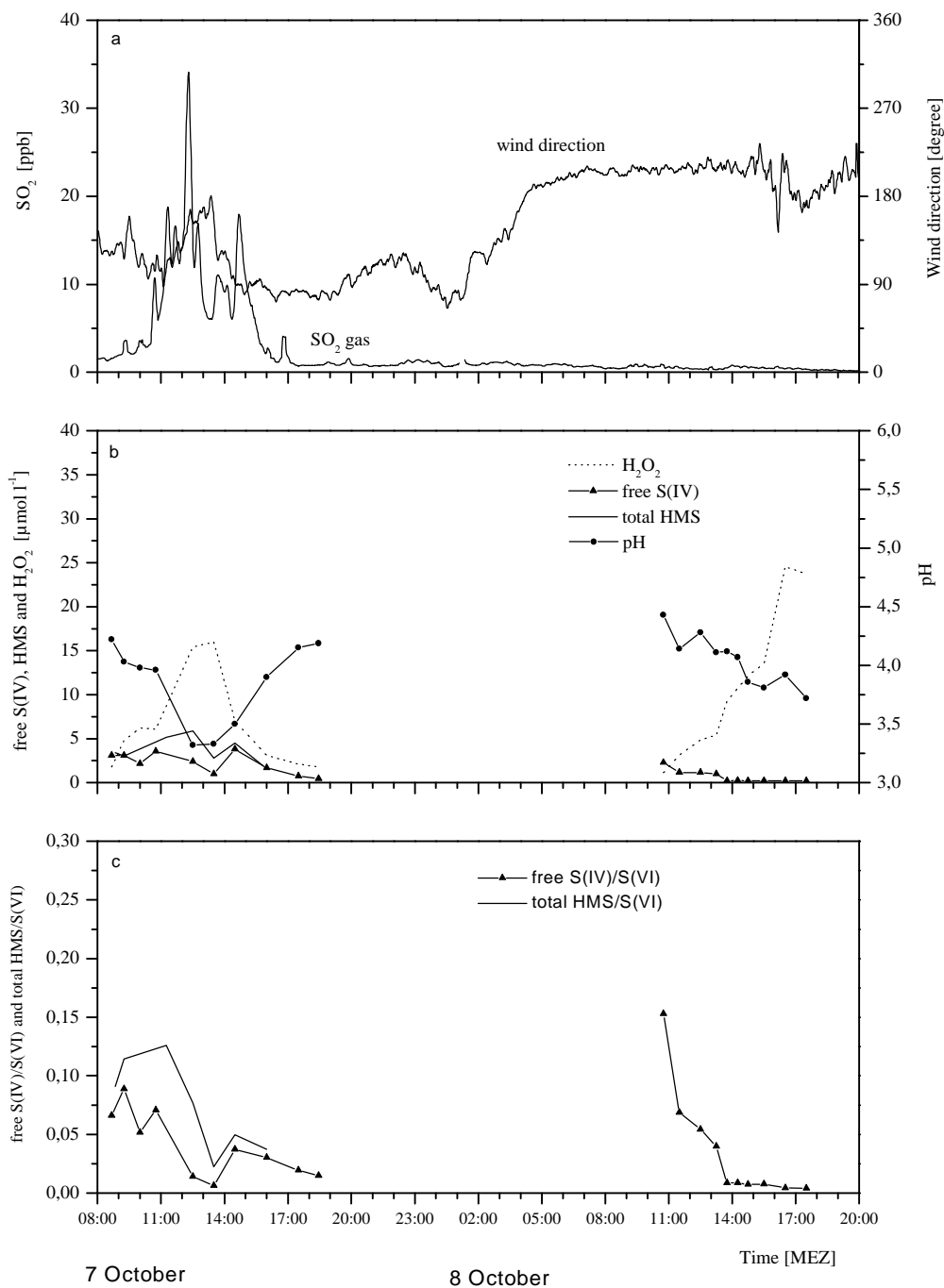


Fig. 3.17. As for Fig. 3.4 but for event #4.

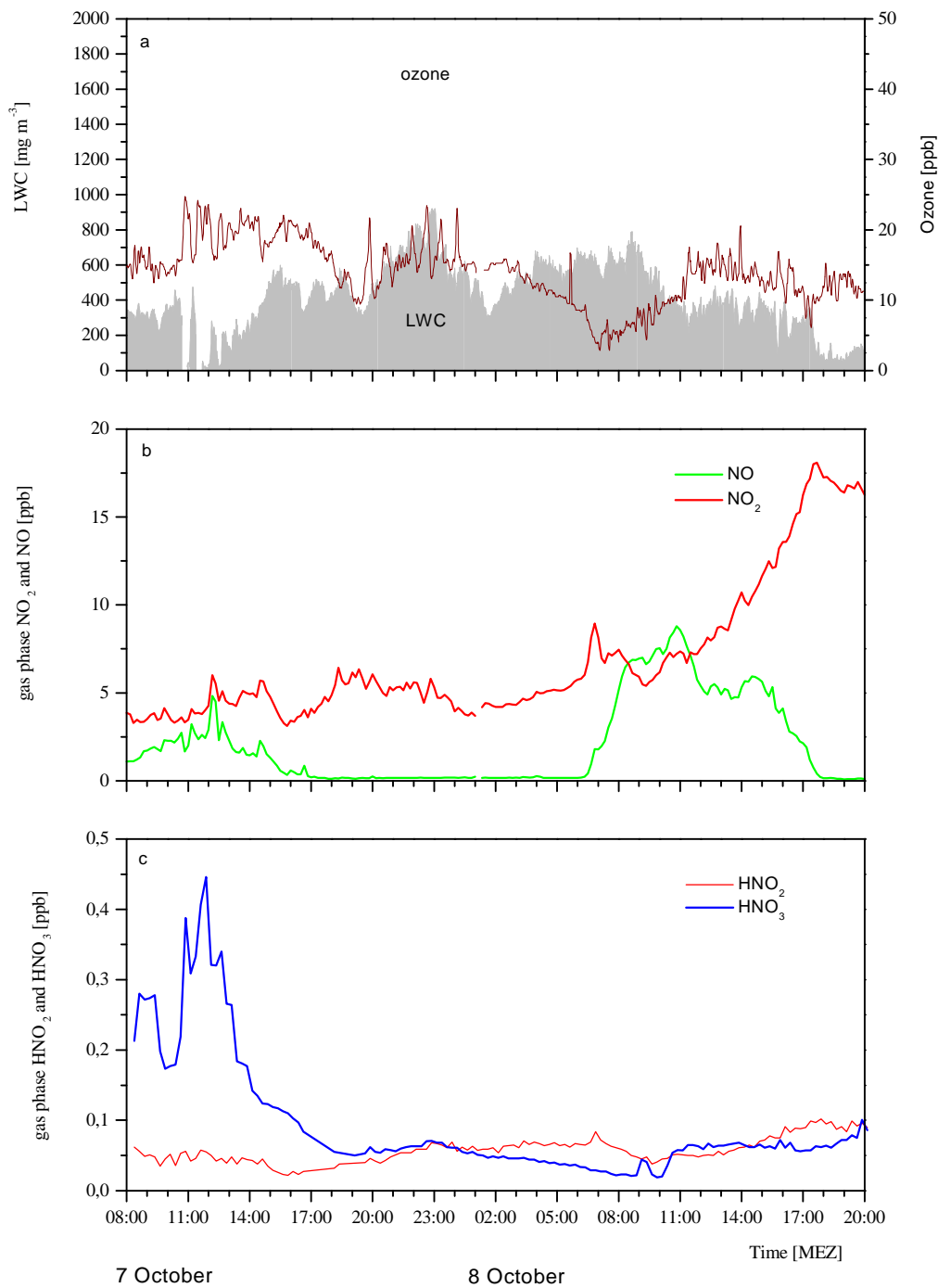


Fig. 3.18. As for Fig. 3.5 but for event #4.

during this event are mainly stratus nebulosus or stratus fractus. Sampling was done only on the daytime of 7<sup>th</sup> and 8<sup>th</sup>. Therefore, our discussion is divided into two separate parts: October 7<sup>th</sup>, 8:00-20:00 and October 8<sup>th</sup>, 10:00-18:00.

### **October 7<sup>th</sup>, 8:00-20:00**

#### **LWC and cloud base height**

From 10:00 to 12:00 the ceilometer measured a cloud base height of less than 700 m above sea level as LWC was lower than 200 mg m<sup>-3</sup> (Fig. 3.16a). Visual observation showed that the station was near cloud top during the period. Similar to event #3, we had the possibility to study the microphysical and chemical characteristics of cloudwater near cloud top.

#### **Ion concentrations**

Ion concentrations in this event were significantly lower than those in other events (Fig. 3.16b,c). The cloudwater during this period contained extremely low concentrations of Ca<sup>2+</sup> and NH<sub>4</sub><sup>+</sup>. Similar to event #3, the highest LWC normalized sulfate and nitrate concentrations were observed, when the site is slightly below the cloud top. Consequently the conductivity of the samples collected near cloud top was 5 times higher than that in other samples. At 14:00 it began to rain and our cloudwater samples from passive samplers were partly mixed with rainwater. Via the dilution effect of rainwater and washout of ions by rainwater, the ion concentrations in the cloudwater decreased. Sulfate concentrations were higher than that of nitrate, were very low, the increase of sulfate and nitrate indicates that either highly acidic which is typical for southeast trajectories. Since concentrations of Ca<sup>2+</sup> and NH<sub>4</sub><sup>+</sup> aerosol particles were entrained or the oxidation of SO<sub>2</sub> and NO<sub>x</sub> contributed significantly to the sulfate and nitrate concentrations of the cloudwater. However, the pH values of aerosol samples (interstitial aerosols) from 9:30-13:30 and from 13:35-17:35 (Tab. 3.3) are higher than 5.0. Consequently, the scavenging of gaseous SO<sub>2</sub> and NO<sub>x</sub> by the cloudwater and their further oxidation to sulfate and nitrate in the liquid phase must be the main reason of increased sulfate and nitrate concentrations in the cloudwater near the cloud top.

**pH, gas phase SO<sub>2</sub>, H<sub>2</sub>O<sub>2</sub>, free S(IV), HMS and S(VI)**

In the time period from 10:00 to 16:00 concentrations of up to 40ppb gas phase SO<sub>2</sub> were observed (Fig. 3.17a). The wind came from southeast with a velocity of only 3m s<sup>-1</sup>, which means that the air mass movement is quite slow. The sharp increase of SO<sub>2</sub> gas phase concentration is therefore most likely from local influence. As already mentioned in event #2, the high concentration of SO<sub>2</sub> gas is very likely caused by the heating in Schierke, which is during this period also in cloud or 100 m below cloud base. SO<sub>2</sub> concentration dropped to under 2ppb after 16:00.

According to the Henry balance, free S(IV) should increase with increasing SO<sub>2</sub> gas phase concentration. However, the observed free S(IV) concentration in the cloudwater was less than 4μmol l<sup>-1</sup> without strong variation. Similar to event #3, H<sub>2</sub>O<sub>2</sub> reached its maximum (15μmol l<sup>-1</sup>) as the station was at the top of the cloud (Fig. 3.17b). At the same time the pH value decreased and was during this period mainly lower than 4.0 with a minimum of 3.3. The high concentrations of H<sub>2</sub>O<sub>2</sub> lead to a continuous oxidation of SO<sub>2</sub> by H<sub>2</sub>O<sub>2</sub> and thus sulfuric acid was produced. The increase of acidity results in a decrease of the solubility of SO<sub>2</sub> into the cloudwater. Therefore, the high SO<sub>2</sub> concentrations caused by the influence of local sources did not lead to a high concentration of free S(IV) in the cloudwater.

At the cloud top, the photochemical reactions are much more active than in deeper cloud layer due to the reflection of solar radiation by the cloud droplets. This can be clearly seen in the increased concentrations of ozone and gaseous HNO<sub>3</sub> (Fig. 3.18).

During the same time period, we performed measurements of total S(IV). In stabilized samples it showed similar trend as free S(IV) with slightly higher concentrations. The original HMS concentration, which can be calculated from the difference of total S(IV) and free S(IV), is quite low. Under conditions of high concentration of H<sub>2</sub>O<sub>2</sub> and high acidity in cloudwater, the HMS formation was limited due to the oxidation of free S(IV) by H<sub>2</sub>O<sub>2</sub>. The ratio of free S(IV)/S(VI) ranged between 0.01 and 0.1. In average 3% of sulfur was in the form of free S(IV).



## **October 8<sup>th</sup> 10:00-18:00**

### **LWC and cloud base height**

On October 8<sup>th</sup> from 10:00 to 18:00 a continuous increase of cloud base resulted in a continuous decrease of LWC (Fig. 3.16a). We monitored the vertical variation of chemical and physical parameters of cloudwater from about 400 m above cloud base to cloud base. The wind direction changed from E to SSW in the early morning of 8<sup>th</sup>. At about 18:00 stratocumulus fractus cloud was replaced by stratocumulus cloud.

### **Ion concentrations**

Like on October 7<sup>th</sup>, ion concentrations were quite low (Fig. 3.16b,c). However, on 8<sup>th</sup> nitrate was the dominant anion, which is typical for the SSW trajectories. Main ion concentrations increased continuously as the cloud base descended slowly.

The spectrum of droplets during this period showed that with the decrease of cloud base, the number concentration of small size droplets (2-4 $\mu$ , 4-6 $\mu$ , 6-8 $\mu$  and 8-10 $\mu$ ) increased obviously whereas the number concentration of large droplets slightly decreased. That means that the entrainment of fresh air from the layers below cloud base produced more small newly activated cloud droplets and at the same time large droplets are partly evaporated. We measured ion concentrations in two drop size ranges: 4<D<10 $\mu$ m and 10<D<31 $\mu$ m. In the fraction of smaller droplets more sulfate was found as the cloud base decreased, while in deeper cloud layer sulfate was concentrated in the fraction of larger droplets (Wieprecht et al., 1999).

### **pH, gas phase SO<sub>2</sub>, H<sub>2</sub>O<sub>2</sub>, free S(IV), HMS and S(VI)**

Gas phase SO<sub>2</sub> concentration was lower than 1 ppb on 8<sup>th</sup> (Fig. 3.17a). The concentration of H<sub>2</sub>O<sub>2</sub> in the liquid phase increased drastically as LWC decreased. Only the unstabilized cloudwater samples were collected on October 8<sup>th</sup>. Free S(IV) concentration in these samples decreased to less than 300 nmol l<sup>-1</sup> as H<sub>2</sub>O<sub>2</sub> concentration in the liquid phase increased.

The pH value of the cloudwater decreased 0.7 unit in this period (from 4.4 to 3.7), which is partly due to production of sulfate acid from free S(IV) and partly due to production of nitric acid. Gaseous HNO<sub>3</sub> and NO<sub>x</sub> concentration increased near cloud

base due to the entrainment of fresh air masses and their dissolution and further reactions in the liquid phase led to the observed increase of nitrate in the cloudwater.

The concentration of free S(IV) in the cloudwater was lower than that on October 7<sup>th</sup>. However, free S(IV)/S(VI) ratio was in average 0.066, i.e. about 7% of sulfur was found in the form of S(IV) in the cloudwater. This ratio dropped to nearly zero as the site was near the base of the cloud. A high value of the ratio between free S(IV) and total sulfur can be found when the concentrations of sulfate and oxidants are low. This indicates that especially in the unpolluted atmosphere, where the number concentration of sulfate aerosol was relatively low, free S(IV) is an important form of sulfur even if the concentration of gaseous SO<sub>2</sub> is low.

### **Short summary**

In this event we observed a variation of ion concentrations near the cloud top (7<sup>th</sup>) and near the cloud base (8<sup>th</sup>). In both cases the concentration of free S(IV) was low as long as high H<sub>2</sub>O<sub>2</sub> concentrations were observed. However, due to the low concentration of sulfate ions in the cloudwater, the ratio of free S(IV)/S(VI) is significantly high on 8<sup>th</sup>. From the data on 7<sup>th</sup> we can also conclude that high concentrations of SO<sub>2</sub> alone can not lead to a high amount of free S(IV) in cloudwater, when the acidity is high and there are enough oxidants available.

### **3.5 Summaries and conclusions**

From Tab. 3.4 to 3.6, we can see that liquid phase H<sub>2</sub>O<sub>2</sub> concentration, pH value and LWC are the main limiting factors for free S(IV) concentrations and free S(IV)/sulfate ratios in cloudwater. The concentrations of free S(IV) and the ratio of free S(IV)/S(VI) decrease with increasing concentrations of liquid phase H<sub>2</sub>O<sub>2</sub> (Tab. 3.4). Under low concentration (<1ppb) of gas phase SO<sub>2</sub> the concentrations of free S(IV) in cloudwater are negligible in very acid cloudwater. However, with the increase of the pH value, both the average concentration of free S(IV) and the ratio of free S(IV) to sulfate increase significantly (Tab. 3.5). LWC has great influence on the scavenging of trace gases by cloudwater. Low LWCs were mainly observed near cloud base while higher LWC (more than 1000 mg m<sup>-3</sup>) was mainly observed just below cloud top. The highest free S(IV) concentration and the highest value of free S(IV)/S(VI) ratio were measured when

LWC was high (Tab. 3.6). Even in the cases with  $\text{SO}_2 < 1\text{ppb}$ , in average more than  $5\mu\text{mol l}^{-1}$  free S(IV) was measured in cloudwater.

Table 3.4. Summary of free S(IV) concentrations and the values of free S(IV)/S(VI) ratio under different concentrations of liquid phase  $\text{H}_2\text{O}_2$ .

	$\text{SO}_2 < 1\text{ppb}$		$1\text{ppb} < \text{SO}_2 < 5\text{ppb}$		$\text{SO}_2 > 5\text{ppb}$		total	
	Free S(IV)	Free S(IV)/S(VI)	Free S(IV)	Free S(IV)/S(VI)	Free S(IV)	Free S(IV)/S(VI)	Free S(IV)	Free S(IV)/S(VI)
$\text{H}_2\text{O}_2$ [ $\mu\text{mol l}^{-1}$ ]								
$\text{H}_2\text{O}_2 < 1$	4.20	0.061	4.96	0.083	---	---	4.37	0.066
$1 < \text{H}_2\text{O}_2 < 5$	1.96	0.019	3.30	0.038	4.00	0.046	2.34	0.030
$\text{H}_2\text{O}_2 > 5$	0.42	0.004	---	---	2.98	0.032	1.16	0.017
Total	3.03	0.040	4.01	0.058	3.34	0.037	3.17	0.045

Table 3.5. Summary of free S(IV) concentration and the value of free S(IV)/S(VI) ratio under different values of pH.

PH	$\text{SO}_2 < 1\text{ppb}$		$1\text{ppb} < \text{SO}_2 < 5\text{ppb}$		$\text{SO}_2 > 5\text{ppb}$		total	
	Free S(IV)	S(IV)/S(VI)	Free S(IV)	S(IV)/S(VI)	Free S(IV)	S(IV)/S(VI)	Free S(IV)	S(IV)/S(VI)
pH < 4	0.24	0.002	1.32	0.018	3.34	0.037	1.40	0.018
$4 < \text{pH} < 5$	3.09	0.042	5.63	0.081	---	---	3.51	0.053
pH > 5	3.58	0.043	---	---	---	---	3.58	0.043

Table 3.6. Summary of free S(IV) concentration and the value of free S(IV)/S(VI) ratio under different LWC.

LWC [ $\text{mg m}^{-3}$ ]	$\text{SO}_2 < 1\text{ppb}$		$1\text{ppb} < \text{SO}_2 < 5\text{ppb}$		$\text{SO}_2 > 5\text{ppb}$		total	
	Free S(IV)	Free S(IV)/S(VI)	Free S(IV)	Free S(IV)/S(VI)	Free S(IV)	Free S(IV)/S(VI)	Free S(IV)	Free S(IV)/S(VI)
LWC < 400	0.28	0.003	2.52	0.066	2.98	0.032	1.40	0.048
$400 < \text{LWC} < 1000$	1.96	0.021	2.58	0.035	4.00	0.046	2.17	0.023
LWC > 1000	5.45	0.082	8.45	0.124	---	---	7.10	0.092

We have collected cloud samples near cloud base, in deeper cloud layer and near cloud top. Microphysical parameters like LWC and droplet size have different

characteristics in the three parts of a cloud. Accordingly, we observed different concentration of free S(IV) and the ratio of free S(IV)/S(VI) in the three parts of clouds.

Near cloud base, free S(IV)/S(VI) ratio is negligibly low, while total S(IV)/S(VI) ratio is significantly high. Even under low gas phase SO<sub>2</sub> (lower than 1ppb), considerable concentration of HMS was measured near cloud base. That means the concentration of formaldehyde might be the limiting factor of the formation of HMS in cloudwater.

In deeper cloud layer, normally low concentration of H<sub>2</sub>O<sub>2</sub> and relatively high concentration of free S(IV) (3~5 μmol l<sup>-1</sup>) were observed in cloudwater. It is due to the low production of gaseous H<sub>2</sub>O<sub>2</sub> in the deeper layer of clouds.

Near cloud top, not only LWC reaches the highest value, but also the entrainment from cloud top is strong. The result is, SO<sub>2</sub> gas is scavenged very efficiently by small cloud droplets which have much higher number density near cloud top than in the deeper layer of cloud. Therefore, significantly high concentration of free S(IV) was measured.

The free S(IV)/S(VI) ratio ranged from zero to 0.18, with mean value of 0.03 whereas total HMS/S(VI) ratio ranged from zero to 0.3, with mean value of 0.04 during our experiment at Mt. Brocken from September, 23<sup>rd</sup> to October, 8<sup>th</sup>, 1998. Compared to the experiment at Berlin-Frohnau, the fraction of S(IV) in total sulfur in cloudwater is much lower than that in rainwater. Most of sulfur exist in the oxidized form. However, under certain circumstances, e.g. near cloud top with high LWC and in deeper cloud layer with low concentrations of oxidants, free S(IV) can be an important form of sulfur in cloudwater and thus is not negligible. When clouds dissipate, the part of free S(IV) in cloudwater will turn back to gas phase SO<sub>2</sub> and take part in the next cloud cycle or will be oxidized in the gas phase.

## Chapter 4

# **One-dimensional physical-chemical stratiform cloud model**

### **4.1 Introduction**

Numerous cloud physical and chemical models have been developed to investigate the dynamical, microphysical and chemical processes going on in a cloud or clouds system (Hegg et al., 1986; Trembley and Leighton, 1986; Lee et al., 1986; Hu et al., 1986; Qin et al., 1986, 1992; Lelieveld and Crutzen, 1991; Möller and Mauersberger, 1992b; Colvile et al., 1994; Liu et al., 1997; Hallberg et al., 1997). The degree of elaboration of the cloud models range from the simple box model to a three dimensional model. The complexity of physical and chemical processes included in these models vary according to their researching focuses. The results vary with different parameterization of microphysical and chemical processes. The simplest type of cloud chemical model is box model or flow-through reactor (Möller and Mauersberger, 1992b) which is quite useful to investigate the chemical evolutions of a cloud system without meteorological or dynamical considerations. One-dimensional time-dependant model is popular to investigate stratiform as well as simple cumulous cloud processes (Lee et al., 1986; Qin, 1992). Three dimensional cumulous cloud models can properly describe complicated dynamics of a cloud, however, they are also computationally time-costing. In some models only in-cloud transformation and redistribution of air pollutants were considered (Qin et al., 1986). Sub-cloud scavenging of trace gases by rainwater plays an important role in the acidification of rainwater especially in heavily polluted areas. Some publications have treated this process separately from cloud model (Wang et al., 1988; Liu and Wang, 1992; Asman, 1995; Jensen and Asman, 1995).

A one-dimensional physical-chemical stratiform cloud model is in many cases sufficient to describe the basic chemical processes leading to aqueous transformation of  $\text{SO}_2$  to sulfate. Since our aim of this work is to estimate the S(IV)/S(VI) ratio in cloud- and rainwater and the important physical and chemical factors which affect the scavenging of  $\text{SO}_2$  in the sub-cloud layer, we believe that an assumption of horizontal homogeneity inside cloud is acceptable. The proper estimation of the S(IV)/S(VI) ratio in cloud- and rainwater and the wet deposition of sulfite can be very useful in some regional and global models which put their emphases on the atmospheric sulfur cycle (Langner and Rohde, 1991; Chin et al., 1996; Lelieveld et al., 1997).

Simplification or parameterization is a must in every model. On one hand, it is due to instrumental or measurement limitations which makes it impossible to measure every parameter needed in models. On the other hand, it is due to the limit of our knowledge, computer facility and computing time, etc. Therefore, it is a serious problem in each model to compare model results with observations.

Our model was initialized based on the data from our field experiments (see Chapter 2 and 3), and the results from modelling were used to compare with our observations qualitatively. The data from other experiments were used for the parameters we have not measured due to the lack of measurement instruments.

The microphysical part of this model is based on Hu et al. (1986), in which a series of simplifying parameterization for microphysical processes controlling cloud- and raindrop formation were made. The distribution of cloud and rain droplets are parameterized and the chemical composition of droplets is assumed to be not size-dependent. The mass transfer of gas to cloudwater, and subsequently to rainwater is reached using mass-continuity equations.

The chemical part of this model was divided into a gas phase chemical mechanism, so-called RADM2 (Regional Acid Deposition Model, version 2) (Stockwell et al., 1990) and an aqueous phase chemical mechanism from Möller and Mauersberger (1992b). They were coupled by the mass transfer processes based on the method of Schwartz (1986) to investigate trace gas production and scavenging during cloud events and precipitation. The change of chemical species in the gas and liquid phase within a precipitating cloud process was studied by the means of continuity equations. We paid

main attention in our model to chemical mechanisms which are important for sulfate production.

As we have learned from Chapter 3, near cloud base and cloud top, due to the strong entrainment from outside the cloud layer, many new small cloud droplets can be produced due to the activation of aerosol particles which act as cloud condensation nuclei. Accordingly, gaseous SO<sub>2</sub> can be better scavenged by the cloudwater near cloud base and cloud top than in the deeper cloud layer. However, in our model the number concentration of cloud droplets are assumed to be vertically the same and constant throughout the evolution of the cloud. Cloud base height and the top boundary of the cloud are also assumed to be constant. Air mass entrainment from the boundaries is not included. Therefore, it is impossible to discuss with this model the vertical variation of S(IV) to S(VI) ratio in cloudwater which is strongly dependant on entrainment from the boundaries and droplet number variations near the cloud base and the cloud top. Our main emphasis of this model study is, therefore, on the increase of S(IV) deposition from the cloud base to the ground due to sub-cloud scavenging of SO<sub>2</sub> by rainwater. The results are qualitatively compared to the experimental observations from Berlin-Frohnau experiment (see Chapter 2).

## 4.2 Cloud physics

The dynamic of a warm stratiform cloud can be described using temperature, humidity and vertical velocity. Because of vertical advection, warm humid air mass is raised up to a certain height at which water vapor begins to condense and thus a cloud is formed. Horizontal homogeneity was assumed and initial vertical distribution of temperature, humidity, vertical velocity and pressure is given as shown in Fig 4.1. Pressure was given according to barometric law. The cloud base height was assumed to be 1000 m. The updraft velocity increases in the function of height and reaches its maximum of 0.2 m s<sup>-1</sup> in the middle of the cloud layer. In stratiform clouds, the vertical updraft are quite weak and therefore the transport via eddy diffusion can be important. We assumed here that the transport is proportional to the eddy diffusion coefficient  $K$  (20 m<sup>2</sup> s<sup>-1</sup>) (Qin et al., 1986). Water vapor, cloudwater and rainwater are considered and the mass continuity equations between the three species are given as follows:

$$\frac{\partial Q_v}{\partial t} = -W \frac{\partial Q_v}{\partial z} - S_{vr} - S_{vc} + K \frac{\partial^2 Q_v}{\partial z^2} \quad (1)$$

$$\frac{\partial Q_c}{\partial t} = -W \frac{\partial Q_c}{\partial z} + S_{vc} - C_{cr} - A_{cr} + K \frac{\partial^2 Q_c}{\partial z^2} \quad (2)$$

$$\frac{\partial Q_r}{\partial t} = -(W - V_r) \frac{\partial Q_r}{\partial z} + S_{vr} + C_{cr} + A_{cr} + K \frac{\partial^2 Q_r}{\partial z^2} \quad (3)$$

$$\frac{\partial N_r}{\partial t} = -(W - V_r) \frac{\partial N_r}{\partial z} + NC_{rr} + NA_{cr} + NS_{vr} + K \frac{\partial^2 N_r}{\partial z^2} \quad (4)$$

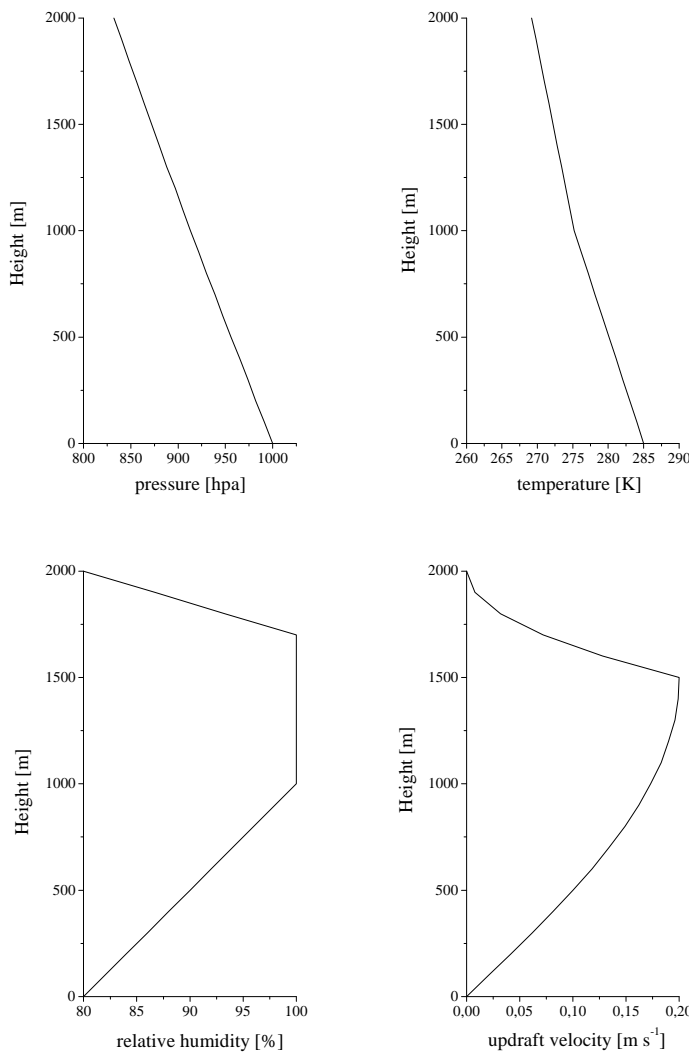


Fig. 4.1. The initial profiles of pressure, temperature, relative humidity and updraft velocity.



Here  $Q_v$ ,  $Q_c$  and  $Q_r$  represent the mass amounts of vapor, cloudwater and rainwater in the unit of g per kg air ( $\text{g kg}^{-1}$ ),  $N_r$  the number of rain droplets per kg air,  $S_{vc}$  and  $S_{vr}$  are vapor condensation on (or evaporation of) cloud and rain droplets respectively,  $C_{cr}$  is the rate of conversion of cloudwater to rainwater by collision and coalescence,  $A_{cr}$  is autoconversion rate,  $NA_{cr}$  is the rate of raindrop production by autoconversion rate,  $NC_{rr}$  is the rate of raindrop production (or lost) by collision and coalescence between different size rain droplets.  $S_{vc}$ ,  $S_{vr}$ ,  $C_{cr}$ ,  $A_{cr}$  have the unit of  $\text{g kg}^{-1} \text{ s}^{-1}$ ,  $NC_{rr}$ ,  $NA_{cr}$ ,  $NS_{vr}$  have the unit of  $\text{kg}^{-1} \text{ s}^{-1}$ .

$\Gamma$ -distribution was assumed for the cloud and rain droplets, in which  $\alpha$  is 2 and 0 for cloud droplets and rain droplets respectively:

$$dN = N_0 D^\alpha e^{-\lambda D} dD$$

$D$  (cm) is the cloud- or raindrop diameter,  $dN$  is the number of droplets in per unit air mass ( $\text{kg}^{-1}$ ) with diameter between  $D$  and  $D + dD$ ,  $N_0$  and  $\lambda$  are parameters. However, all rain droplets are assumed to fall with mean velocity. Group terminal velocity of rain droplets  $V_r$  ( $\text{cm s}^{-1}$ ) is

$$V_r = 2.97 A_{vr} \lambda^{-0.8} \quad (5)$$

where  $A_{vr} = 2100 \text{ cm}^{0.2} \text{ s}^{-1}$ .

The number of cloud droplets does not change much in cloud level except at the cloud base and cloud top. So we just assumed the total number of cloud droplets

$$N_c = \int_0^{\infty} N_{0c} D^2 e^{-\lambda_c D} dD \quad (6)$$

as constant.

The triggering mechanisms for the development of rain is the process in which cloud droplets grow to size large enough to be called small raindrops, so-called ‘‘autoconversion’’, which initiates the ‘‘warm’’ rain. The raindrops continue to grow by accretion of droplets. The rate of autoconversion is considered to be zero when the trigger function  $F$  is smaller than 1. If  $F$  is greater than 1, then the rate of autoconversion is

$$A_{cr} = \frac{J\rho Q_c^2}{60} \left(6 + \frac{0.02N_c}{D_c\rho Q_c}\right)^{-1} \quad (7)$$

in which  $J$  is a normalization factor, here considered to be 0.25,  $\rho$  air density ( $\text{kg m}^{-3}$ ).

Trigger function  $F$  follows a differential equation

$$\frac{\partial F}{\partial t} = -W \frac{\partial F}{\partial z} + K \frac{\partial^2 F}{\partial z^2} + \frac{\rho Q_c}{60} \left(2 + \frac{0.02N_c}{D_c\rho Q_c}\right)^{-1} \quad (8)$$

The increasing rate of raindrop number due to autoconversion is

$$NA_{cr} = A_{cr} / Q_{r0} \quad (9)$$

where  $Q_{r0}$  taken as  $5 \cdot 10^{-7}$  g.

Condensation of water vapor to cloud ( $S_{vc}$ ) and rainwater ( $S_{vr}$ ) can be described as

$$S_{vc} = (Q_v - Q_{sw}) / dt \quad (10)$$

$$S_{vr} = 4\pi D_w N_r R_r f(R_r) (Q_v - Q_{sw}) \quad (11)$$

$$D_w = 0.211 \left(\frac{T}{T_0}\right)^{1.94} \left(\frac{P_0}{P}\right) \text{ cm}^2 \text{ s}^{-1} \quad (12)$$

ventilation factor  $f(R_r)$  is given by Frossling's equation

$$f(R_r) = 1 + 0.23(2R_r V_r / \nu)^{0.5} \quad (13)$$

where  $Q_{sw}$  ( $\text{g kg}^{-1}$ ) is the saturated water vapor under the temperature of  $T$ ,  $D_w$  diffusivity of water vapor in air,  $\nu$  the kinematic viscosity of air ( $0.165 \text{ cm}^2 \text{ s}^{-1}$ ),  $T_0$  is melting temperature of ice,  $T$  is the temperature of air mass,  $P_0$  is standard atmosphere pressure and  $P$  is the pressure of air mass. In stratiform warm cloud the vertical advection is much smaller than that in cumulous cloud, the supersaturation rate is also quite small, hence we can assume that all saturated water vapor will be condensed quickly.

As the raindrops fall through the sub-cloud layer, in which air humidity is less than 100%, small rain droplets will evaporate to particles and this part of rainwater can not arrive the ground. The lost of rain drop number due to evaporation can be described as

$$NS_{vr} = S_{vr} \cdot N_r / Q_r \quad (14)$$

The rate of conversion of cloudwater to rainwater due to collision and coalescence is

$$C_{cr} = \frac{\pi}{4} \Gamma(3.8) A_{vr} \rho Q_c E \left( \frac{Q_r}{6 A_{mr} N_r} \right)^{\frac{2.8}{3}} N_r \left( \frac{P_0}{P} \right)^{0.286} \quad (15)$$

where  $E$  is the mean collision-coalescence efficiency, taken to be 0.8.  $A_{mr}$  is  $0.524 \text{ g cm}^{-3}$ . The collision among raindrops change only the number of raindrops and the drop distribution.

$$NC_{rr} = 4 \cdot 10^{-8} \rho N_0^2 \left( -\exp^{-0.152\lambda_r} + S_r \exp^{-0.23\lambda_r} \right) \quad (16)$$

$$S_r = 3$$

Temperature ( $T$  in K) in each layer changes as the cloud develops. Water vapor releases latent heat as it condenses and heats the air mass surrounded. On the contrary, evaporation is followed with the cooling of surrounding air. Temperature  $T$  in each layer is thus calculated as follows:

$$\frac{\partial T}{\partial t} = -W \frac{\partial T}{\partial z} - 0.0098 * W + 2.5 \times (S_{vc} + S_{vr}) \quad (17)$$

$0.0098 \text{ } ^\circ\text{C m}^{-1}$  is the dry adiabatic decreasing rate of temperature.

### 4.3 Scavenging of aerosols and dissolution of gases into the liquid phase

Aerosols will be transferred to the liquid phase either by acting as condensation nuclei or by coagulating with an existing droplet. In our model the activation process of aerosols was simplified without considering different activation efficiency of different sized aerosol particles. Nucleation scavenging is the main part of in-cloud scavenging and also the beginning of cloud chemistry. As liquid droplets form on the hygroscopic particles which serve as cloud condensation nuclei (CCN), all the soluble substances contained in the CCN will make up the initial chemical compositions of cloud droplets. Because of the lack of adequate information on aerosol activity spectrum and chemical composition of active part of aerosols from experimental point of view, an initial concentrations of cloudwater ions were given. However, in the future work size dependence of aerosol chemical compositions and nucleation activation should be considered in more detail. Since a great part of aerosols in the cloud layer will be transferred to the aqueous phase via nucleation scavenging, the uptake of aerosols by cloudwater by coagulation is not considered in our model. Aerosol particles will be

removed by rainwater via impaction. Aerosol scavenging efficiency by falling rain droplets is parameterized as

$$\Lambda = 4.2 \cdot 10^{-4} \cdot 0.8 \cdot (Q_r \cdot V_r \cdot \rho)^{0.79} \quad (18)$$

where  $V_r$  is the mean falling velocity of raindrops and  $\rho$  is the density of air mass.

As soon as water droplets form, mass transfer of gas species to liquid drops will happen. As mentioned in Chapter 1, the process include different steps in which chemical reactions in droplets are mainly rate determining. The mass transfer of gases to the liquid phase follows the theory of Schwartz (1986). The density of flux of gas toward the drop can be shown as

$$F = \frac{K_g}{RT} \left( g - \frac{c}{H_{eff}} \right) \quad (19)$$

$$K_g = \left( \frac{r^2}{3D_g} + \frac{4r}{3v\alpha} \right)^{-1} \quad (20)$$

where  $g$  is the bulk gas-phase concentration (atm),  $c$  the aqueous-phase concentration ( $\text{mol l}^{-1}$ ),  $R$  the gas constant ( $1 \text{ atm mol}^{-1} \text{ K}^{-1}$ ),  $T$  the temperature in K,  $H$  the efficient Henry constant ( $\text{mol l}^{-1} \text{ atm}^{-1}$ ),  $K_g$  mass transfer coefficient ( $\text{s}^{-1}$ ),  $r$  drop radius (cm),  $D_g$  the gas-phase diffusion coefficient ( $\text{cm}^2 \text{ s}^{-1}$ ),  $v$  the mean molecular speed ( $5 \times 10^4 \text{ cm s}^{-1}$ ) and  $\alpha$  the accommodation coefficient (dimensionless).

The mass transfer of gases to falling raindrops should take the ventilation factor  $f(r)$  into consideration. Therefore,  $D_g$  in equation (20) should be replaced by  $D_g \cdot f(r)$ .

$$f(r) = 1 + 0.3 \left( \frac{2 \cdot r \cdot V_r}{0.133} \right)^{-0.5} \quad (21)$$

where rain drop falling velocity  $V_r$  has the unit of  $\text{cm s}^{-1}$ .

#### 4.4 RADM2 gas phase chemical reaction system

Atmospheric gas phase chemistry is based on RADM2 (Stockwell et al., 1990). The chemical mechanism consists of an explicit set of inorganic reactions and a lumped organic chemistry scheme. The concentrations of abundant stable gas phase species  $\text{O}_2$ ,  $\text{N}_2$  and  $\text{H}_2\text{O}$  were parameterized.

About 1970 it was found that hydroxyl radical play a critical role in tropospheric chemistry. As mentioned in chapter 1, reaction of  $\text{SO}_2$  with the OH radical is the only gas phase process that is fast and efficient enough to account for most of the sulfuric acid production in the gas phase processes. OH radicals are generated via the reaction of excited oxygen atoms, which are produced by photolysis of ozone with  $\text{H}_2\text{O}$ .

The importance of photochemistry in the oxidation of sulfur dioxide is that oxidants such as  $\text{H}_2\text{O}_2$  can be produced via photochemical reactions. In the gas phase,  $\text{H}_2\text{O}_2$  is formed from the interactions of Hydroperoxy ( $\text{HO}_2$ ) and hydrated hydroperoxy ( $\text{H}_2\text{O}\cdot\text{HO}_2$ ) radicals, which are produced by the photochemical reactions of atmospheric trace gases such as ozone and volatile organic compounds. The removal mechanisms for  $\text{H}_2\text{O}_2$  from the gas phase are photolysis of  $\text{H}_2\text{O}_2$ , reaction with OH radicals, and heterogeneous processes such as washout, rainout and dry deposition.

Another important oxidant of  $\text{SO}_2$  in the liquid phase is ozone. Ozone is also produced via photochemistry in the gas phase. Photochemical production of formaldehyde is also taken into consideration in this model.

#### **4.5 Aqueous phase chemical reaction system**

A cloud aqueous phase chemistry mechanism based on the work of Möller and Mauersberger (1992b) was used here to study the aqueous phase sulfur chemistry. Among the thousands of liquid phase reactions are known until now, we selected only the reactions relevant to the S(IV) multiphase chemistry. 38 liquid phase species are used in the model from which 20 species exist also in the gas phase. The mass transfer of these species from the gas phase to the aqueous phase are considered as reversible. Oxidants  $\text{H}_2\text{O}_2$  and ozone are also generated in aqueous phase.

The radical pathway of sulfate production in the liquid phase is ignored in our model. According to the model study of Möller (1995), from the different sulfate production pathways in the liquid phase the percentage of radical reactions is less than 10% in the daytime.  $\text{H}_2\text{O}_2$  is the dominant oxidant in summer and ozone plays important role in winter daytime. Only in winter night, radical reactions can be important. Since our cloud model simulates a precipitation process in the daytime of November, we assume that sulfate production via radical reactions in the liquid phase can be ignored.

#### 4.6 Numerical solvers

The time step of integration for physical processes is 10 seconds. The equations describing physical terms are calculated with the finite differential method. For the chemical equations initial time step of 10 seconds is given. The system of the chemical rate equations is numerically integrated using a hybrid integration technique (Young and Boris, 1977). The evolution time of clouds is 3 hours.

#### 4.7 Initial and boundary conditions

According to the vertical profile of relative humidity, at time=0 water vapor above 1000 m was saturated and ready for condensing. Cloudwater and rainwater content were assumed to be zero at all layers at the beginning. On the ground surface, continuity condition is assumed for the rainwater.

As long as CCN aerosols activated into cloudwater, the following initial values were accepted for the concentrations of ions (in the unit of  $\mu\text{g}$  ion amount in per cubic meter air volume) in cloudwater:

Tab. 4.1. Initial concentrations of ions in cloudwater [ $\mu\text{g m}^{-3}$ ]

Ion	Concentration	Ion	Concentration	Ion	Concentration
$\text{SO}_4^{2-}$	2.4	$\text{H}^+$	0.003	Fe(II)	$6.7 \times 10^{-3}$
$\text{NO}_3^-$	3.1	Cu(I)	$1.9 \times 10^{-4}$	Fe(III)	$1.3 \times 10^{-2}$
$\text{NH}_4^+$	0.85	Cu(II)	$1.9 \times 10^{-6}$	Mn(II)	$4.8 \times 10^{-3}$
$\text{Ca}^{2+}$	0.4			Mn(III)	$1.6 \times 10^{-6}$

The initial concentrations of Fe(II) and Fe(III) in cloudwater are accepted from the result of Brocken experiment at June 7<sup>th</sup>, 1994, which was carried out by our institute in cooperation with the Institute for tropospheric research (IFT).

The initial concentrations of main gaseous species are listed in Tab. 4.2. Background concentration of gas phase formaldehyde is 0.5 ppb according to our measurement in Berlin in summer 1998. Since Mt. Brocken is in the area without special pollution, and not far away from Berlin, we assume that 0.5 ppb formaldehyde concentration is also available for Mt. Brocken.

Tab. 4.2. Initial concentrations of main gaseous species referred in this work [ppb]

Species	concentration	species	Concentration	species	Concentration
NO <sub>2</sub>	5	O <sub>3</sub>	30	CO <sub>2</sub>	330×10 <sup>3</sup>
NO	0.2	H <sub>2</sub> O <sub>2</sub>	0.1	CO	200
NH <sub>3</sub>	3	SO <sub>2</sub>	10	CH <sub>4</sub>	1.7×10 <sup>3</sup>
HNO <sub>3</sub>	0.1	HCHO	0.5		

The initial ion concentrations of aerosol we used in our model has strong alkaline characters for the purpose to test the buffer effect of alkaline aerosols for the wet deposition of sulfite by rainwater.

Table 4.3. Initial concentrations of ions in aerosol [ $\mu\text{g m}^{-3}$ ]

Ion	Concentration	Ion	Concentration
SO <sub>4</sub> <sup>2-</sup>	0.96	NH <sub>4</sub> <sup>+</sup>	0.72
NO <sub>3</sub> <sup>-</sup>	1.24	Ca <sup>2+</sup>	0.4

## 4.8 Results and discussions

### 4.8.1 Physical model results

Temporal and vertical variations of  $Q_c$  and  $Q_r$  are presented in Fig. 4.2a and 4.2b respectively. Cloudwater is first produced in the middle levels of the cloud. Accordingly, raindrops are also first produced in the middle levels of the cloud. Fig. 4.3 shows the development of rain intensity and precipitation on the ground. After about 135 minutes of simulation time, the precipitation begins. The rain intensity increases rapidly to a maximum of  $1.1 \text{ mm hr}^{-1}$  in the next 15 minutes and then decrease to a steady rain intensity on the ground. The steady state of rain intensity is caused by our assumption that updraft velocity is constant throughout the simulation and there is no entrainment of dry air from lower boundary.

In Chapter 2 we discussed if the evaporation of rainwater during the falling period of rain droplets from the tower to the ground is negligible or not. Here we will calculate the percentage of evaporated rainwater in the total rainwater content with theoretical functions (see Functions 11-13) based on Hu et al. (1986). We assume that the relative

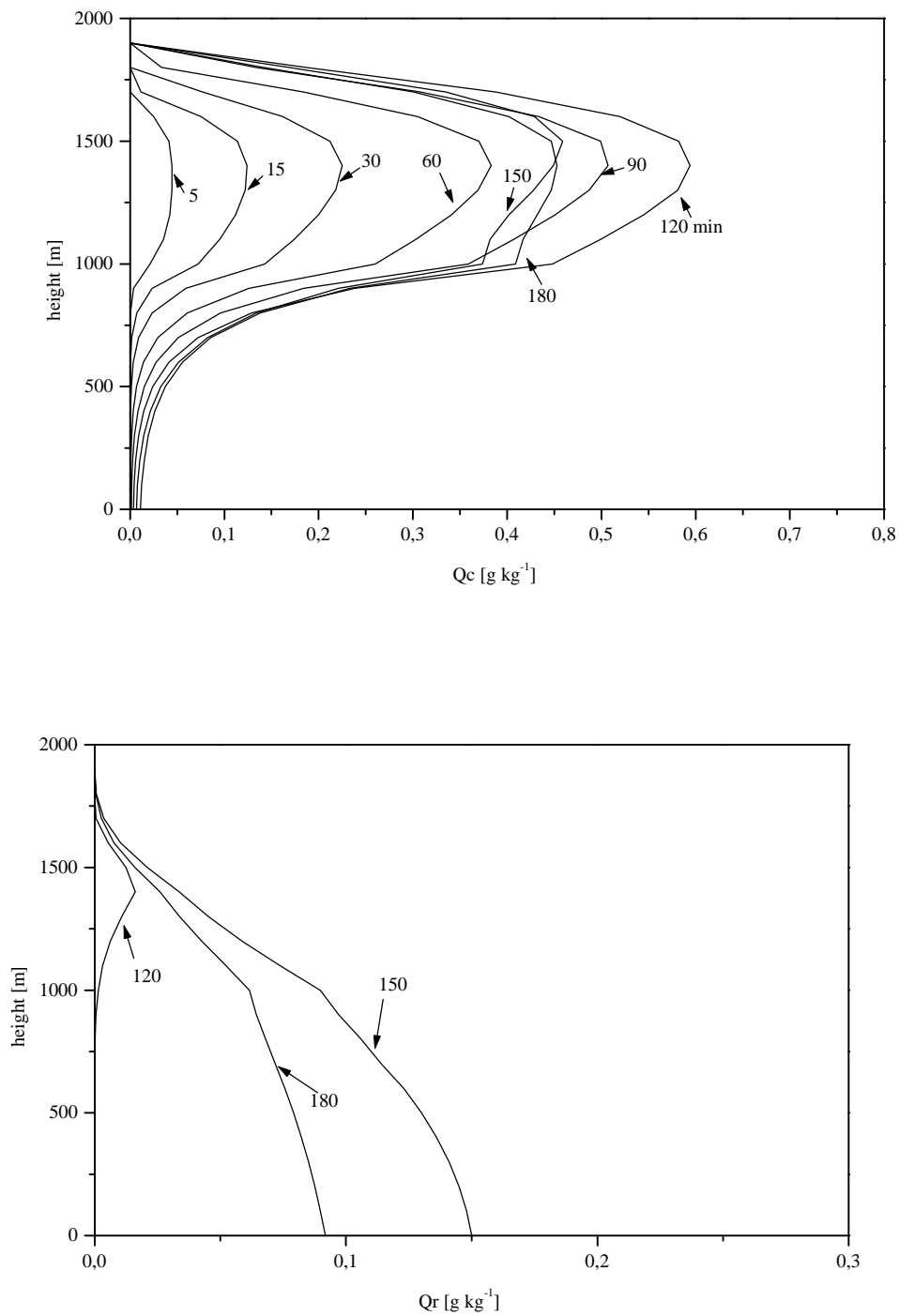


Fig. 4.2. (a) the mixing ratios of cloudwater,  $Q_c$ ; (b) the mixing ratio of rainwater as a function of height.



humidity in the sub-cloud layer is 80% which is typical in Frohnau experiment. According to our model test, the group terminal falling velocity of rain droplets is in the order of  $2 \text{ m s}^{-1}$ , the mean radius of rain droplets is 0.01 cm. Based on the functions 11-13, we can calculate that less than 2% of rainwater will evaporate during the falling period of rain droplets from the tower to the ground. Therefore we can ignore the evaporation of rain droplets during their falling period from the tower to the ground.

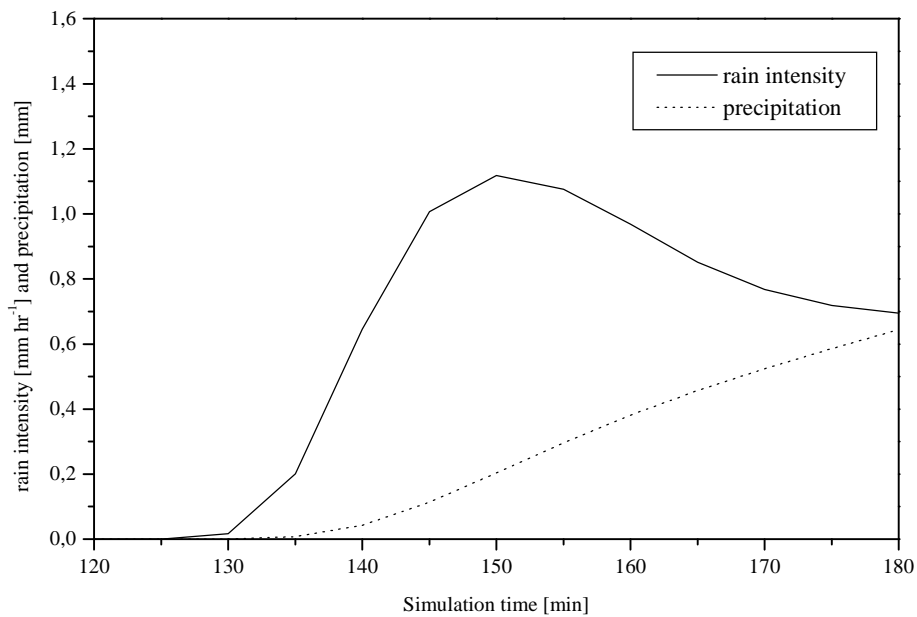


Fig. 4.3. The rain intensity and precipitation amount at the surface as a function of time.

Table 4.4. Comparison of rain evolution under different values of maximal updraft velocity and turbulence coefficient

Conditions	$K = 20 \text{ m}^2 \text{ s}^{-1}$ $W = 0.2 \text{ m s}^{-1}$	$K = 20 \text{ m}^2 \text{ s}^{-1}$ $W = 0.3 \text{ m s}^{-1}$	$K = 10 \text{ m}^2 \text{ s}^{-1}$ $W = 0.2 \text{ m s}^{-1}$
Time of initial rain (minutes)	135	110	120
Max. rain intensity ( $\text{mm hr}^{-1}$ )	1.12	1.97	1.03
Precipitation in 3hours (mm)	0.64	1.29	0.68

The updraft velocity and turbulence coefficient are the two factors which directly influence the rain evolution. We made several tests changing the two parameters and compared the values of maximum rain intensities on the ground. The results are listed in

Tab. 4.4. We can conclude from the tests that updraft velocity is the limiting parameter of the rain evolution. Under the condition of the maximum updraft velocity of  $0.3 \text{ m s}^{-1}$  the maximum rain intensity is significantly higher and the time of initial rain is also earlier than under the condition of the maximum updraft velocity of  $0.2 \text{ m s}^{-1}$ .

#### 4.8.2 Chemical model results

From Chapter 2 and 3 we have learned that there are several factors (gaseous  $\text{SO}_2$  concentration, the pH value,  $\text{NH}_3$  and  $\text{HCHO}$  concentration in the gas and liquid phase, etc.) which influence the sub-cloud scavenging of  $\text{SO}_2$  by rainwater as well as the concentration of free S(IV) and the ratio of S(IV) and S(VI) in cloudwater. One of the important questions we attempt to answer with this model is whether the ratio of S(IV) to S(VI) in the liquid phase increases linearly with increasing gas phase  $\text{SO}_2$  concentration. Moreover, we will also discuss the factors which are important for the variation of S(IV) deposition in the sub-cloud layer. This question is especially crucial in highly sulfur polluted regions. For this purpose, we made several tests with different initial conditions. The different conditions are listed in Tab. 4.5.

Table 4.5. Initial conditions of tests

Tests	Initial conditions
1	Initial concentrations of gaseous and aqueous chemical compositions as listed in Tab. 4.1 and 4.2; without aerosol;
2	as test 1 but with gaseous $\text{SO}_2 = 1\text{ppb}$
3	as test 1 but with gaseous $\text{SO}_2 = 100\text{ppb}$
4	as test 1 but with gaseous $\text{NH}_3$ on the ground level = $0.3\text{ppb}$
5	as test 1 but with gaseous $\text{NH}_3$ on the ground level = $10\text{ppb}$
6	as test 1 but with gaseous $\text{H}_2\text{O}_2 = 1\text{ppb}$
7	as test 1 but with gaseous $\text{HCHO} = 0.1\text{ppb}$
8	as test 1 but with gaseous $\text{HCHO} = 5\text{ppb}$
9	as test 1 but with ozon = $60\text{ppb}$
10	as test 1 but with aerosol (Tab. 4.3)

We use symbol  $\gamma$  to represent the ratio of free S(IV) deposition ( $[\text{free S(IV)}] \times \text{rain intensity (RI)}$ ) at the ground and at the cloud base. In the case of test 1,  $\gamma$  increases rapidly at the beginning of the rain event (Fig. 4.4a). The maximum value of  $\gamma$  is reached 5 min after the beginning of the rain event. After 15 min,  $\gamma$  became almost constant. This can be explained by the buffer effect of  $\text{NH}_3$ .  $\text{NH}_3$  is dissolved into rainwater as the rain event starts and increases the pH value of rainwater. Accordingly, the solubility of  $\text{SO}_2$  will increase with decrease of rainwater acidity. Therefore, at the beginning of the rain event much more sulfite can be found at the ground than at the cloud base. However, with the consumption of gaseous  $\text{NH}_3$ , the buffer effect of  $\text{NH}_3$  for the acidity of the rainwater will decrease and the scavenging of  $\text{SO}_2$  by rainwater is not as significant as at the beginning of the rain event.

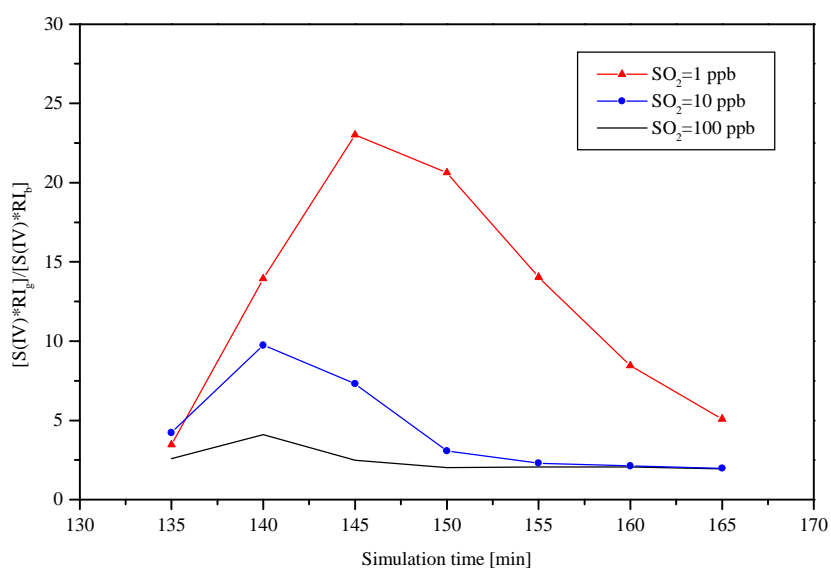


Fig. 4.4a. The time variation of the ratio of free sulfite deposition- $[\text{S(IV)}] \times \text{RI}$  (rain intensity)-between the ground (g) and the cloud base (b) under different concentrations of gaseous  $\text{SO}_2$ . The ratio is represented with symbol  $\gamma$  in the text.

If we increase the initial concentration of gaseous  $\text{SO}_2$  from 1 ppb (test 2) to 10 ppb (test 1) and 100 ppb (test 3), the value of  $\gamma$  decreases with the increase of gaseous  $\text{SO}_2$  concentration (Fig. 4.4a). The maximum value of  $\gamma$  in test 2 is about 10 times of that in

test 3. This means that under low concentration of gaseous  $\text{SO}_2$ , the contribution of sub-cloud scavenging of  $\text{SO}_2$  to the free S(IV) deposition is much higher than under high concentration of gaseous  $\text{SO}_2$ . However, the concentration of free sulfite in rainwater at the ground increases drastically with the increase of initial gaseous  $\text{SO}_2$  concentration. For example, at the beginning of the rain, free sulfite concentration in rainwater in test 3 is about 30 times as in test 2 (Fig. 4.4b). Nevertheless, we should notice that the increasing factor of free sulfite is not linear to the increasing factor of initial gaseous concentration of  $\text{SO}_2$ . From Fig. 4.4b

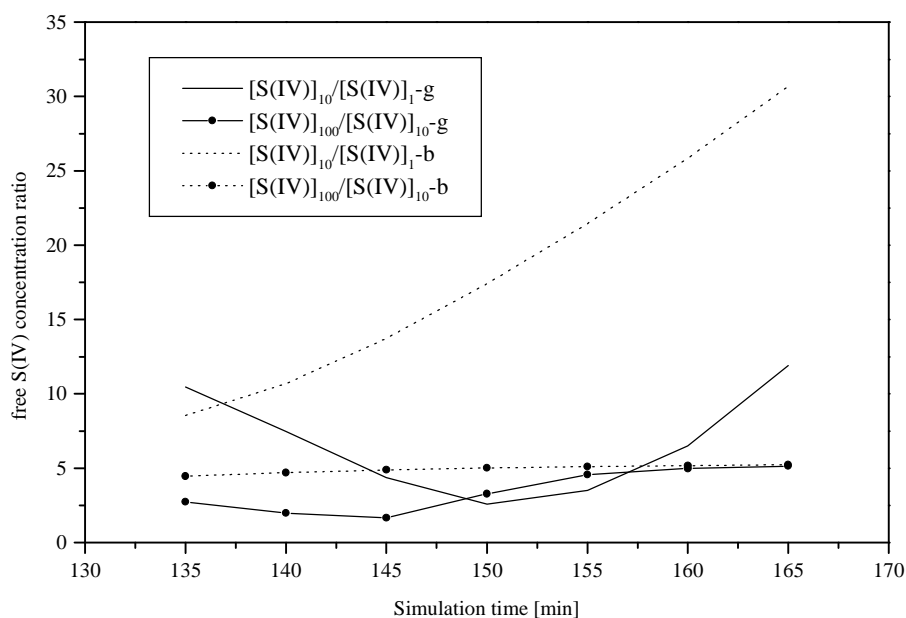


Fig. 4.4b. The variation of free S(IV) concentration ratios between test 1 ( $\text{SO}_2 = 10$  ppb), test 2 ( $\text{SO}_2 = 1$  ppb) and test 3 ( $\text{SO}_2 = 100$ ppb) at the ground (g) and at the cloud base (b).

we can see that when the initial concentration of  $\text{SO}_2$  increase from 10 ppb to 100 ppb, the concentration of free S(IV) in rainwater at the ground increases maximal 5 times. However, when the initial concentration of  $\text{SO}_2$  increase from 1 ppb to 10 ppb, the concentration of free S(IV) in rainwater at the ground increases more than 10 times. This shows that in heavily polluted areas, the scavenging of  $\text{SO}_2$  by rainwater is limited.

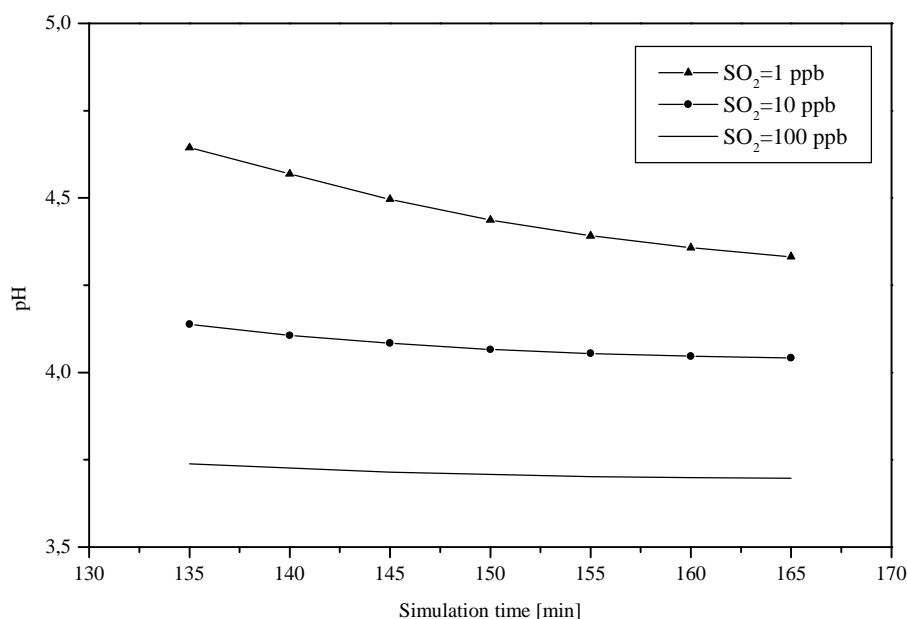


Fig. 4.4c. The variation of the pH value of the rainwater at the cloud base in test 1, 2 and 3.

It is obvious that the acidity of rainwater both at the ground and at the cloud base increases with increasing initial SO<sub>2</sub> concentration. The pH value influences not only the solubility of SO<sub>2</sub> but also the aqueous phase oxidation rate of free S(IV) with H<sub>2</sub>O<sub>2</sub> and ozone. In test 2 free S(IV) concentration in rainwater at the cloud base decreases to less than 1 μmol l<sup>-1</sup> with the evolution of the rain event. Although the initial gaseous SO<sub>2</sub> concentration in test 1 is 10 times as in test 2, the ratio of free S(IV) concentration between test 1 and 2 at the cloud base is much higher than 10. This is due to the increasing rate of conversion of free S(IV) to S(VI) by ozone at the pH value near 4.5 which is typical in test 2 (Fig. 4.4c).

The ratio of free S(IV) to S(VI) is much higher at the ground than at the cloud base (Fig. 4.4d and 4.4e). Obviously this is due to the scavenging of SO<sub>2</sub> in the sub-cloud layer. This ratio is the highest in the case with 100 ppb SO<sub>2</sub>, ranging from 0.35 to 0.9. This means that in heavily polluted area free S(IV) is a very important form of sulfur in rainwater.

Low (0.3 ppb) and high (10 ppb) initial concentration of  $\text{NH}_3$  are used in test 4 and 5 to compare the influence of  $\text{NH}_3$  buffer effect on the sub-cloud scavenging of  $\text{SO}_2$  by rainwater (Fig. 4.5). In the case with 0.3 ppb  $\text{NH}_3$  at the ground, wet deposition of free S(IV) at the ground is even lower than that at the cloud base at the beginning of the rain event. This is due to the oxidation of free S(IV) by  $\text{H}_2\text{O}_2$  which dissolves rapidly into rainwater with the formation of rain. This indicates that the ratio of initial  $\text{NH}_3$  and  $\text{H}_2\text{O}_2$  is a limiting factor for the deposition of free S(IV) by rainwater. With the initial concentration of 10 ppb  $\text{NH}_3$  the maximum value of  $\gamma$  is approximately 3 times as with 3 ppb  $\text{NH}_3$ . This means that the increase of wet deposition of free S(IV) in rainwater is almost linear to the increase of  $\text{NH}_3$  concentration. Therefore,  $\text{NH}_3$  is an efficient factor to limit the sub-cloud scavenging of  $\text{SO}_2$  by rainwater.

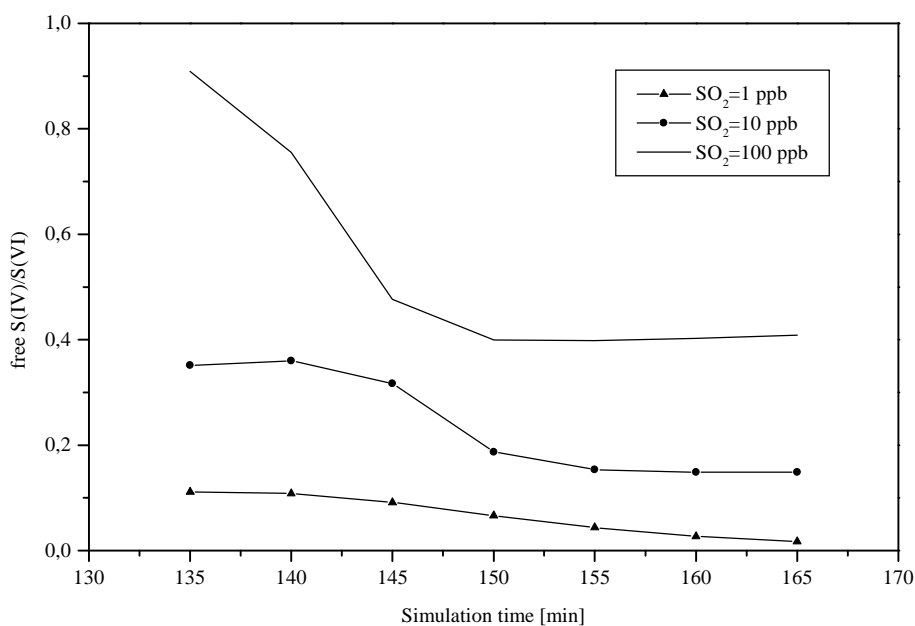


Fig. 4.4d. The variation of free S(IV) to S(VI) ratio of the rainwater at the ground in test 1, 2 and 3.

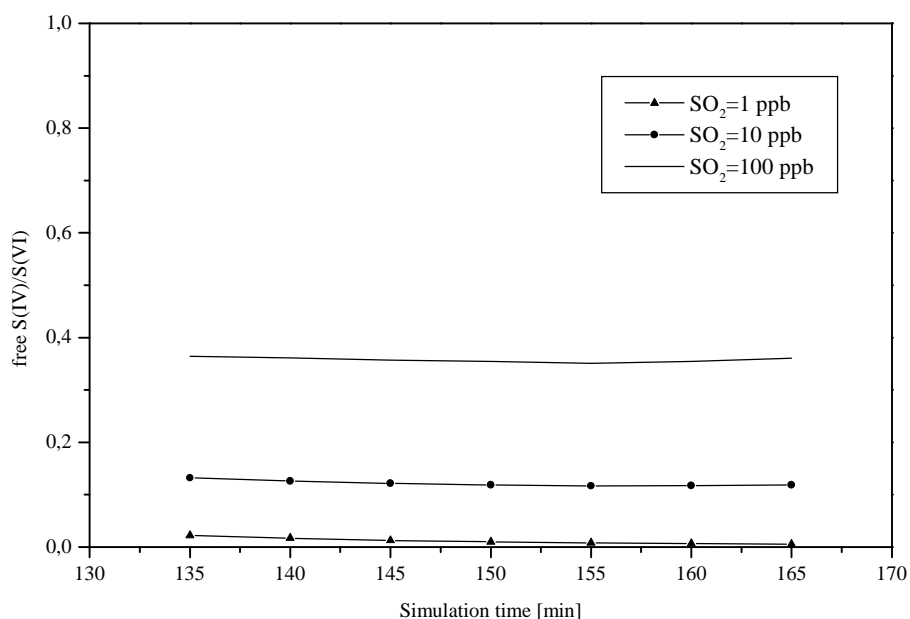


Fig. 4.4e. As for Fig. 4.4d but at the cloud base.

We have already observed from Brocken experiment (see Chapter 3) that there is a negative correlation between  $\text{H}_2\text{O}_2$  and free S(IV) in cloudwater. As an efficient oxidant of free S(IV) in the liquid phase,  $\text{H}_2\text{O}_2$  can strongly influence the acidity of cloud and rainwater. In test 6 we set an initial concentration of 1 ppb for gaseous  $\text{H}_2\text{O}_2$ . The  $\gamma$  value is significantly lower in test 6 than in test 1 and the variation trend of the value is also quite different from test 1 (Fig. 4.6). Instead of reaching maximum with the evolution of rain event, a minimum value of  $\gamma$  is reached after 10 min of raining. The reason is the low pH value caused by the oxidation of free S(IV) with high concentration of  $\text{H}_2\text{O}_2$  in rainwater.

As already discussed in Chapter 3, formaldehyde is the limiting factor of HMS formation in cloudwater. Based on the fact that near cloud base we measured significantly high concentration of HMS even under low  $\text{SO}_2$  concentration in the gas phase ( $<1$  ppb), we compared the free S(IV) deposition and HMS deposition changing initial gaseous formaldehyde concentration from 0.1 ppb (test 7) to 0.5 ppb (test 1) and 5 ppb (test 8). With 5 ppb HCHO as initial condition, there is little difference between free sulfite deposition at the cloud base and at the ground (Fig. 4.7). This shows that

under high concentration HCHO, even during the short falling period of rain droplets from the cloud base to the ground, most of dissolved  $\text{SO}_2$  will be adducted with HCHO to form HMS.

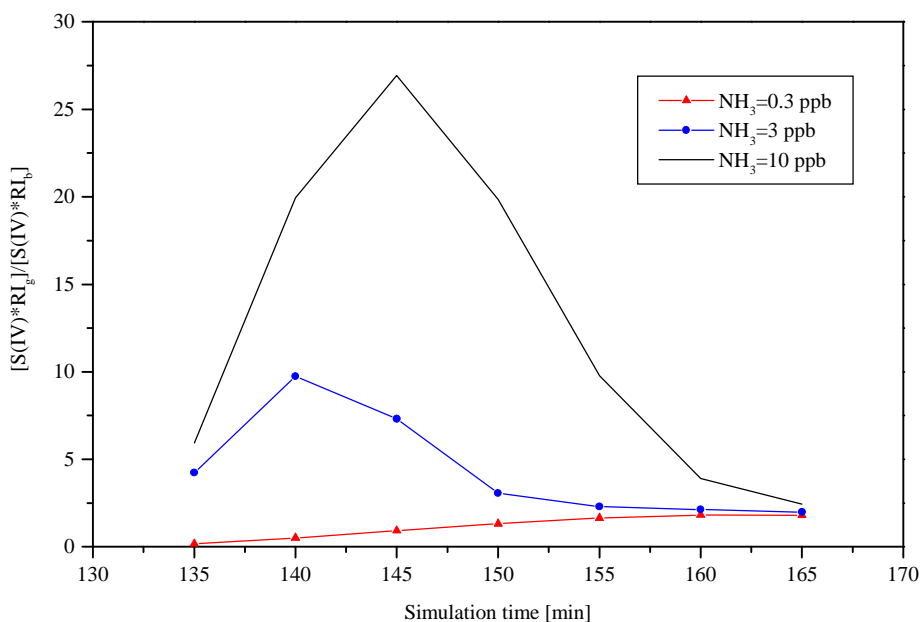


Fig. 4.5. As for Fig. 4.4a but under different concentrations of  $\text{NH}_3$ .

The conversion rate of free S(IV) to S(VI) via the reaction with ozone is known to be efficient with pH value higher than 4.5. In test 9 we used 60 ppb initial ozone concentration and compared the free sulfite deposition with test 1. From Fig. 4.8 we can see that with the condition of 60 ppb ozone, the  $\gamma$  value is slightly lower than in test 1. The difference is not as significant as in Fig. 4.6 where  $\text{H}_2\text{O}_2$  concentration is increased from 0.1 ppb to 1 ppb.

Sub-cloud scavenging of aerosols by falling rain droplets can strengthen or buffer the acidity of rainwater depending on the chemical composition of aerosols. We made test 10 with alkaline aerosols below cloud base. As we can see from Fig. 4.9, with and without scavenging of aerosols by rainwater makes no significant difference to the value of  $\gamma$ .



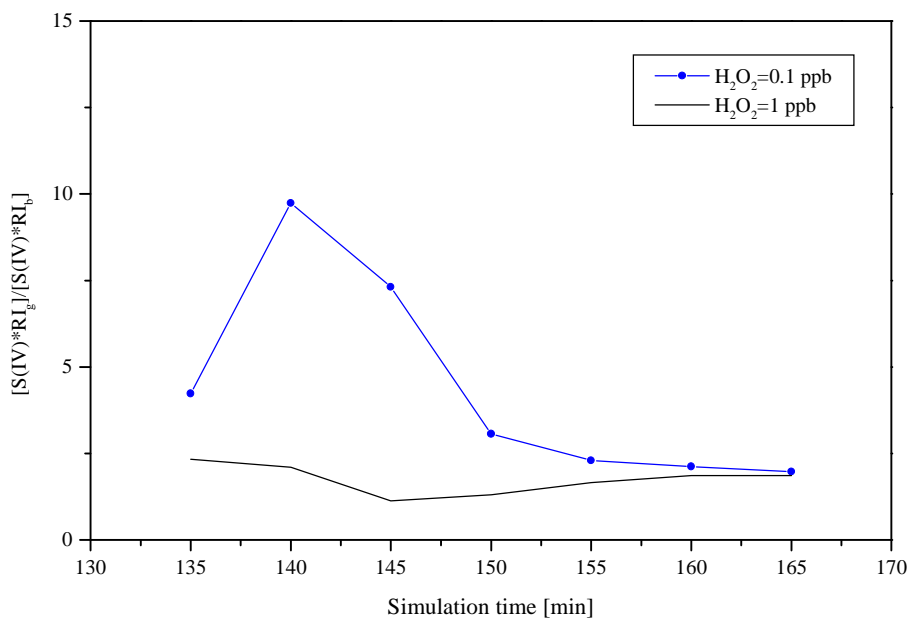


Fig. 4.6. As for Fig. 4.4a but under different concentrations of H<sub>2</sub>O<sub>2</sub>.

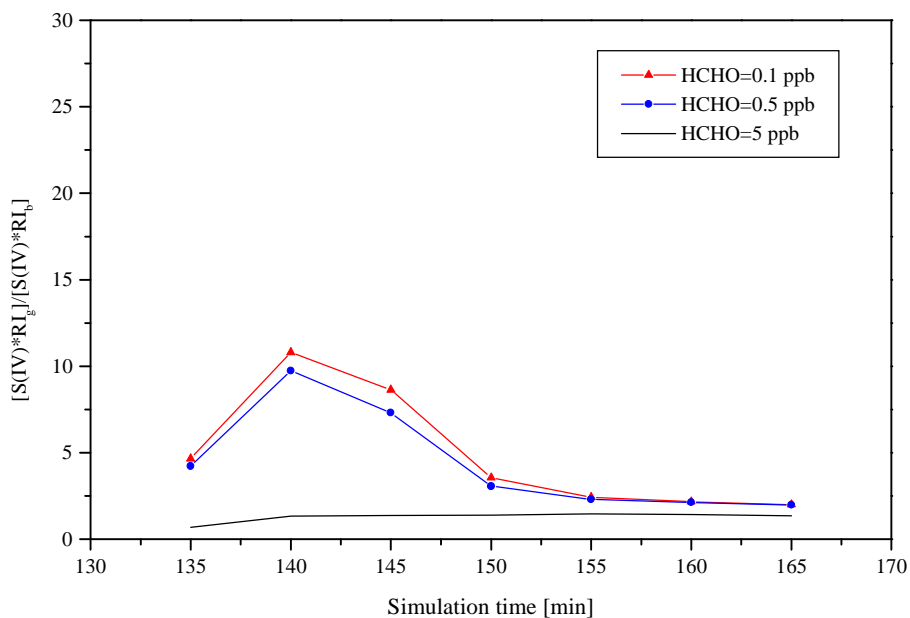


Fig. 4.7. As for Fig. 4.4a but under different concentrations of HCHO.

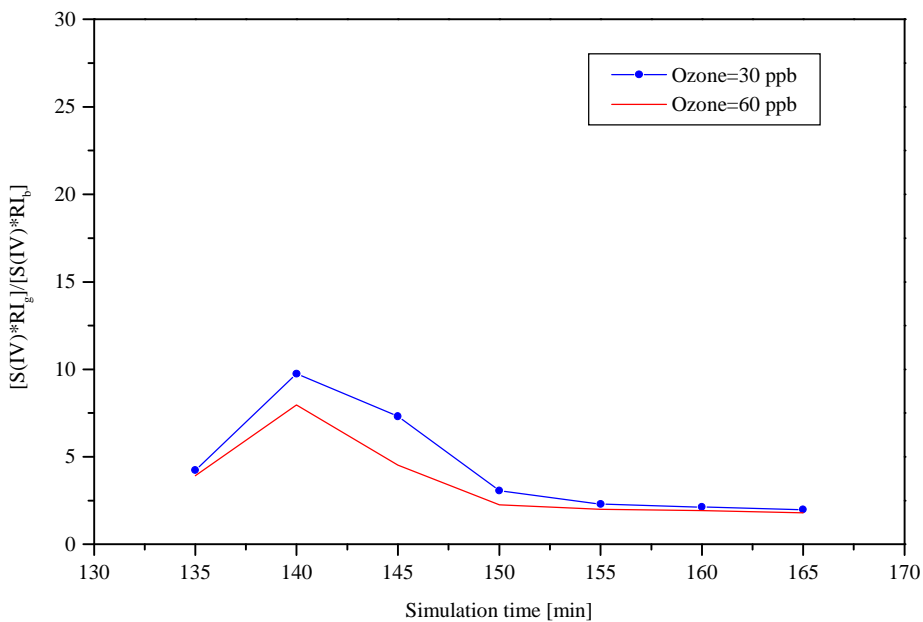


Fig. 4.8. As for Fig. 4.4a but under different concentrations of ozone.

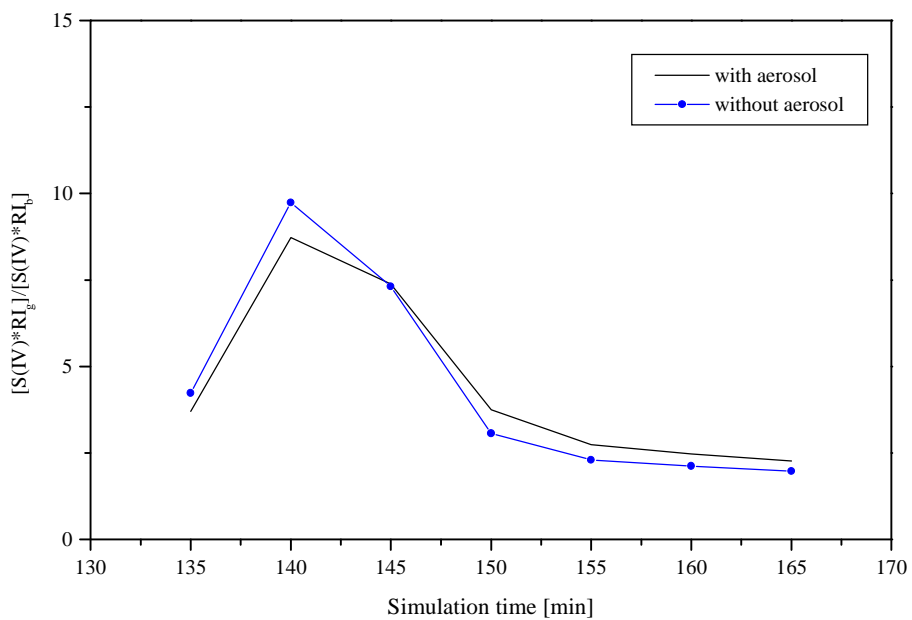


Fig. 4.9. As for Fig. 4.4a but with and without aerosol scavenging by rainwater.

#### 4.9 Summaries and conclusions

Our model calculations indicate that the removal of  $\text{SO}_2$  by rainwater in sub-cloud layer can be strongly influenced by the concentrations of other chemical species. Among the species,  $\text{NH}_3$  and  $\text{H}_2\text{O}_2$  are most important.  $\text{NH}_3$  can buffer the acidity of rainwater and thus enhance the solubility of  $\text{SO}_2$  into the liquid phase. Under high concentration of  $\text{NH}_3$  the wet deposition of free S(IV) in rainwater is significantly enhanced. On the contrary,  $\text{H}_2\text{O}_2$  can efficiently consume free S(IV) in rainwater via oxidation reaction.

Under low concentration of gaseous  $\text{SO}_2$ , the contribution of sub-cloud scavenging of  $\text{SO}_2$  to the free S(IV) wet deposition is much higher than under high concentration of gaseous  $\text{SO}_2$ . It indicates that in heavily polluted areas, the relative scavenging effect of  $\text{SO}_2$  by rainwater is limited. However, the concentration of free sulfite in rainwater at the ground increases drastically with the increase of initial gaseous  $\text{SO}_2$  concentration.

The ratio of free S(IV) to S(VI) is much higher at the ground than at the cloud base due to the scavenging of  $\text{SO}_2$  in the sub-cloud layer. In heavily polluted area this ratio is as high as 0.9. This means that free S(IV) is a very important form of sulfur in rainwater in the areas with high sulfur dioxide emissions.



## Chapter 5

### Summary and outlook

In this chapter our main experimental and theoretical findings and conclusions will be presented. Two field experiments and a cloud model simulation were carried out with the aim to investigate the ratio of S(IV) to S(VI) in rainwater and cloudwater. The transformation of dissolved SO<sub>2</sub> to sulfate in the aqueous phase is one of the most important chemical transformations in the hydrometeors. The transformation is the main cause of different air pollution problems like acid rain, forest decline and negative climate forcing. With the aim to reduce the global production of sulfate aerosols it is necessary to first investigate the partitioning of sulfur in the forms of S(IV) and S(VI) in the aqueous phase.

In our experiments several weeks of measurements were carried out to measure free S(IV) and HMS concentrations in the aqueous phase. Moreover, meteorological and microphysical parameters as well as chemical species relevant to the sulfur chemistry in the aqueous phase were measured.

During our first experiment, a 324 m high telecommunication tower at Berlin-Frohnau is used to collect rainwater simultaneously from two different levels. From the difference of the wet deposition of S(IV) from the two levels, we estimated the effect of sub-cloud scavenging of SO<sub>2</sub>. Measured S(IV) concentrations in rainwater are in the range of 1.44 to 27.36 μmol l<sup>-1</sup>. On average about 36% (13-51%) of total sulfur in rainwater on the ground site is in the form of S(IV), indicating the significant contribution of S(IV) to the total sulfur wet deposition. Taking into account the dilution effect of rainwater from the tower to the ground, about 60% of wet deposited S(IV) comes from sub-cloud scavenging below the 324m level. This means that the main part

of dissolved  $\text{SO}_2$  in the sub-cloud layer remains as S(IV) and will not be oxidized into sulfate.

This result is further confirmed in our theoretical part using a one-dimensional time-dependant physical-chemical cloud model. Our model calculation focuses on the increase of free S(IV) in rainwater from cloud base to the ground. According to our calculation, the increase of free S(IV) deposition in rainwater from cloud base to the ground is significant, with increasing factor ranging from 2 to 25. An interesting phenomenon found from the model simulation is that the contribution of sub-cloud scavenging of  $\text{SO}_2$  to the free S(IV) deposition is much higher under low concentration of gaseous  $\text{SO}_2$  than under high concentration of gaseous  $\text{SO}_2$ . This indicates that in heavily polluted areas the contribution of sub-cloud scavenging to the total wet deposition of free S(IV) is not as high as in less polluted areas. Our calculations show also that the scavenging of  $\text{SO}_2$  by rainwater in the sub-cloud layer can be highly variable with different conditions of gaseous  $\text{NH}_3$  and  $\text{H}_2\text{O}_2$ . For example with 10 ppb gas phase  $\text{NH}_3$  and 10 ppb gas phase  $\text{SO}_2$  on the ground site, the increasing factor of free S(IV) deposition in rainwater from cloud base to the ground can be as high as 27. On the contrary,  $\text{H}_2\text{O}_2$  can efficiently consume free S(IV) in rainwater via oxidation reaction. For example, with 1 ppb  $\text{H}_2\text{O}_2$  the increasing factor of free S(IV) deposition in rainwater is less than 2.5.

The ratio of free S(IV) to S(VI) is much higher at the ground than at the cloud base due to the scavenging of  $\text{SO}_2$  in the sub-cloud layer. In heavily polluted areas (e.g. 100 ppb  $\text{SO}_2$ ) this ratio can be as high as 0.9 according to model calculations. With initial concentration of 10 ppb  $\text{SO}_2$  in the gas phase, which is typical during Berlin-Frohnau experiment, this ratio ranges between 10-40 % according to our model calculations.

Our second experiment is carried out at Mt. Brocken. Following conclusions can be made based on the case studies of different cloud events. Free S(IV) concentration in cloudwater is relatively low compared to that in rainwater (Berlin-Frohnau) according to our experiment. The average concentration of free S(IV) in cloudwater ( $3.2 \mu\text{mol l}^{-1}$ ) is less than half of that in rainwater ( $7.4 \mu\text{mol l}^{-1}$ ). It is well known that the ion concentrations of cloudwater are generally much higher than in rainwater. Taking this dilution effect of rainwater into account, we can estimate that the difference of free S(IV) amount in rain and cloudwater should be even much higher than 2. The ratio of

free S(IV) to S(VI) ranges from zero to 0.18, averaging 0.03 in cloudwater at Mt. Brocken during our experiment, which is much lower than that we observed in rainwater at Berlin-Frohnau (0.35 as a mean value). This indicates that most of sulfur in cloudwater exist in the oxidized form. However, this ratio can be as high as 0.2 in several situations. One is in the atmosphere with relatively low sulfate burden. In this case the sulfate ion content in cloudwater is relatively low. Therefore, even low concentration of free S(IV) can make up a considerably high fraction of total sulfur in cloudwater. A second one is in the deeper layer of a cloud where the production of oxidant like  $\text{H}_2\text{O}_2$  is limited. A third one is the local transportation of  $\text{SO}_2$  into the cloud layer which will obviously increase the concentration of free S(IV) in cloudwater.

Our experiments have shown that the liquid phase concentration of  $\text{H}_2\text{O}_2$  and pH are the main limiting factors for the free S(IV) concentrations. The ratio of free S(IV) to S(VI) decrease with increasing concentrations of  $\text{H}_2\text{O}_2$  in the liquid phase. With the increase of cloudwater pH, this ratio increases significantly.

We can conclude from our experimental and modeling findings that free S(IV) is an important form of sulfur in rainwater and stems mainly from sub-cloud scavenging of rainwater. Free S(IV) in cloudwater seems less important compared to that in rainwater. However, we should also notice that the cloud events we observed at the Mt. Brocken during our experiment last generally at least one day. Free S(IV) in such long period clouds has enough time to be almost totally oxidized into sulfate. Therefore, we believe that in cloud events with shorter life time, the S(IV)/S(VI) ratio should be greater than what we measured. Hence, it is necessary to observe more different kinds of clouds in the future work.

From our experiments we have found that formaldehyde can be the limiting factor of HMS formation in the aqueous phase. In the further research, formaldehyde concentrations in the gas phase and liquid phase should be monitored to better understand the formation of HMS in the aqueous phase. It is also suggestable to collect cloudwater and rainwater simultaneously during one precipitation process to compare free S(IV) concentrations in cloud- and rainwater. Our model calculations have shown that in differently polluted areas the ratio of S(IV) to S(VI) have different characteristics. To access the ratio of S(IV) to S(VI) in hydrometeors on the global scale, more similar experiments in other sites are necessary.

Our findings suggest that considerable part of emitted  $\text{SO}_2$  will not be transformed to sulfate especially in the sub-cloud layer. Therefore, the production of climate affecting sulfate aerosol via aqueous phase transformation of dissolved  $\text{SO}_2$  is more limited than believed by climate modellers.



## References

- Acker, K., Möller, D., Wieprecht, W. and Naumann, St. (1995a) Mt. Brocken, a site for a cloud chemistry measurement programme in central Europe. *Water, Air and Soil Pollution* 85, pp. 1979-1984.
- Acker, K., Wieprecht, W., Möller, D., Mauersberger, G., Naumann, S. and Oestreich, A. (1995b) Evidence of ozone destruction in clouds. *Naturwissenschaften* 82, pp. 86-89.
- Acker, K., Möller, D., Marquardt, W., Brüggemann, E., Wieprecht, W., Auel, R. and Kalaß, D. (1998a) Atmospheric research program for studying changing emission patterns after German unification. *Atmospheric Environment* Vol. 32, No. 22, pp. 3435-3443.
- Acker K., Möller, D., Wieprecht, W., and Kalaß, D. (1998b) Investigations of ground-based clouds at the Mt. Brocken. *Fresenius J Anal. Chem.* 361, pp. 59-64.
- Acker, K., Möller, D., Auel, R., Wieprecht, W., Kalass, D., Schmidt, V. (1999) Wolken - eine Quelle für HNO<sub>2</sub>? Meßtechnik-Feldexperiment am Brocken-Ergebnisse und Ausblick. BMBF AFS-Statusseminar München, 24.-25. 6. 1999
- Anderson, T.L., Wolfe, G. V. and Warren, S.G. (1992) Biological sulfur, clouds and climate. *Encyclopedia of Earth System Science* Volume 1, pp. 363-376.
- Andreae, M.O. (1990) Ocean-atmosphere interaction in the global biogeochemical sulfur cycle. *Mar. Chem.* 30, pp. 1-29.
- Asman, W.A.H. (1995) Parameterization of below-cloud scavenging of highly soluble gases under convective conditions. *Atmos. Environ.* Vol. 29, pp. 1359-1368.
- Ayers, G. P., Ivey, J.P. and Goodman H.S. (1986) Sulfate and methansulfonate in the maritime aerosol at Cape Grim. *J. Atmos. Chem.* 4, pp. 173-185.
- Botha, C.F., Hahn, J., Pienaar, J.J. and Eldik, R.V. (1994) Kinetics and mechanism of the oxidation of sulfur(IV) by ozone in aqueous solutions. *Atmos. Environ.* 28, pp. 3207-3212.

- Brandt C. and Eldik, R.V. (1995) Transition metal-catalyzed oxidation of sulfur(IV) oxides. Atmospheric-relevant processes and mechanisms. *Chem. Rev.* 95, pp. 119-190.
- Brimblecombe, P. and Spedding, D.J. (1974) The reaction order of the metal ion catalysed oxidation of sulphur dioxide in aqueous solution. *Chemosphere* No. 1, pp. 29-32.
- Calvert, J.G. et al. (1985) Chemical mechanisms of acid generation in the troposphere. *Nature* 317, pp. 27.
- Cape, J.N. et. al. (1999) Field observation of S(IV) in cloud. *Atmospheric Research* 50, pp. 345-358.
- Charlson, R.J. and Wigley, T.M.L.(1994) Sulphate aerosol and climate change. *Scientific American*, February 1994, pp. 28-35.
- Charlson, R.J., Lovelock, J.E., Andreae, M.O. and Warren, S.J. (1987) Oceanic phytoplankton, atmospheric sulfur, cloud albedo and climate. *Nature*, Lond. 326, pp. 655-661.
- Chin, M. and Davis, D. (1993) Global sources and sinks of OCS and CS<sub>2</sub> and their distributions. *Global Biogeochemical Cycles* 7, pp. 321-337.
- Chin, M., Jacob, D.J. Gardner, G.M. and Savoie, D.L. (1996) A global three-dimensional model of tropospheric sulfate. *J. Geophys. Res.* Vol. 101, D13, pp. 18667-18690.
- Choulaton, T.W., Bower, K.N. and Gallagher, M.W. (1997) The effect of sulphur chemistry on the scattering properties of particles. *Phil. Trans. R. Soc. Lond. B* 352, pp. 213-220.
- Clarke, A. G. and Rodojevic, M. (1987) Oxidation of SO<sub>2</sub> in Rainwater and its Role in Acid Rain Chemistry. *Atmos. Environ.* Vol. 21, No. 5, pp. 1115-1123.
- Colvile, R.N., Sander, R., Choulaton, T.W. et al. (1994) Computer modelling of clouds at Kleiner Feldberg. *J. Atmos. Chem.* 19, pp 189-229.
- Cowling, E.B. (1982) Acid precipitation in historical perspective. *Environ. Sci. Technol.* 16, pp. 110A-123A.

Cox, R.A. (1997) Atmospheric sulphur and climate- What have we learned? *Phil. Trans. R. Soc. Lond. B* 352, pp. 251-254.

Dasgupta P. K. (1982) Technical note on the ion chromatographic determination of S(IV). *Atmos. Environ. Vol. 16, No. 5*, pp. 1265-1268.

Davies, T. D. (1974) Determination of the local removal of sulphur dioxide by precipitation. *Observation and measurement of atmospheric pollution. WMO-No. 368 World Meteorological Organisation, Geneva.* pp. 567-578.

Davies, T.D. (1976) Precipitation scavenging of sulphur dioxide in an industrial area. *Atmos. Environ. Vol. 10*, pp. 879-890.

Davies T. D. (1979) Dissolved sulphur dioxide and sulphate in urban and rural precipitation (Norfolk, U.K.). *Atmos. Environ. Vol. 13*, pp. 1275-1285.

Dixon, R.W. and Aasen, H. (1999) Measurement of hydroxymethanesulfonate in atmospheric aerosols. *Atmos. Environ. Vol. 33*, pp. 2023-2029.

Eisele, E.L. and McMurry, P.H. (1997) Recent progress in understanding particle nucleation and growth. *Phil. Trans. R. Soc. Lond. B* 352, pp. 191-201.

Facchini, M.C., Fuzzi, S. Kessel, M., et al. (1992) The chemistry of sulfur and nitrogen species in a fog system. A multiphase approach. *Tellus 44B*, pp. 505-521.

Fuzzi, S. et al., (1992) The Po Valley Fog Experiment 1989- An Overview. *Tellus 44B*, pp. 448-468.

Galloway, J.N., Likens, G.E., Keene, W.C., and Miller, J.M. (1982) The composition of precipitation in remote areas of the world. *J. Geophys. Res.* 87, 8771-8786.

Gerber H. (1984) Liquid water content of fogs and hazes from visible light scattering. *J. Climate Appl. Meteor.* 23, pp. 1247-1252.

Gravenhorst, G. et al. (1980) Sulphur dioxide absorbed in rain water. Effects of acid precipitation of terrestrial ecosystems, Edited by T.C. Hutchinson and M. Havas, Plenum Publishing Corporation.

Gravenhorst, G., Kreilein, H., Schnitzler, K.-G., Ibrom, A. and Nützmann, E. (2000) Trockene und nasse Deposition von Spurenstoffen aus der Atmosphäre. In *Handbuch*

der Umweltveränderungen und Ökotoxikologie. Band 1B, (ed. Rober Guderian). Springer.

Grgic, I., Poznic, M. and Bizjak, M. (1999) S(IV) autoxidation in atmospheric liquid water: The role of Fe(II) and the effect of oxalate. *J. of Atm. Chem.* 33, pp. 89-102.

Guiang, S. F., Sagar, III, Krupa, V. and Pratt, G. C. (1984) Measurements of S(IV) and organic anions in Minnesota rain. *Atmos. Environ.* Vol. 18, No. 8, pp. 1677-1682.

Hales, J.M. and Dana, M.T. (1978) Regional-scale deposition of sulfur dioxide by precipitation scavenging. *Atmos. Environ.* Vol. 13, pp. 1121-1132.

Hallberg, A., Wobrock, W., Flossmann, A.I. et al. (1997) Microphysics of clouds: model vs measurements. *Atmos. Environ.* Vol. 31, No. 16, pp. 2453-2462.

Hegg, D.A., Rutledge, S.A. and Hobbs, P.V. (1986) A numerical model for sulfur and nitrogen scavenging in narrow cold-frontal rainbands 2. discussion of chemical fields. *J. Geophys. Res.* Vol. 91, No. D13, pp. 14403-14416.

Hoffmann, M.R. and Calvert, J.G. (1985) Chemical transformation modules for Eulerian acid deposition models. Volume II. The Aqueous-Phase Chemistry. National Center for Atmospheric Research, Boulder, CO.

Hoffmann, M.R. and D. J. Jacob (1984) Kinetics and mechanisms of the catalytic oxidation of dissolved sulfur dioxide in aqueous solution: An application to nighttime fog water chemistry. In *SO<sub>2</sub>, NO and NO<sub>2</sub> oxidation mechanisms: Atmospheric considerations*. J. G. Calvert (Ed.), Butterworth, pp. 101-172.

Hoffmann, M.R. (1986) On the kinetics and mechanism of oxidation of aquated sulfur dioxide by ozone. *Atmos. Environ.* Vol. 20, No. 6, pp. 1145-1154.

Hu Z.J. and Yan C.F. (1986) Numerical simulation of microprocesses in stratiform cloud – (1) Microphysical model *J. Academy of Meteorological Science* (in Chinese), Vol. 1, No.1, pp. 37-52.

Huang, M., Liu, S. and Ueda, H. (1993) Comparison and analysis of chemical characteristics of precipitation in China and Japan. *Chinese Journal of Atmospheric Sciences*, Vol. 17, No. 1, pp. 21-34.

Huang, M., Shen, Z., Liu, S. and Wu, Y. (1995) A study on the formation processes of acid rain in some areas of southwest China. *Scientia Atmospherica Sinica* (in Chinese), Vol. 19, No. 3, pp. 359-366.

Husain, L., Dutkiewicz, V. and Das, M. (1998) Evidence for decrease in atmospheric sulfur burden in the eastern United States caused by reduction in SO<sub>2</sub> emissions. *Geophysical Research Letters*. Vol. 25, No. 7, pp. 967-970.

Jaeschke, W. (1990) Untersuchungen zur Chemie des Schwefels in der Atmosphäre. Report of Environmental Research Center in J.W. Goethe Universität, Frankfurt/M, J.W. Goethe Universität, Frankfurt/M, Nr. 11.

Jaeschke, W. (1989) Atmospheric liquid phase chemistry. *Promet Meteorologische Fortbildung* 19, ¾ pp. 86-94.

Jensen, P.K. and Asman, W.A.H. (1995) General chemical reaction simulation applied to below-cloud scavenging. *Atmos. Environ.* Vol. 29, pp. 1619-1625.

Johnson, C. A., Sigg, L. and Zobrist, J. (1987) Case studies on the chemical composition of fogwater: The influence of local gaseous emissions. *Atmos. Environ.* Vol. 21, No. 11, pp. 2365-2374.

Kames, J. and Schmidt, R.W.H. (1992) NO<sub>y</sub>-Analytik in der Atmosphärenchemie. *Labor 2000*. pp. 12-23.

Lagrange, J., Pallares, C., Wenger, G. and Lagrange, P. (1996) Kinetics of sulphur(IV) oxidation by hydrogen peroxide in basic aqueous solution. *Atmos. Environ.* Vol. 30, No. 7, pp. 1013-1018.

Laj, P. et al., (1997) Cloud processing of soluble gases. *Atmos. Environ.* Vol. 31, pp. 2589-2598.

Lammel, G. and Metzger, G. (1991) Multiphase chemistry of orographic clouds: observations at subalpine mountain sites. *Fresenius J. Anal. Chem.* 340, pp. 564-574.

Lammel, G. (1996) Sensitive method for the determination of different S(IV) species in cloud and fog water. *Fresenius J. Anal. Chem.* 356, pp. 107-108.

- Lammel, G. and Metzigg, G. (1998) On the occurrence of nitrite in urban fogwater. *Atmosphere* 37, pp. 1603-1614.
- Langner, J. and Rodhe, H. (1991) A global three-dimensional model of the tropospheric sulfur cycle. *J. Atmos. Chem.* 13, pp 225-263.
- Lee, Y.N., Shen, J., Klotz, P.J., Schwarz, S.E. and Newman, L. (1986) Kinetics of hydrogen peroxide-sulfur(IV) reaction in rainwater collected at a northeastern U.S. site. *J. Geophys. Res.* Vol.91, No. D12, pp. 13264-13274.
- Lei, H.C., Tanner, P.A., Huang, M.Y., Shen, Z. L. and Wu, Y.X. (1997) The acidification process under the cloud in southwest china: Observation results and simulation. *Atmos. Environ.* Vol. 31, No. 6, pp. 851-861.
- Lelieveld, J. (1990) The role of clouds in tropospheric photochemistry. Thesis, Univ. of Utrecht, Netherlands.
- Lelieveld, J. and Crutzen, P.J. (1991) The role of clouds in tropospheric photochemistry. *J. Atmos. Chem.* 12, pp. 229-267.
- Lelieveld, J., Roelofs, G.-J., Ganzeveld, L., Feichter, J. and Rodhe, H. (1997) Terrestrial sources and distribution of atmospheric sulfur. *Phil. Trans. R. Soc. Lond. B* 352, pp. 149-158.
- Lelieveld, J., Ramanathan, V. and Crutzen, P.J. (1999) The global effects of asian haze. *IEEE Spectrum*, December, pp. 50-54.
- Liu, X. and Wang, M. (1992) Physico-chemical scavenging factors in the gaseous pollutants below clouds. *Journal of Nanjing Institute of Meteorology* Vol. 15, No. 2, pp. 30-36.
- Liu, X., Mauersberger, G. and Möller, D. (1997) The effects of cloud processes on the tropospheric photochemistry: An improvement of the EURAD model with a coupled gaseous and aqueous chemical mechanism. *Atmos. Environ.* Vol. 31, No. 19, pp. 3119-3135.
- Lovelock, J. (1997) A geophysicologist's thoughts on the natural sulfur cycle. *Phil. Trans. R. Soc. Lond. B.* 352, pp. 143-147.

- Maahs, H.G. (1982) Sulfur-dioxide/water equilibria between 0° and 50°C: An examination of data at low concentrations. In *Heterogeneous atmospheric chemistry*. D.R. Schryer (Ed.), Geophysical Monograph 26, American Geophysical Union, Washington DC, pp. 187-195.
- Maahs, H.G. (1983) Kinetics and mechanism of the oxidation of S(IV) by ozone in aqueous solution with particular reference to SO<sub>2</sub> conversion in nonurban tropospheric clouds. *J. Geophys. Res.* 88, pp. 10721-10732.
- Martin A. and Barbar F. R. (1978) Some observations of acidity and sulphur in rainwater from rural sites in central England and Wales. *Atmos. Environ.*, Vol. 12, pp. 1481-1487.
- Martin, L.R. (1984) Kinetic studies of sulphite oxidation in aqueous solutions. In *SO<sub>2</sub>, NO and NO<sub>2</sub> oxidation mechanisms: Atmospheric Considerations. Acid precipitation series*, Vol. 3. Butterworth, Boston. J.G. Calvert (Ed.), Chapter 2, pp. 63-100.
- Mohnen V.A. (1989) Cloud chemistry research at Whiteface Mountain. *Tellus* 41B, pp. 79-91.
- Möller, D. (1990) The Na/Cl ratio in rainwater and the seasalt chloride cycle. *Tellus* 42B, pp. 254-262.
- Möller, D. and Mauersberger, G. (1992a) Modelling of cloud water chemistry in polluted areas. In: *Precipitation Scavenging and Atmosphere-Surface Exchange*, Vol. 1. (ed. By S.E. Schwartz and W.G.N. Slinn), Hemisphere Publ. Corp., Washington, pp. 551-562.
- Möller, D. and Mauersberger, G. (1992b) Cloud chemistry effects on tropospheric photooxidants in polluted atmosphere—model results. *J. Atmos. Chem.* 14, pp. 153-165.
- Möller D. (1995a) Sulfate aerosol and their atmospheric precursors. In: *Aerosol Forcing of Climate* (ed. By R.J.Charlson, J. Heinzenberg), John Wiley & Sons Ltd, pp. 73-90.
- Möller, D. (1995b) Cloud Processes in the troposphere. *NATO ASI Series*, Vol. I 30: *Ice Core Studies of Global Biogeochemical Cycles*. pp. 39-63.

- Möller D. and Mauersberger G. (1995) An aqueous phase chemical reaction mechanism. In: Cloudsmodels and mechanism, EUROTRAC Int. Sci. Secr. Gramisch-Partenkirchen, pp. 77-93.
- Möller, D., Wieprecht, W., Kalaß, D., Acker, K., Auel, R. and Oestreich, A. (1996a) Physico-chemical characteristics of clouds at the Brocken summit. Proceedings of EUROTRAC Symposium 96, pp. 93-99.
- Möller, D., Acker, K. and Wieprecht, W. (1996b) A relationship between liquid water content and chemical composition in clouds. Atmospheric Research 41, pp. 321-335.
- Möller, D. (1996c) Experimentelle Untersuchungen der Transformation und Entfernung atmosphärischer Spurenstoffe in stratiformen Wolken auf dem Brocken (Harz). Abschlußbericht
- Möller, D. (2000) Atmosphärische Multiphasenchemie. In Handbuch der Umweltveränderungen und Ökotoxikologie. Band 1B, (ed. Rober Guderian). Springer.
- Munger, J.W. et al. (1984) The occurrence of bisulfite-aldehyde addition products in fog- and cloudwater. J. Atmos. Chem. 1, pp. 335-350.
- Munger J.W., Tiller C. and Hoffmann M.R. (1986) Identification of hydroxymehtanesulfonate in fog water. Science 231, pp. 247-249.
- Naumann, St. (1996) Relation of physico-chemical properties of clouds at Mt.Brocken (Harz) to transport and different-scale meteorological parameters. Dissertation, Free University Berlin, dept. of geosciences.
- Olson T.M and Hoffmann M.R. (1989) Hydroxyalkylsulfonate formation: Its role as a S(IV) reservoir in atmospheric water droplets. Atmos. Environ. Vol. 23, No. 5, pp. 985-997.
- Otto P. and Georgii H.W. (1992) Untersuchungen zur Bestimmung von S(IV) in Wolken- und Niederschlagsselementen. Report of Environmental Research Center in J.W. Goethe Universität, Frankfurt/M, Nr. 19.
- Pahl, S. and Winkler, P. (1995) Höhenabhängigkeit der Spurenstoffdeposition durch Wolken auf wälder. Abschlußbericht.



Penkett, S. A., Jones, B.M:R., Brice, K.A. and Eggleton, A.E.J. (1979) The importance of atmospheric ozone and hydrogen peroxide in oxidising sulphur dioxide in cloud and rainwater. *Atmos. Environ.* Vol. 13, pp. 123-137.

Finlayson-Pitts, B.J. and Pitts, Jr., J. N.(1986) *Atmospheric Chemistry: Fundamentals and Experimental Techniques*. John Wiley & Sons, New York.

Preiss M., Maser, R., Franke, H., Jaeschke, W. and Graf, J. (1994) Distribution of trace substances inside and outside of clouds. *Beitr. Phys. Atmosph.*, November, pp. 341-351.

Preiss M. et al. (1994) Measurements of S(IV) and H<sub>2</sub>O<sub>2</sub> in gas and liquid phase at Great Dun Fell. *Proceedings of EUROTRAC Symposium 94* (ed. by P.M. Borrell et al.) pp. 1129-1132.

Pruppacher, H.R. and Klett, J.D. (1997) *Microphysics of clouds and precipitation*. Atmospheric and Oceanographic Sciences Library. Kluwer Academic Publishers.

Qin Y. (1992) Numerical simulation of pollutants removal by precipitation. *J Atmos. Chem.* 14, pp. 143-151.

Qin Y. and Chameides, W.L. (1986) The removal of soluble species by warm stratiform clouds. *Tellus*, 38B, pp. 285-299.

Radojevic, M. (1985) Discussion to Measurements of S(IV) and organic anions in Minnesota rain. *Atmos. Environ.* Vol. 19, No. 4, pp. 685-686.

Radojevic M. et al., (1990) Field studies of the SO<sub>2</sub>/aqueous S(IV) equilibrium in clouds. *Atmos. Environ.* Vol. 24A, No. 2, pp. 323-328.

Radojevic M. (1992) SO<sub>2</sub> and NO<sub>x</sub> oxidation mechanisms in the atmosphere. In *Atmospheric Acidity: Sources, Consequences and Abatement*. (Radojevic, M. and Harrison, R.M.) Elsevier Applied Science, London, pp. 73-137.

Radojevic M., Tyler B.J. Hall S. and Penderghest N. (1995) Air oxidation of S(IV) in cloudwater samples. *Water, Air and Soil Pollution* 85, pp. 1985-1990.

Rao, X. and Collet, J.L.Jr. (1995) Behavior of S(IV) and Formaldehyde in a chemically heterogeneous cloud. *Environ. Sci. Technol.* 29, pp. 1023-1031.

Richards L. W. et al. (1983) Preliminary communication Hydrogen peroxide and sulphur(IV) in Los Angeles cloud water. *Atmos. Environ.* Vol. 17, No. 4, pp. 911-914.

Richards, L.W. (1995) Airborne chemical measurements in nighttime stratus clouds in the Los Angeles basin. *Atmos. Environ.* Vol. 29, No. 1. pp. 27-46.

Rohde, H. (1999) Human impact on the atmospheric sulfur balance. *Tellus* 51A-B, pp. 110-122.

Schmidt V. (1995) Auswahl und Anpassung eines Verfahrens zur Bestimmung von S(IV) in Proben atmosphärischen Flüssigwassers. Diplomarbeit.

Schwartz, S.E. and Freiberg, J.E. (1981) Mass-transport limitation to the rate of reaction of gases in liquid droplets: Application to oxidation of SO<sub>2</sub> in aqueous solutions. *Atmos. Environ.* Vol. 15, pp. 1129-1144.

Schwartz, S.E. (1986) Mass-transport considerations pertinent to aqueous phase reactions of gases in liquid-water clouds. In *Chemistry of Multiphase Atmospheric Systems*. (Ed. W. Jaeschke), Springer, Berlin, Germany. pp. 415-471.

Sedlak, D.L. et al. (1997) The cloudwater chemistry of iron and copper at Great Dun Fell, U.K. *Atmos. Environ.* 31, pp. 2515-2526.

Seinfeld, J.H. (1986) *Atmospheric Chemistry and Physics of Air Pollution*. John Wiley and Sons.

Stockwell, W.R., Middleton, P., Chang, J.S., Tang, X.(1990) The second generation regional acid deposition model chemical mechanism for regional air quality modelling. *J. Geophys. Res.*, 95, pp. 16343-16367.

Streets, D.G. and Waldhoff, S.T. (2000) Present and future emissions of air pollutants in China: SO<sub>2</sub>, NO<sub>x</sub>, and CO. *Atmos. Environ.* 34, pp. 363-374.

Tremblay, A. and Leighton, H. (1986) A three-dimensional cloud chemistry model. *Journal of climate and applied meteorology*. Vol. 25, pp. 652-671.

Wang, M., Liu, X. and Yang, H. (1988) The scavenging of SO<sub>2</sub> by raindrops below cloud base. *Scientia meteorologica Sinica* Vol. 8, pp. 27-36.

Warneck, P. (1988) *Chemistry of the natural atmosphere*. Academic Press, New York.

- Warneck, P. (1989) Sulfur dioxide in rain clouds: Gas-liquid scavenging efficiencies and wet deposition rates in the presence of formaldehyde. *J. Atmos. Chem.* 8, pp. 99-117.
- Warneck, P. (1991) Chemical reactions in clouds. *Fresenius J. Anal. Chem.* 340, pp. 585-590.
- Warneck, P. (1996) *Heterogeneous and liquid-phase processes.* Springer, Berlin.
- Watts, S.F. (2000) The mass budgets of carbonyl sulfide, dimethyl sulfide, carbon disulfide and hydrogen sulfide. *Atmos. Environ.* 34, pp. 761-779.
- West, P.W. and Gaeke, G.C. (1956) Fixation of sulfur dioxide as Disulfitomercurate (II) and subsequent colorimetric estimation. *Journ. of Industr. Engineering, Anal. Chem.* Vol, 28, pp. 1816-1819.
- Wieprecht, W, Möller, D., Acker, K. and Naumann, S. (1995) Influence of cloud physical parameters on chemical composition of clouds. *Air Pollution III: Engineering and Management*, pp.199-205.
- Wieprecht, W., Acker, K., Möller, D., Auel, R., Kalass, D., Schmidt, V. (1999) Reservoiraufteilung von Ruß, organischen Bestandteilen, Gesamtkohlenstoff, löslichen Substanzen u. Aerosolpartikeln (Anzahl und Masse) in der Tropfen- und Zwischenraumphase von Wolken – Feldexperiment 1998 am Brocken. BMBF AFS-Statusseminar München, 24.-25. 6. 1999.
- WMO-Reports 85 (1992) and 102 (1994) WMO CH-1211 Geneva, Switzerland.
- Wobrock, et al. (1994) The Kleiner Feldberg cloud experiment 1990. An overview. *J. Atmos. Chem.* 19, pp. 3-36.
- Young, T.R. and Boris, J.P. (1977) A numerical technique for solving stiff ordinary differential equations associated with the chemical kinetics of reactive-flow problems. *J. Physical Chemistry.* Vol. 81, No. 25, pp. 2424-2427.



## Appendix

### Measurement Methods and Instruments

#### **Ceilometer CT25K (Vaisalla)**

The cloud base was measured with ceilometer. The operating principle of the CT25K ceilometer is based on measurement of the time needed for a short pulse of light (905nm) to traverse the atmosphere from the transmitter of the ceilometer to a backscattering cloud base and back to the receiver of the ceilometer. The measurement range of CT25k ceilometer is from zero to 25,000ft (7616.67m). To eliminate the noise which can exceed the backscattered signal, a large number of laser pulses are used and the return signal are summed, so the random noise cancel partially itself.

#### **CFCL (continuous flow chemiluminescence)-S(IV)-Analyser**

Stauff und Jaeschke (1978) developed a method named C.L. method to measure free S(IV) in the liquid phase. This method is based on a TCM-absorptions solution, whose disulfitmercuratecomplex dissociate under the addition of a strong oxidant like  $\text{KmnO}_4$  and the bisulfite will be oxidized in a chemiluminescence reaction into sulfate. From the intensity of free C.L. radiation we can determine the quantative mass of S(IV) content in the liquid phase sample. C.L.- method was improved by Otto in 1992 and used as the basis of the CFCL-S(IV)-Analyser which we used in our experiment (Otto and Georgii, 1992). The CFCL-method has detection limit of  $5\text{nmol l}^{-1}$  S(IV). This method has also other advantages like high sensitivity, good reproductivity and less preparation work (Schmidt, 1995).

#### **Gerber Particulate Volume Monitor (PVM)**

Liquid water content (LWC) of clouds was measured continuously using forward scattering of laser beam by cloud droplets in the open air along 40cm path (Gerber Particulate Volume Monitor). This instrument can measure in situ and in real time the

integrated volume of suspended water droplets with a stated precision of  $0.002 \text{ g m}^{-3}$  (Gerber 1984). Under conditions of field experiments the PVM signal is controlled daily and if necessary new calibrated by the light diffusion disc. The average uncertainty becomes no greater than  $0.009 \text{ g m}^{-3}$ .

### **H<sub>2</sub>O<sub>2</sub> analyser (AL-1002)**

An H<sub>2</sub>O<sub>2</sub> analyser (AL-1002) was used to measure liquid phase H<sub>2</sub>O<sub>2</sub> in the field just after sampling of rain- and cloudwater. The measurement principle is based on the liquid phase reaction of peroxides with P-Hydroxyphenylacetic Acid catalyzed by peroxidase. This reaction produce a fluorescent dimer, that can be excited at 326 nm (Cd-lamp) and detected between 400 and 420 nm. The detection limit of H<sub>2</sub>O<sub>2</sub> analyser is  $0.002 \mu\text{mol l}^{-1}$  for the liquid phase. Interferences from O<sub>3</sub> and NO are 30 ppt H<sub>2</sub>O<sub>2</sub> per 100 ppb and 12 ppt H<sub>2</sub>O<sub>2</sub> per 100 ppb respectively.

### **Ion chromatography for HMS**

Ion chromatography with chemical suppression was used for the determination of HMS. Variation of the eluent composition using a separator column Dionex AS9-SC 4 mm (precolumn AG9-SC 4 mm) showed that a good separation was obtained using  $0.89 \text{ mmol l}^{-1} \text{ NaHCO}_3$  and  $67 \text{ mmol l}^{-1}$  paraformaldehyde (pH = 6) as eluent. HMS was not stable throughout the elution without adding paraformaldehyde to the eluent. An eluent flow of  $1.65 \text{ ml min}^{-1}$  was applied. For chemical suppression  $12.5 \text{ mmol l}^{-1} \text{ H}_2\text{SO}_4$  was used. Standards were made from sodium hydroxy methanesulfonate. Retention times obtained under the above mentioned conditions were HMS =  $6.6 \text{ min} \pm 15 \%$ . The detection limit of this measurement method for HMS is  $50 \text{ nmol l}^{-1}$ .

### **Ion chromatography for main ions in rain and cloudwater**

The anion chromatographic system consists of a SYKAM pump, a separation column AS14-4 mm (with precolumn AG14-4 mm), a micromembrane suppressor Dionex ASRS-II, a SYKAM conductivity detector, a JASCO sampler and the eluent contains  $3.5 \text{ mmol l}^{-1} \text{ Na}_2\text{CO}_3/1.0 \text{ mmol l}^{-1} \text{ NaHCO}_3$ . For analysis of cations a SYKAM pump, a separation column Waters IC-Pak CM/D, a SYKAM conductivity detector, a JASCO sampler a  $0.1 \text{ mmol l}^{-1} \text{ EDTA}/ 3.9 \text{ ml l}^{-1} \text{ HNO}_3$  are used. The data obtained with ion

chromatography correspond to the dissolved fraction. The acceptance criteria for ion balance and for conductivity (measured/calculated), respectively, are defined in the Reports 85 and 102 of the World Meteorological Organisation for all activities within the Global atmospheric Watch (GAW) Program and also we follow rigorously these standard practice. The whole measurement and analytical procedure is laid down in standard operating procedures. Annual samples of the WMO/GAW laboratory intercomparison program organised by the U.S. EPA and since 1996 by QA/SAC Americas are analysed (Acker 1998b).

### **Passive string collector**

Passive string collector (ASRC-type) was used to collect cloud water on the Brocken. Such kind of passive cloud-water collectors depend on ambient wind speed to impact droplets onto 0.4-mm Teflon wires string between two circular disks (Mohnen, 1989). The efficiency of such collectors depend on wind speed in a large extent. Cape et al. 1999 used the same method to collect cloud water at the summit of Great Dun Fell, and they estimated that the capture efficiency was likely to be better than 90 % for all droplet sizes larger than 5  $\mu\text{m}$  diameter.

### **TSP high volume sampler**

Aerosol samples were collected with TSP high volume sampler. Digital-aerosol sampler DHA-80 can work fully automatically to sample exact volume of air mass. The flow of air mass ranges between 100-1000  $\text{l min}^{-1}$  and thus it belong to high volume sampler. The filter (Whatman GF/C) was stored in a bottle for later analyse in Berlin laboratory with ion chromatography. The filter was first weighed and then in 100ml bottle together with 50 ml destiled water shaken for one hour. After this process, 0.45  $\mu\text{m}$  filter was used to select out the larger nucleiis.





## Lebenslauf

### Zur Person

Name	Xiangshan Tian-Kunze geb. Tian
Adresse	Wilhelm-Ostwald-Str. 5 12489 Berlin
geboren am	18. März 1970 in Jilin, Volksrepublik China
Familienstand	verheiratet

### Schulbildung

1977-1982	Grundschule in Yanji, Volksrepublik China
1982-1988	Mittelschule in Yanji, Volksrepublik China
7.1988	Allgemeine Hochschulreife

### Studium

9.1988-7.1992	Studium der Luftphysik an der Peking Universität, Beijing, Volksrepublik China
7.1992	Bachelor's Degree
9.1993-7.1996	Studium der Luftchemie an der Peking Universität, Beijing, Volksrepublik China
7.1996	Master's Degree
9.1996-6.2000	Promotion an der Technischen Universität Cottbus, Cottbus

### Beruflicher Werdegang

9.1992-8.1993	Tätigkeit als wissenschaftliche Mitarbeiterin an der Peking Universität, Beijing, Volksrepublik China
---------------	--